Title
Phase Transitions in Nuclear Organization and Function

Author
Strom, Amy R

Publication Date
2018

Peer reviewed|Thesis/dissertation

Phase Transitions in Nuclear Organization and Function

by

Amy Rose Strom

A dissertation submitted in partial satisfaction of the

requirements for the degree of

Doctor of Philosophy

in

Molecular and Cell Biology

in the

Graduate Division

of the

University of California, Berkeley

Committee in charge:
Professor Gary H. Karpen, Chair
Professor Iswar K. Hariharan
Professor Dirk Hockemeyer
Professor Ke Xu

Spring 2018

Abstract

Phase transitions in Nuclear Organization and Function

by

Amy Rose Strom

Doctor of Philosophy in Molecular and Cell Biology

University of California, Berkeley

Professor Gary H. Karpen, Chair

Compartmentalization is a theme used throughout all kingdoms of biology to create functionally distinct units within a complex cellular environment. In addition to membrane-bound organelles, compartments can exist in the cell that are not membrane bound, yet are still physically distinct from surrounding space. The cell contains many of these membraneless organelles (nucleoli, stress granules, PML bodies, etc.), which are thought to be formed by liquid-liquid phase separation. We find that in early Drosophila embryos, a distinct chromatin domain (heterochromatin) forms by nucleating multiple Heterochromatin Protein 1a (HP1a) foci that grow individually, then fuse together into the final domain. This formation process is reminiscent of liquid-like fusion of nucleoli, which led us to comprehensively study whether heterochromatin could also be a phase-separated system within the nucleus. We utilized Fluorescence Correlation Spectroscopy (FCS) methods to investigate protein diffusion dynamics and determine if heterochromatin displays characteristics associated with phase separation. We find that, similar to other membraneless organelles, the heterochromatin domain is indeed capable of liquid-like fusion, is selectively permeable, and the hetero-euchromatic interface is a barrier to protein diffusion. Additionally, Drosophila HP1a protein is capable of liquid demixing in vitro and mediates domain formation in vivo. This work is the first to demonstrate that the heterochromatin domain is subject to phase separation principles, which suggests that phase interaction, rather than steric hindrance due to chromatin compaction, defines accessibility of heterochromatic areas. It has been suggested that phase separation could be a general organizing property for many membraneless organelles; therefore this model has broad implications for understanding the mechanism of nuclear and genome organization.

Table of Contents

Acknowledgements

To begin, I would like to acknowledge my mentor and friend, Gary Karpen. Your positivity and support have been instrumental in guiding my scientific curiosity and growth as a researcher and a person. Your unbridled idealism and passion for basic scientific inquiry are an inspiration and I hope to be half as wonderful of a mentor as you someday.

To my office-mate Aniek Janssen, who lifts my spirit on Monday mornings and cathartically complains with me when times are tough. Thank you for reading many of my first drafts, I attribute any future grant successes at least in part to you for teaching me to be a better communicator. To W. Kyle Mills, fellow graduate student who went through the challenges and exciting times of graduate school with me. Thank you for being a touchstone for my progress during our time at Berkeley, for organizing adventurous lab trips and always being ready with a beer and a listening ear when I needed it.

To the other members of the Karpen lab, past and present. Serafin Colmenares, thank you for always sharing reagents and a helping hand. Grace Lee, for our mutual love of dogs! Weiguo Zhang, your stories always bring a smile to my face. David Acevedo, for supporting us without complaint and being the rock of the lab. Sasha Langley, your unique perspectives always improve my scientific stories. As for the newest members Shelby and Collin, the lab is lucky to have both of you. Enjoy your years in the Karpen lab and at Berkeley, I know you will do great things! My students—Debbie Staijen, Braedi Ego, and Ryan Chung. Thank you for the years of hard work you have dedicated to these projects. I wish you all the best in your futures, scientifically and personally.

Thank you to my collaborators, near and far. Mustafa Mir and Xavier Darzacq, for believing in such a bold project from the beginning and contributing your time and effort to making it better. Dmitry Fyodorov and Alexander Emelyanov, for investigating the same project from a new perspective and adding to its foundation from a new direction. Sam Safran and Dan Deviri, for hosting Gary during his sabbatical in Israel and teaching both of us the physics behind the phenomenon we were studying biologically. You are to thank for our stronger understanding of the fundamental processes that guide these data, and I hope our fruitful collaborations continue.

To my parents. Thank you for nurturing my curiosity as a child, building my logical thinking with games and puzzles, and supporting my education always. I only began on this scientific path because of you, and my heart swells knowing you are proud of me and my work. To Akshay Tambe, who hiked with me up countless mountains and added perspective to my life and my projects. My roommates and friends, for helping me to maintain a healthy work life balance and always being willing to try my new favorite hobby, whether ukulele, sailing, watercolors, or dog walking.

Finally, thank you to my dissertation committee, Dirk Hockemeyer, Iswar K. Hariharan, and Ke Xu. Your critical and balanced views guided my projects and my own path toward success throughout these years and I am forever grateful. You let me explore new and different aspects of science and navigated me in when I didn't know which path to choose. I will remember your advice for many years to come.

Chapter 1

Introduction: Nuclear organization and function of constitutive heterochromatin

Introduction to Epigenetics—nucleosomes, modifications

Each nucleus in a multicellular organism contains the same DNA, but actively utilizes a distinct set of genes that allow it to become a certain cell type. How the DNA is packaged, on many scales, determines cell identity, health, and can contribute to physiological phenotypes like tissue function and aging.

On the smallest scale, DNA is wrapped around nucleosomes (Richmond & Davey, 2003). Nucleosome occupancy can determine fine-scale accessibility of DNA sequences to DNA-binding proteins of various function (Noll & Kornberg, 1977). Nucleosomes can be post-translationally modified on their flexible tails in order to influence nucleosome stability and binding, which in turn can recruit specific enzymes to the underlying sequences (Jenuwein & Allis, 2001). Proteins that catalyze epigenetic marks are called 'writers,' ones that recognize those marks are called 'readers,' and enzymes that remove marks are called 'erasers.' Histone tails can be modified by acetylation, methylation, ubiquitination, and sumoylation, with each having a specific effect on function of the underlying DNA sequence. For example, acetyl modifications are negatively charged and slightly repel the backbone of wrapped DNA, leading to opening of the DNA and lower stability of the DNA-nucleosome interactions. Acetylated histones are thus more easily removed, and tend to lead to increased transcription (Lee, Hayes, Pruss, & Wolffe, 1993).

A second and third layer of complexity are added by understanding that the histone modification can occur at multiple sites and multiple times. For example, lysines of histone H3 at positions four, nine and thirty-six can each be mono-, di-, or tri-methylated, and each of these will direct a specific outcome (Jenuwein & Allis, 2001). Additionally, adjacent nucleosomes need not be modified in the same way, but can influence function of the same underlying sequence. For even more complexity, DNA bases themselves can be methylated and have epigenetic outcomes. However, this is exceedingly rare in *Drosophila melanogaster* (Urieli-Shoval, Gruenbaum, Sedat, & Razin, 1982), our organism of choice, and will therefore be largely overlooked in this dissertation. Therefore, the epigenetic state of a chromatin locus is an integration of the combined modifications on nucleosomes within a range of the locus.

Nuclear Organization

Like the cytoplasm, the nucleus is organized into many physically distinct compartments that tend to organize sequences into groups by function. Breakthroughs in mechanics of the organization processes necessary for compartmentalization have revealed the role of phase separation in compartmentalization of the nucleus. Originally applied to cytoplasmic membraneless organelles, the theory of phase separation provides a novel way to consider regulation of chromatin via basic biophysical principles.

Gene structure of exons and introns, enhancer-promoter interactions, transcription factor binding sites, histone modifications; these describe what is happening at a single locus. Organizational data for whole genomes, like Hi-C, Dam-ID, and oligo paints, tells us there are many levels of pairwise interactions, but the nucleus is coordinating hundreds or thousands of loci at once, constantly re-evaluating its

environment and tuning transcription to respond. We have little understanding how the nucleus accomplishes this great feat.

Of note, chromosomal loci are often organized in 3D space based on their regulatory state (Heard & Bickmore, 2007). Examples include, X chromosome inactivation (Clemson, Hall, Byron, McNeil, & Lawrence, 2006), Polycomb bodies (Mao, Zhang, & Spector, 2011), repair foci(Aten et al., 2004). Take constitutive heterochromatin as an example; it is largely composed of simple repetitive sequences(Peacock et al., 1978) and transposons, which must be transcriptionally silenced and prevented from recombining in order to maintain genome integrity(Peng & Karpen, 2009). These heterochromatic sequences are found in pericentromeric and subtelomeric regions of linear chromosomes, are epigenetically marked with methylation on histone H3 (H3K9me2/3), and are bound by Heterochromatin Protein 1a (HP1a). In a nucleus, these sequences are organized into one or a few compartments that each contain sequences from multiple chromosomes. In this way, the cell can use this compartmentalization to coregulate all the sequences in the heterochromatin domain. The nucleus can ensure that the heterochromatin domain is depleted for polymerases and recombinases, and thus all the sequences in the heterochromatic compartment will not be transcribed or recombined.

We recently published the discovery that cell achieves this heterochromatic compartmentalization through a biophysical process called phase separation (Strom et al., 2017) (also see Chapter 1). Similar to oil and water, liquid-liquid phase separation is the process by which two (or more) types of molecules, when mixed, can demix from one another based on their interaction preferences. Biological phase separation has been invoked in the formation of nonmembranous organelles in the cytoplasm (P granules, stress granules) and nucleus (nucleoli) (Brutlag, Carlson, Fry, & Hsieh, 1978; Hyman, Weber, & Jülicher, 2014). Here we suggest that compartmentalization of chromatin within the nucleus could occur through the same processes. Invoking phase separation provides a possible explanation for why coregulated sequences tend to cluster together in space, and how the cell could control so many loci in a quick, sensitive, and coordinated fashion.

What is phase separation?

Liquid-liquid phase separation is the process of a solution separating into two immiscible liquids. It requires that at least one of the liquid components has a tendency to interact with itself more than with the other component. Given self-interaction, when these two components are mixed, they will tend to bind to like molecules more than unlike, and eventually concentrating like molecules into an area that is depleted for unlike molecules, called a phase.

To understand whether two liquids will phase separate, we turn to their phase diagram. On the x axis is the relative concentration of each component, and on the y axis is $1/\chi$ where χ is the interaction coefficient, which is the strength of self-interaction (Figure 1).

At one interaction strength, increasing concentration will lead to crossing the critical concentration from the one-phase regime into the two-phase regime. At or above this concentration, liquid droplets will form. Continuing to increase the concentration will lead to larger phase droplets, then two equal sized compartments, then droplets of first phase within background of second, and finally crossing the other side of the diagram, past the critical concentration of the second component (Figure 1). Imagine a set amount of water, to which is added a small amount of oil. Very small concentrations of oil within the water are not strong enough to separate themselves from the water molecules. Keep adding oil, however, and droplets of oil will begin to emerge. Continue to add oil and the system will reach a point at which there is equal parts oil and water, then more oil than water, and water will become droplets inside of the oil phase. Still adding oil will result in a point at which there is not enough water to separate itself from the oil.

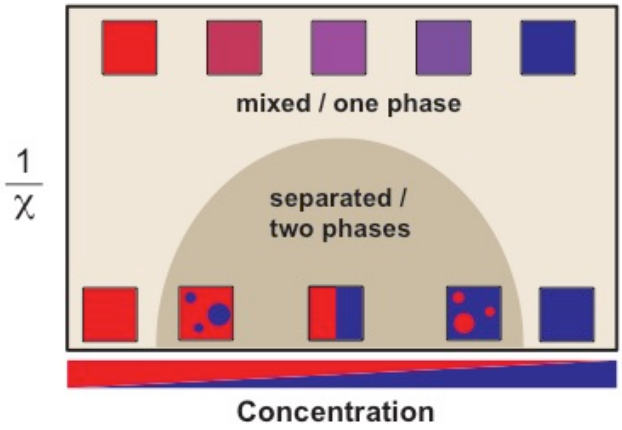

Figure 1: Example of a Phase Diagram
At low temperature, increasing concentration of blue particles within red background will lead to blue droplets. Continuing to increase blue concentration will lead to equal volumes of both phases, then to red droplets within blue background. Increasing temperature of this type of system will lead to mixing of red and blue into one phase.

Altering the interaction strength, usually by increasing temperature, results in raising the energy of the system over the threshold of interaction energy between the two components, leading to mixed / one phase. Imagine a mixture of oil and water that results in oil droplets within water phase. Next, imagine raising the temperature of this mixture while keeping concentrations of oil and water steady. The system will reach some critical temperature at which oil and water mix back into one phase.

Biological Phase Separation

In most biological systems that undergo phase separation, it is believed that proteins are the driving component. Canonical protein-protein interactions happen between hydrophobic faces on well-folded proteins, called the ‘lock-and-key model,’ resulting in specific interactions over very short distances between two proteins (Figure 2). In phase separation, proteins tend to be disordered, lack specific structure, interact

more weakly and on a slightly longer length scale, and tend to interact with multiple partners at once (multivalency) to build a mesh-like network.

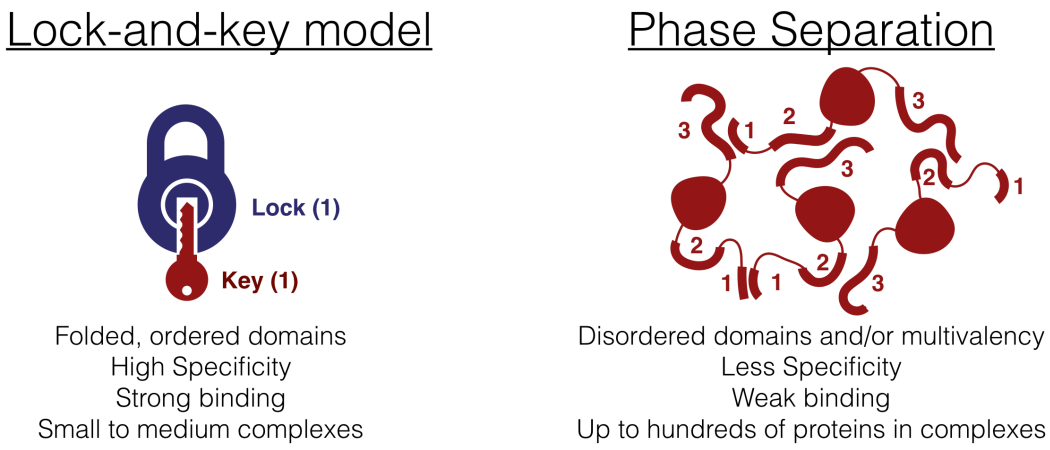

Figure 2: Contribution of Disorder and Multivalency to liquidity and phase separation
Lock-and-key model of protein interaction occurs when two well-folded proteins interact specifically with one another. This model explains most protein complex formation and enzymatic functions. Phase separation occurs when proteins have low complexity or intrinsically disordered domains that are more flexible and have high multivalency, meaning they can interact with more than two other proteins at once. These multiple weak interactions result in flexible, short-lived interactions that can result in emergent formation of a liquid-like phase.

Proteins that mediate phase separation *in vivo*, when expressed exogenously from bacteria and purified *in vitro*, are capable of liquid demixing from aqueous solutions (Hyman et al., 2014). Intriguingly, most known examples do not demix at physiological salt and protein concentrations—usually the critical concentration of protein at physiological salt concentration is much higher than the measured endogenous protein concentration. This could mean that the *in vivo* system requires additional components, modifications or regulators in order to phase separate. In that vein, many phase-separation-capable proteins have RNA-binding properties, and in multiple cases, addition of RNA to purified protein *in vitro* results in significant lowering of the critical protein concentrations required for formation of phase droplets (Lin, Protter, Rosen, & Parker, 2015).

Because the field of biological phase separation is relatively young, and purification and biochemical manipulation of intrinsically disordered proteins is technically difficult, as yet there does not exist an *in vitro* system that perfectly recreates the phase separation properties of *in vivo* domain formation. This is an ongoing area of research in 2018. Additionally, the molecular grammar of phase interactions is poorly understood. It is still difficult to accurately predict which proteins will be able to undergo phase separation, and what the selective permeability properties of the resultant domain will be. Some labs are performing specific studies of the grammar of phase separating protein composition, and others are attempting high-throughput characterization of protein sequence function prediction. It will be pertinent to connect findings from both of these types of studies in order to fully understand and predict presence and function of biological phase separation.

Utility of Compartmentalization

Because of the distinct chemical environments of each liquid phase, the nucleus can use phase separated compartments to concentrate specific factors inside and exclude others. This can be large molecules like proteins (polymerases excluded from heterochromatin), but also metabolites and other small molecules. Concentrating or excluding these factors in certain areas allow for functionalization of each compartment through selective permeability. With two compartments that are created from incompatible components (Figure 3), things that are compatible with X will enter domain X but not Y, and things that are compatible with Y will enter domain Y but not X. For example, the fibrillar core of the nucleolus is a compartment rich in RNA pol I, which transcribes ribosomal DNA (rDNA). rRNA from the fibrillar core becomes concentrated in the liquid phase separated exterior of the nucleolus, where it folds into proper tertiary structure and complexes with RNPs. After folding, the completed ribosomal subunits are shuttled from the outside of the nucleolus to the cytoplasm to begin their function translating mRNAs into proteins (Feric et al., 2016). Each subcompartment promotes the function necessary at that step of the assembly line-- high concentration of RNA Pol I at transcription site, allowing time for folding before moving to next compartment.

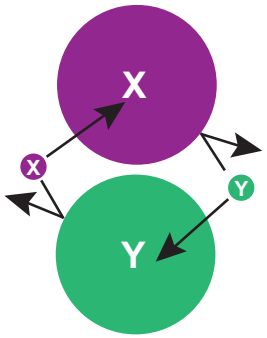

Figure 3: Selective Permeability Particles compatible with phase X are able to enter domain X but be excluded from domain Y, and vice versa.

Utility of liquidity

Liquid-liquid phase separation allows for high concentration of components while maintaining high mobility inside the dense phase. This allows the separation to be quickly and easily reversible. If multivalency instead leads to irreversible aggregation, the cell would not be able to regulate these domains, and the aggregates could be toxic. Examples of irreversible aggregates include prions and amyloid plaques (Brundin, Melki, & Kopito, 2010). Indeed, some liquid-phase forming proteins have the propensity to adopt a conformation that results in irreversible aggregation, which can lead to disease. Disease-causing mutations of FUS tend to aggregate into fibrils rather than liquid droplets (Patel et al., 2015). Maintaining compartments as liquids is advantageous to their regulation and reversibility.

The cell could shift the system across the boundary of the one to two phase regimes with small alterations in protein concentration, binding partner associations, and post-translational modifications. Alternatively, the cell could use the sensitive nature of phase transitions to respond to environmental changes like pH and temperature. For example, stress granules are phase separated domains that form upon exposure to stressors like heat shock (Grousl et al., 2009) (Kramer et al., 2008) or acute oxidative

damage (Lian & Gallouzi, 2009). Stress granules are cytoplasmic bodies that aid in a rapid and robust translational switch. Upon prolonged starvation or heat shock in yeast, mRNAs from the cytoplasm accumulate in ribosome-deficient stress granules. Ribosomes are then free to quickly produce high levels of heat shock proteins from newly transcribed heat shock gene transcripts (Grousl et al., 2009). The liquidity of these heat shock compartments allows them to be quickly formed and dissolved so that the cell can robustly respond to stress and change translational programs.

Physical process of forming a phase: Nucleation, growth, coalescence

Starting with a mix of evenly distributed particles with self-aggregation properties, over time they move via brownian motion, creating small areas of higher or lower concentration. This small area of higher concentration can continue to aggregate other molecules, or can spontaneously dissolve. Once the small droplet reaches a critical radius, it will become stabilized (nucleation) and be able to continue growing and attracting more similar molecules (growth) (Figure 4). Generally, the attraction of like molecules and repulsion of unlike molecules energetically favors formation of droplets with the lowest possible surface area to volume ratio; a sphere. These nucleated droplets continue to grow as spheres until they reach equilibrium, with the same number of molecules entering the dense phase as leaving it.

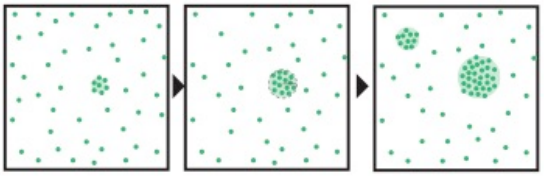

Figure 4: Nucleation and growth
Individual particles with self-association properties randomly diffuse, bind and unbind until a concentration of greater than the critical radius is formed. Once beyond the critical radius, the droplet will continue to grow and accumulate particles into the phase-separated droplet.

They can also physically run into another droplet, in which case they can fuse together. Colloidal particles within fused droplets tend to rearrange themselves until they again reach the lowest energy state--lowest surface area to volume ratio—a spherical shape. This is sometimes referred to as ‘rounding up,’ and is dependent on surface tension.

In the process of reaching equilibrium, the number of phase droplets is controlled by a balance of nucleation and growth. Early in droplet growth, each nucleated droplet that passes above the critical radius will continue to grow, but then when there are many different sizes of droplets, the larger ones win out. Larger droplets continue to grow while smaller actually shrink until below critical radius, then disappear. This is a process called Ostwald ripening, in which differences in curvature impacts the stability of molecules on the surface of the droplets. Specifically, larger droplets are able to maintain contacts with multiple partners and continue to grow, while molecules on the edge of smaller droplets are less stable, and tend to shrink (Hyman et al., 2014).

Nucleation can be aided by a non-random process that results in increased concentration of components in an area. For example, in a system very close to the critical concentration, components binding to a scaffold would bring enough in close proximity to push over the critical radius and stably nucleate.

Growth-limited and nucleation-limited systems

In growth-limited phase separating systems, nucleation occurs easily and droplets are maintained as they grow, resulting in multiple small droplets. Nucleation-limited systems forming a new droplet, but once they're established they are stable and will grow, resulting in fewer, larger droplets.

In development of the fruit fly *Drosophila melanogaster*, the nucleolus is established in nuclear cycles 12-14 post-fertilization. Nucleoli appear synchronously, one per nucleus, after a wave of mitosis. They nucleate on the ribosomal DNA (rDNA) locus and grow as ribosomal RNAs (rRNAs) are both accumulated at the site from the nucleoplasm, and transcribed from the locus. This is an example of a growth-limited system. In a mutant that lacks the nucleating rDNA, formation of nucleoli is stochastic and happens at varying times during interphase, sometimes multiple times in one nucleus, indicating the system has switched to nucleation-limited (Falahati, Pelham-Webb, Blythe, & Wieschaus, 2016). In this case, the nucleating rDNA allows for synchronous formation of nucleoli in all cells.

Growth-limiting systems also allow for specified localization of membraneless organelle formation. Providing a nucleation point drives formation of the organelle at a specific location, i.e. at the rDNA locus. Organization of the number and size of membraneless organelles is an ongoing area of research, but knowledge of growth-limited and nucleation-limited phase-separated systems provides a potential explanation for how a cell would easily create multiple smaller domains or fewer larger domains; A growth-limited system would allow for formation of multiple, smaller domains while nucleation-limited would result in fewer larger domains.

Three or more component systems

With two-component phase systems, the above diagram is applicable and compartments will form only in one of two ways; B droplets in A background, or A droplets in B background. However, the nucleus is complex and contains more than two types of compartments. Adding a third immiscible liquid to the first two allows us to understand the possibilities of more complex systems (Figure 5).

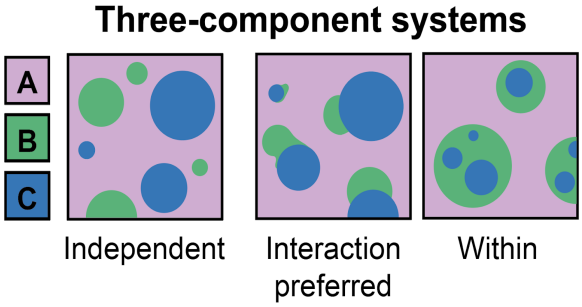

Figure 5: Three-component systems
Two self-aggregating phases, B and C, can form droplets in background solution of A in multiple ways. If B and C components are independent, their droplets will be exclusive. If B and C components have less of an energetic cost to interact with each other than to interact with A, they will form droplets as in 'Interaction preferred.' If C has strong energetic cost of interaction with A, but only weak cost with B, it will partition entirely inside B droplets, as in 'within.'

In A background, droplets of B and C could be independent of one another, and be formed and regulated completely separately. Alternately, B and C could prefer interacting with one another over interacting with A, leading to a conformation in which the B and C compartments are adjacent. Additionally, if C strongly prefers interaction with B, and B can interact with either A or C, it could lead to a conformation in which the C compartment is contained entirely within the B compartment. With these possibilities in mind, one can begin to imagine how a nucleus could use multiple miscible and

immiscible liquids to organize genomic sequences into specific nuclear conformations, and be able to regulate each one independently.

How is compartment identity imparted onto the chromatin fiber?

In addition to phase separated systems made of individual colloidal particles, polymers made of monomers with self-associative properties can be units of phase separation as well. Polymers made of two types of monomers (X and Y) arranged into blocks (e.g. X-X-X-X-Y-Y-Y-Y) are called block copolymers (Figure 6). These polymers phase separate into domain structures that depend on their monomer composition and

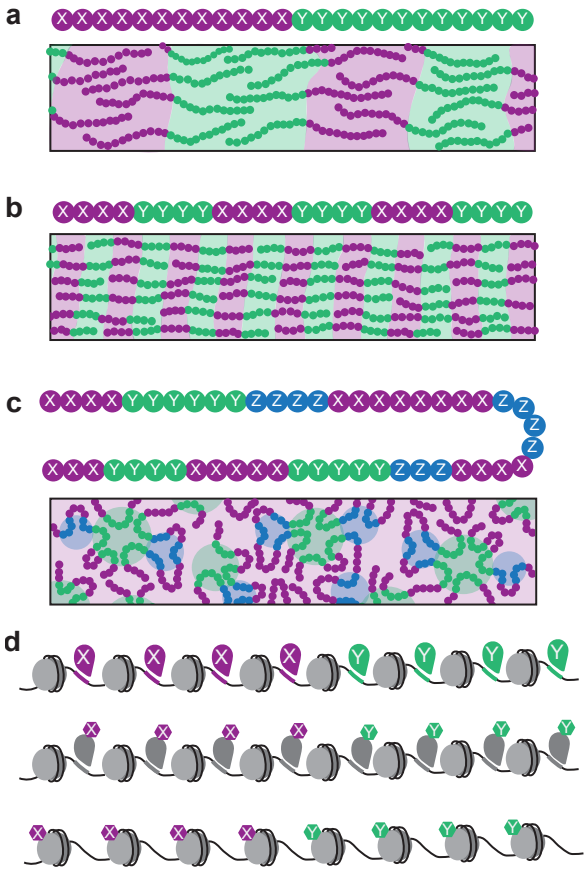

Figure 6: Block copolymers
a. Phase separating materials can be formed by polymers comprised of repeating arrays of self-associating monomers, called block copolymers (top). These polymers associate into phase separated domains depending on their polymer structure (bottom). **b.** A different arrangement of monomers (top) creates a new domain structure (bottom). **c**. A polymer created from more than two monomers (top) can create more complex domain structures (bottom). **d.** Chromatin is a polymer comprised of nucleosomes and DNA. Its monomer identity could be imparted by multiple mechanisms, including direct DNA-binding proteins (top), post-translational modifications on DNA-binding proteins (middle), epigenetic modifications on histones (bottom), or a combination of all of these. Specified areas of chromatin would phase separate into domain areas based on their monomer identity.

order. Simple block copolymers (Figure 6a) create simple two-domain layers while more complex organization can be formed by polymers of longer and more complicated composition (Figure 6b) or even polymers that contain additional monomers (Figure 6c). This type of phase separation is particularly relevant to nuclear organization, as the chromatin fiber is a complex polymer that is organized into phase separated compartments.

In nuclear organization, phase separation would need to include the chromatin fiber inside the phase. In order to properly organize the chromatin fiber, each section must have an identifier that signifies which compartment it belongs in. Compartment identity could be specified on the chromatin fiber in a number of ways, including direct DNA-binding proteins, or modifications on DNA-binding proteins or histones (Figure 6d).

Phase Separation of Constitutive Heterochromatin

In this document, I will explore the roles of phase transitions in nuclear organization and function, using constitutive heterochromatin as a lens. First, in Chapter 2 I will define constitutive heterochromatin and characterize phase separation of HP1a *in vitro* and *in vivo*. Then, in Chapter 3 I describe investigations of a protein that has specific effects on phase separation properties of HP1a without changing its concentration or genomic localization. Lastly, in Chapter 4, I describe the organismal effects of heterochromatic phase separation on aging and longevity.

Chapter 2

Phase separation drives heterochromatin domain formation

Authors: Amy R. Strom[1,2], Alexander V. Emelyanov[3], Mustafa Mir[2], Dmitry V. Fyodorov[3], Xavier Darzacq[2] and Gary H. Karpen[1,2*]
[1] Biological Systems and Engineering Division, Lawrence Berkeley National Laboratory, Berkeley, CA, USA.
[2]Department of Molecular and Cell Biology, University of California, Berkeley, CA, USA.
[3]Albert Einstein College of Medicine, Department of Cell Biology, New York, NY, USA
*Corresponding author

Summary:
Constitutive heterochromatin is an important component of eukaryotic genomes that plays essential roles in nuclear architecture, DNA repair and genome stability(Chiolo et al., 2011), and silencing of transposon and gene expression(Peng & Karpen, 2008). Heterochromatin is highly enriched for repetitive sequences, and is defined epigenetically by methylation of Histone H3 at lysine 9 (H3K9me2/3) and recruitment of its binding partner Heterochromatin Protein 1 (HP1). A prevalent view of heterochromatic silencing is that these and associated factors lead to chromatin compaction, resulting in steric exclusion of regulatory proteins such as RNA polymerase from the underlying DNA(Elgin & Reuter, 2013). However, compaction alone does not account for formation of distinct, membrane-less heterochromatin domains within the nucleus, fast diffusion of proteins inside the domain, and other dynamic features of heterochromatin. Here we present data supporting an alternative hypothesis, that formation of heterochromatin domains is mediated by phase separation, a phenomenon that gives rise to diverse non-membrane-bound nuclear, cytoplasmic and extracellular compartments(Hyman et al., 2014). We find that *Drosophila* HP1a protein undergoes liquid-liquid demixing *in vitro,* and nucleates into foci that display liquid properties during the first stages of heterochromatin domain formation in early *Drosophila* embryos. Further, in both *Drosophila* and mammalian cells, heterochromatin domains exhibit dynamics characteristic of liquid phase-separation, including sensitivity to disruption of weak hydrophobic interactions, and reduced diffusion, increased coordinated movement and inert probe exclusion at the domain boundary. We conclude that heterochromatic domains form via phase separation, and mature into a structure that includes liquid and stable compartments. We propose that emergent biophysical properties associated with phase-separated systems are critical to understand the unusual behaviors of heterochromatin, and how chromatin domains in general regulate essential nuclear functions.

Introduction

Proteins that undergo liquid-liquid demixing *in vitro* and *in vivo* often contain intrinsically disordered regions (IDRs) and/or low-complexity sequences(Kato et al., 2012), which are present in the N-terminal tail and hinge domains of *Drosophila* HP1a (Extended Data Fig. 1a). We therefore expressed and purified *Drosophila* HP1a protein from *E. coli* to determine if it undergoes phase separation *in vitro*. At 22 °C, high protein concentrations and low salt, aqueous solutions of HP1a spontaneously demixed to form droplets (Fig. 1a, b) that reversibly dissolved at 37 °C (Extended Data Fig. 1b), as observed for other phase-separating proteins (Mitrea et al., 2016; Molliex et al., 2015). These droplets are highly spherical and their area distribution fits a power law with exponent -1.5, suggesting that they are liquid-like and undergo coarsening(Huber, 1991) (Extended Data Fig. 1c, d). Large oligomeric complexes of purified HP1a also formed in glycerol gradients in low but not high salt conditions (Extended Data Fig. 1e, f). Independently, Larson et al.[31] report that human HP1α protein also displays liquid demixing *in vitro*, demonstrating a conserved property of diverged HP1 proteins. In contrast to our observations with *Drosophila* HP1a, human HP1α demixing requires N-terminal phosphorylation or DNA binding, which could be due to differences in species-specific amino acid sequences or *in vitro* conditions.

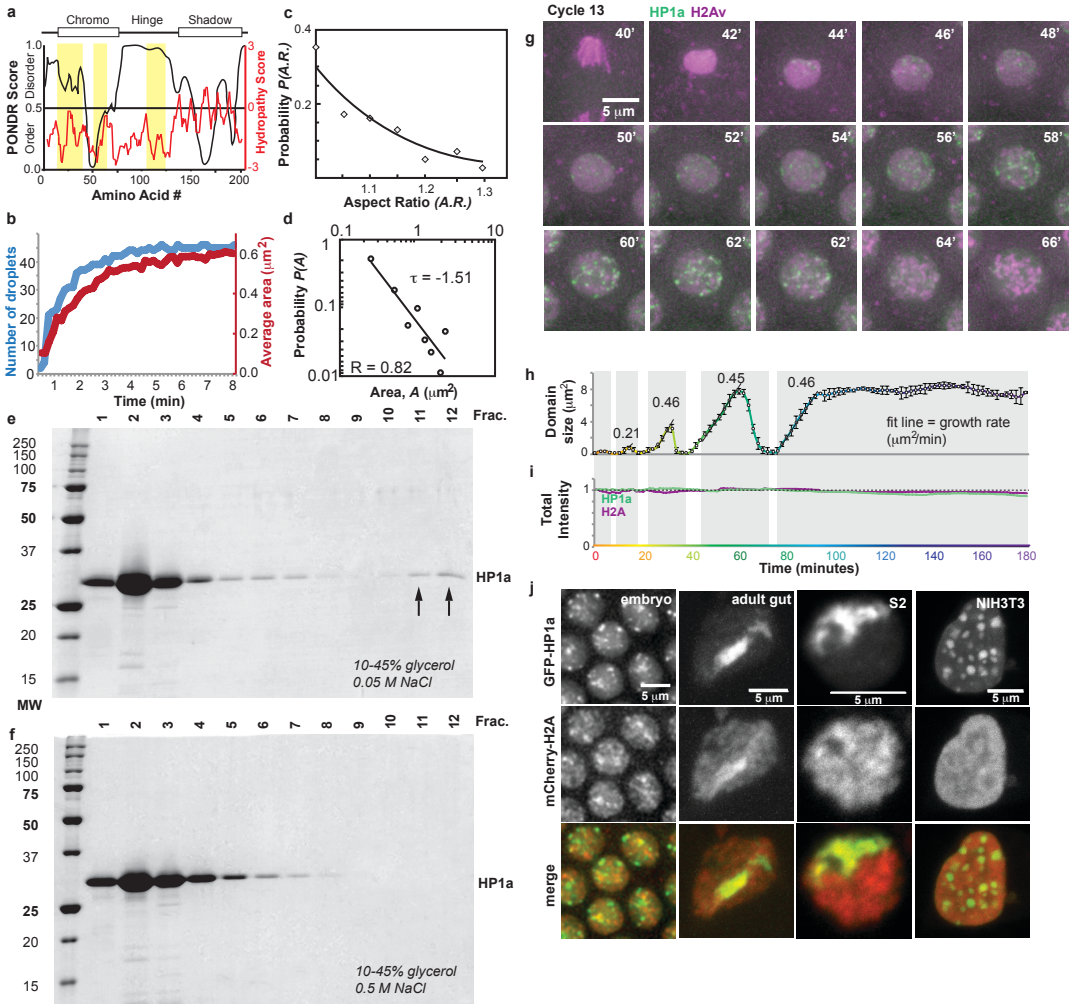

Extended Data Figure 1: HP1a facilitates liquid demixing *in vitro* and *in vivo*
a. Analysis of HP1a 206 aa protein sequence. Top: known domains chromo, hinge, and shadow. Black line: PONDR score for intrinsic disorder, >0.5 is considered disordered. Red line: hydropathy score, positive is hydrophobic. Yellow bars indicate low complexity sequences. **b.** 1 mg/mL HP1a in 50 mM NaCl was incubated at 37°C for 5 minutes, then returned to room temperature (22°C) and imaged with DIC every 5 seconds for 8 minutes. Quantification of average number and area of HP1a droplets formed in a 50x50 μm window, N=3. **c.** Probability distribution of droplet aspect ratio. **d.** Probability distribution of droplet area on a log-log plot follows a power law exponential with τ = -1.5, indicative of aggregating systems. Sediment gradient analysis shows large oligomers of HP1a in 0.05 M NaCl (arrows, **e.**) but not 0.5 M NaCl (**f.**). **g.** Two-color images showing HP1a and H2Av for one nucleus over *Drosophila* embryonic cycle 13. **h.** Quantification of average HP1a domain size per nucleus and **i.** total intensity of HP1a and H2A over embryonic cycles 10-14. Error bars are SD. N=12 embryos of >75 nuclei each. **j.** Two-color images of HP1a and H2A showing differentially shaped heterochromatin domains in *Drosophila* embryos, adult gut and cultured Kc cells, and mouse fibroblast NIH3T3 cells.

To determine the *in vivo* relevance of HP1a demixing, we analyzed the first stages of heterochromatin formation in early *Drosophila* embryos. Heterochromatin begins to form during the short (~8-20 minute) post-fertilization nuclear cycles 11-13, but does not mature into a stable domain until cycle 14, when interphase extends to 1.5 hours (Yuan & O'Farrell, 2016). In each of these cycles, we observe that GFP-HP1a

exhibits the nucleation, growth and fusion dynamics associated with phase-separated, liquid compartments (Hyman et al., 2014; Zhu & Brangwynne, 2015). High-resolution 4D analysis using lattice light-sheet microscopy(B.-C. Chen et al., 2014a) revealed that HP1a is initially diffuse, then forms highly spherical foci that grow, frequently fuse together, and dissolve at the onset of mitotic prophase, when HP1a is removed from chromatin (Fischle et al., 2005) (Fig. 1c, Movies S1-3). Wide-field microscopy shows that in nuclear cycles 11-14, 6-8 HP1a major foci appear simultaneously in early interphase (Fig. 1d-f), grow in cross-section at a rate of 0.45 μm^2/min (Extended Data Fig. 1h), and dissolve during mitosis (Extended Data Fig. 1g). Importantly, the total fluorescence intensity of GFP-HP1a does not change during cycles 10-14 (Extended Data Fig. 1i), suggesting that formation and dissolution of HP1a foci is not controlled by changes in protein concentration.

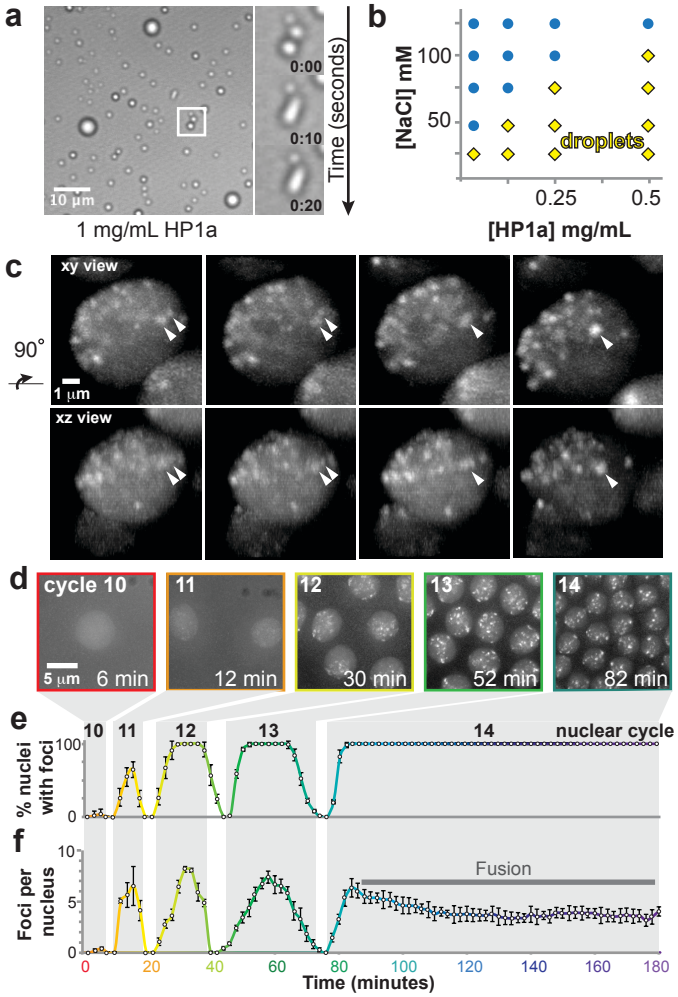

Figure 1: HP1a facilitates liquid demixing *in vitro* and *in vivo*

a. Purified *Drosophila* HP1a forms liquid phase droplets *in vitro* that undergo fusion**. b.** Phase diagram of HP1a droplet formation in varying salt and protein concentrations. **c.** In *Drosophila* embryos, GFP-HP1a forms liquid phase droplets that fuse and round up. **d.** HP1a droplets form in every interphase after nuclear cycle 11. **e.** Quantification of average percent of nuclei with HP1a foci in cycles 10-14. **f.** Quantification of average number of HP1a foci per nucleus in cycles 10-14. For **e.** and **f.,** error bars are SD. N=12 embryos of >75 nuclei each.

Fusion of droplets to form larger, spherical compartments is a property of liquids (Zhu & Brangwynne, 2015). In *Drosophila* embryos, foci round up after fusion to be highly circular (in 2D) in cycle 13 and early cycle 14, but display lower circularity as cycle 14 progresses (Fig. 2a, c, Movie S1-3). Notably, mature heterochromatin domains appear roughly spherical in some eukaryotic cell types like early *Drosophila* embryos, but are aspherical in other cell types (Extended Data Fig. 1j). To assess whether loss of circularity reflects reduced liquid-like behavior, we used FRAP to measure the mobile and immobile HP1a fractions during cycles 10-14, and after gastrulation (stage 8). The immobile fraction was undetectable in cycle 10, measured ~2.5-10% in cycles 11-13 and early cycle 14, and rose to ~30% by late cycle 14 (Fig. 2b), equivalent to stage 8 embryos

(Extended Data Fig. 2a, b). Thus, loss of circularity is accompanied by a significant increase in the HP1a immobile fraction, which we speculate is due to more HP1a associating with the chromatin polymer, whose inherent elasticity introduces shape constraints (Vasquez et al., 2016).

Formation of compartments by phase separation often requires weak hydrophobic interactions among macromolecules, which can account for both high concentrations and high mobility of phase components (Hyman et al., 2014). Therefore, we analyzed the response of heterochromatin domains to 1,6-hexanediol, an aliphatic alcohol that specifically disrupts weak hydrophobic interactions *in vivo* (Ribbeck & Görlich, 2002). Addition of 1,6-hexanediol to *Drosophila* S2 and mouse NIH3T3 cultured cells resulted in significant but incomplete dispersal of HP1 from the heterochromatic domains, then 1,6-hexanediol is washed out after two minutes and partial recovery of heterochromatic HP1 enrichment is observed (Fig. 2d, e). Interestingly, proposed roles for HP1 in compacting chromatin (Hinde, Cardarelli, & Gratton, 2015) predict that HP1a dispersal would decrease histone density in heterochromatin; however, hexanediol treatment did not change histone enrichment, likely due to nuclear dehydration and a decrease in total nuclear size (Extended Data Fig. 2c).

We hypothesized that the HP1 population unresponsive to 1,6-hexanediol is equivalent to the immobile component measured by FRAP. Consistent with this idea, FRAP analysis indicated that the immobile fraction of HP1a in S2 cells, 50%, is similar to the 46% that remains after hexanediol treatment (Fig. 2g, Extended Data Fig. 2d). GFP-HP1a proteins containing point mutations known to disrupt dimerization (I191E) or non-histone partner binding (W200A) (Brower-Toland et al., 2007) displayed significantly increased mobility compared to GFP-HP1a wild-type controls (Extended Data Fig. 2d), and the mutant proteins were nearly completely extracted from the domain by 1,6-hexanediol treatment (Fig. 2f, g). We conclude that the integrity of mature heterochromatin domains relies on weak hydrophobic interactions, and that dimerization and interactions with non-histone binding partners contribute to HP1 immobilization. This is consistent with evidence that networks of multivalent interactions promote demixing *in vitro* and *in vivo* (P. Li et al., 2012; Mitrea et al., 2016). We propose that mature heterochromatic domains consist of both immobile (static) and mobile (liquid) HP1a compartments, similar to recent findings for nucleoli (Feric et al., 2016).

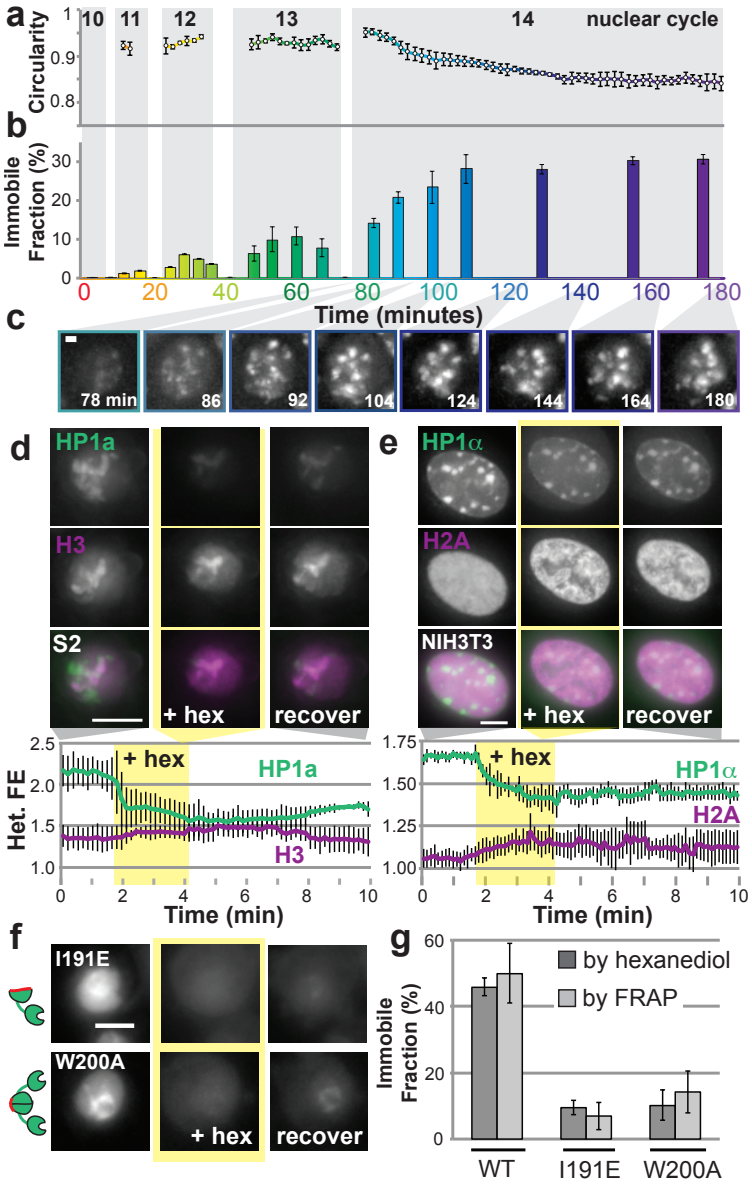

Figure 2: Mature HP1 domains *in vivo* are not purely liquid
a. Quantification of average HP1a droplet circularity over cycles 10-14. **b.** The average immobile component of GFP-HP1a as measured by FRAP in cycles 10-14. N=12 embryos >75 nuclei each, error bars are SD. **c.** Example images of foci during cycle 14. Images and quantification of heterochromatic enrichment of HP1a/α in **d.** S2 cells (N=136 nuclei) and **e.** NIH3T3 cells (N=87 nuclei) treated with medium containing 10% 1,6-hexanediol, error bars are SD. **f.** Representative images of HP1a mutants I191E (non-dimerizing) and W200A (no PxVxL binding) before, during, and after exposure to 1,6-hexanediol. **g.** Immobile fraction by percent of total population for wild type HP1a (WT), and point mutants incapable of dimerizing (I191E) or interacting with binding partners (W200A) in S2 cells. Immobile fractions 'using FRAP' were measured as percent fluorescence intensity unrecovered after 30 seconds, and 'using hexanediol' as percent heterochromatic enrichment remaining after hexanediol treatment for 120 seconds.

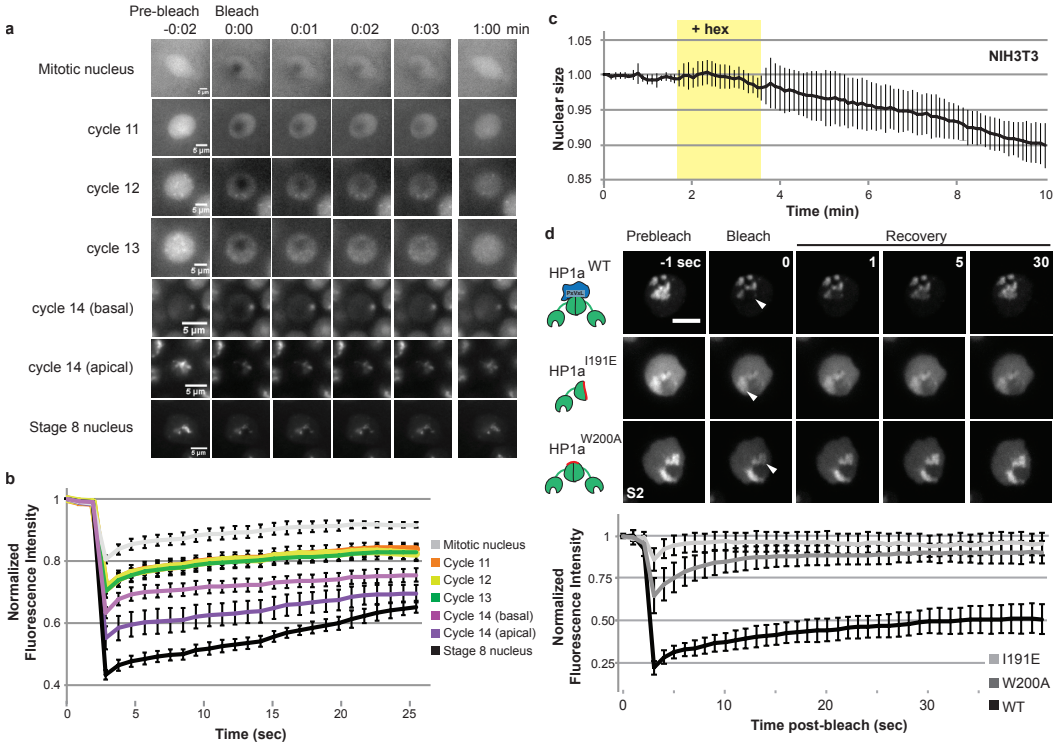

Extended Data Figure 2: Mature *in vivo* HP1 domains are not pure liquid.
FRAP images (**a.**) and average fluorescence intensity over time of bleached area (**b.**) of *Drosophila* embryonic nuclei in cycles 10-14, and Stage 8. In cycle 14, heterochromatin forms in the apical region of the nucleus. N=20 nuclei in each condition, error bars are SD. **c.** NIH3T3 nuclear size after addition of media containing 10% 1,6-hexanediol. N=63 nuclei, error bars are SD. **d.** Images and quantification of FRAP on HP1a wild type (WT) and point mutants incapable of dimerizing (I191E) or interacting with binding partners (W200A) in S2 cells. N=60 nuclei each condition, error bars are SD.

To further test the idea that distinct heterochromatin domains arise through phase separation, we analyzed HP1a dynamics within and outside these domains in more detail. Macromolecules that self-interact to promote demixing become spatially confined because free energy must be expended to break self-interaction and leave the phase. The magnitude of this free energy cost defines the interfacial tension, and also constrains the directionality of a molecule's movement, increasing the likelihood that two molecules near the phase boundary will move in the same direction ('cooperative' or 'coordinated' movement, Extended Data Fig. 3a). Subcellular regions in which fluorescently-tagged proteins undergo coordinated movement can be identified by observing increased fluorescence intensity variance using an FCS derivative called Number and Brightness (Digman, Dalal, Horwitz, & Gratton, 2008) (N&B, Extended Data Fig. 3b). We validated this application of N&B in *Drosophila* S2 cells by first analyzing nucleoli, which are known to arise through phase separation (Falahati et al., 2016). N&B analysis of GFP-fibrillarin highlighted areas of consistently high variance (2.38±0.46 –mers) at the nucleolar boundary, compared to inside (1.28±0.36) or outside

(1.17±0.25) the domain (Extended Data Fig. 3c). Similarly, GFP-HP1a displayed increased variance near the heterochromatin domain boundary (2.06±0.31), compared to inside (1.23±0.38) or outside (0.95 ±0.15) the domain (Fig. 3a). High variance at the heterochromatin boundary was also observed for two other heterochromatin proteins, HP4 and HP5 (Extended Data Fig. 3d, e), and for human HP1α expressed in mouse NIH3T3 cells (Fig. 3b, Extended Data Fig. 3f), similar to previous results in mammalian cells(Hinde et al., 2015). By contrast, HP1c, which is closely related to HP1a but enriched in euchromatin, did not show increased variance near the eu-heterochromatic border (Extended Data Fig. 3g). Together these data demonstrate that HP1a and other heterochromatic proteins exhibit the

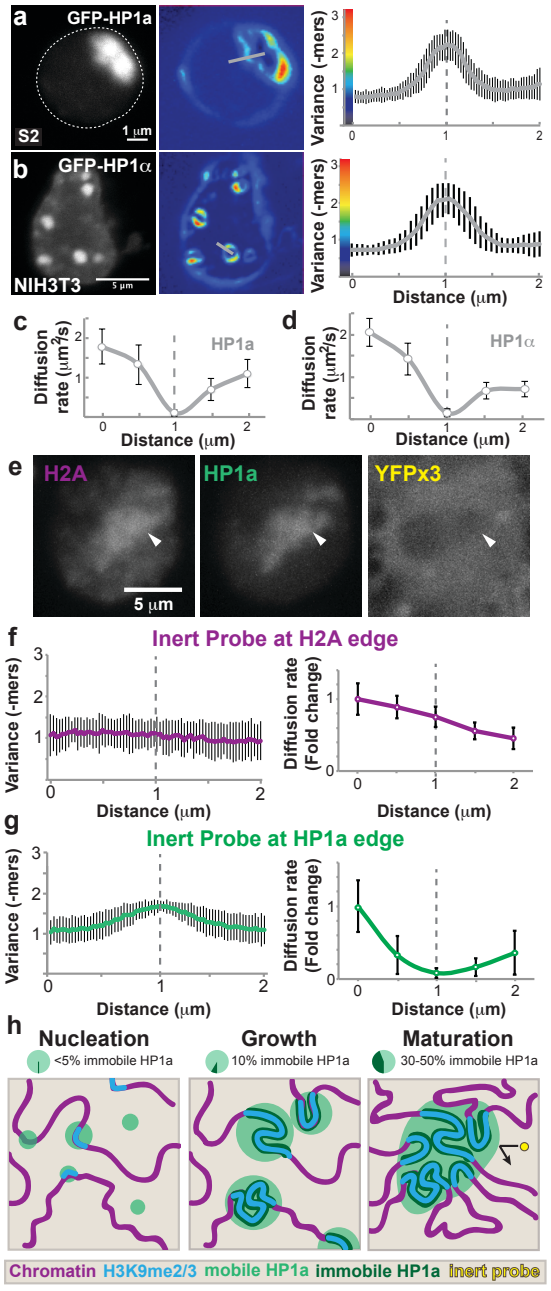

Figure 3: The hetero-euchromatic border is a barrier to protein diffusion

a. A cultured *Drosophila* S2 cell expressing GFP-tagged HP1a (left). Pseudocolored image of fluorescence intensity variance measured by Number and Brightness (middle), color scale represented in quantification graph (right). Quantification of variance (right) across the hetero-euchromatic border from nucleoplasm to heterochromatin (example line drawn in middle). Dotted line represents approximate hetero-euchromatic boundary. N=25 nuclei, error bars are SD. **b.** Image, variance map, and quantified variance of HP1α in mammalian NIH3T3 cells. N=25 nuclei, error bars are SD. Average diffusion rate, *D,* in $\mu m^2/s$, of HP1a and HP1α across the hetero-euchromatic boundary in **c.** S2 and **d.** NIH3T3 cells, respectively. N=25 nuclei, error bars are SD. **e.** Representative image of nucleus expressing mCherry-H2A to mark chromatin, Cerulean-HP1a to mark heterochromatin, and NLS-YFP-YFP-YFP as an inert probe excluded from heterochromatin (arrowhead). **f.** Quantified variance and diffusion rate for inert probe at the edge of an H2A-rich domain (> 2 fold intensity increase in H2A, <1.25 fold intensity increase in HP1a). N=47 nuclei, error bars are SD. **g.** Quantified variance and diffusion rate for inert probe at the edge of an HP1a-rich domain (> 3 fold intensity increase in HP1a, <1.25 fold intensity increase in H2A). N=47 nuclei, error bars are SD. **h.** Model of heterochromatin formation: **Nucleation** (left), where all HP1 is mobile and foci begin to form via liquid phase separation, driven by multivalent, weak hydrophobic interactions between HP1 and other heterochromatin components; **Growth** (middle), where spherical foci become larger through recruitment of more HP1 and coarsening, and some HP1 becomes immobile, most likely due to chromatin fiber binding; and **Maturation** (right), where foci containing heterochromatic sequences from different chromosomes undergo liquid-like fusions to form larger domains, significant subcompartments containing immobile (static) and mobile (liquid) components develop, and selective permeability and other dynamic properties of the phase interface are observed.

coordinated movement predicted to occur at phase interfaces.

Constraints on movement at phase interfaces also predict that diffusion rates will be slower at the boundary compared to inside the domain[20] (Extended Data Fig. 3a). To assess the movement of fluorescently tagged HP1a near the heterochromatin domain boundary, we used Raster Image Correlation Spectroscopy(Rossow, Sasaki, Digman, & Gratton, 2010) (RICS). Here again we validated the approach by analyzing GFP-fibrillarin dynamics in S2 cells, and observed much slower diffusion rates near the inner surface (D = 0.20±0.18 $\mu m^2/s$), compared to the interior (1.78±0.50 $\mu m^2/s$) or outside (1.72±0.77 $\mu m^2/s$) the domain (Extended Data Fig. 3h). Similarly, GFP-HP1a (Fig. 3c) displayed reduced diffusion near heterochromatin domain boundaries (0.10±0.07 $\mu m^2/s$), compared to the interior of the heterochromatin domain (1.09±0.36 $\mu m^2/s$) or the nucleoplasm (1.78±0.45 $\mu m^2/s$). HP4 and HP5 showed similar spatial variation in their dynamics (Extended Data Fig. 3h), and human HP1α shows similar behavior in NIH3T3 cells (near the boundary: 0.15±0.08 $\mu m^2/s$; internal: 0.71±0.18 $\mu m^2/s$; nucleoplasm: 2.05±0.34 $\mu m^2/s$) (Fig. 3d). Thus, two independent methods reveal that that *in vivo* HP1a dynamics in both *Drosophila* and mammalian nuclei are consistent with heterochromatin protein containment within liquid-like, phase-separated compartments.

We next assessed whether HP1a is needed for compartmentalization of heterochromatin *in vivo* by depleting it from cultured *Drosophila* S2 cells and examining impact on the nuclear distribution of HP4(Greil, de Wit, Bussemaker, & van Steensel, 2007). After HP1a depletion, GFP-HP4 loses coordinated movement and becomes dispersed throughout the, in contrast to its restriction to a distinct heterochromatic domain in control cells (*brown* RNAi), or in HP1a-depleted cells rescued by transfection with RNAi-resistant, wild-type HP1a (Extended Data Fig. 3i). We conclude that HP1a is required for heterochromatin domain integrity and compartmentalization, but it is likely that other components and interactions also play an important role.

Inert macromolecular probes such as fluorescent dextrans and some proteins are excluded from heterochromatin(Bancaud et al., 2009), which has been attributed to steric exclusion as a consequence of chromatin compaction. To test whether exclusion might instead reflect selective permeability of heterochromatic compartments, we co-expressed an inert probe (NLS-YFP-YFP-YFP, 89 kDa) with mCherry-H2A and Cerulean-HP1a in S2 cells (Fig. 3e-g), and observed variance and diffusion of the inert probe at areas of high H2A-density or high HP1a-density. If phase interactions most influence probe movement, high HP1a density will have a greater effect than high H2A density on the probe's variance and diffusion (Extended Data Fig. 3j). Consistent with the phase model, variance of the probe did not spatially correlate with H2A density, but was elevated at the edges of HP1a-rich domains (1.45±0.09, Fig. 3f-g). We also observed reduced probe diffusion within H2A-dense regions (45%±14% of the euchromatic rate), suggesting that chromatin density hinders movement. However, the proximity to the heterochromatin border had a much stronger effect on diffusion rates (0.17±0.12, Fig. 3g). Therefore, we conclude that phase interactions and selective permeability play a dominant role over chromatin compaction in inert probe exclusion from the domain (summarized in Extended Data Fig. 3k).

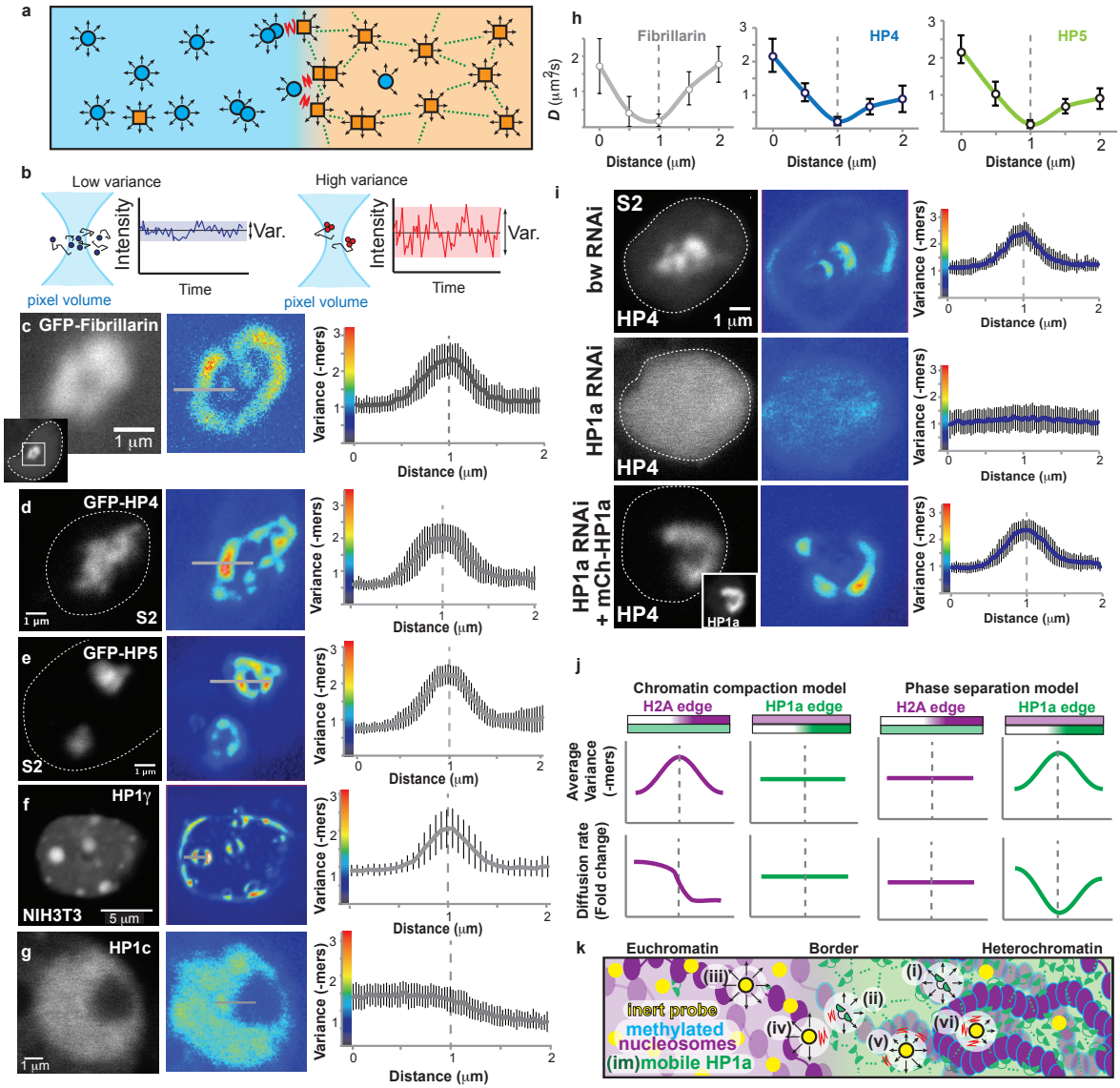

Extended Data Figure 3. The hetero-euchromatic border is a barrier to protein diffusion
a. Schematic illustration of dynamic properties near a phase boundary. Orange particles have self-association properties (green dotted lines) and concentrate into a phase (orange background, right side). An orange particle in the orange phase can move in any direction and encounter only orange particles (eight arrows) until it contacts a blue particle, which prevents self-association between two orange particles and limits the potential diffusion dimensions of the orange particle (red squiggle, loss of arrows). This results in two properties of particles near the phase boundary: 1) net slower diffusion, and 2) higher likelihood that two orange particles will move in the same direction. **b.** Schematic illustrating number and brightness technique(Digman et al., 2008). If particles are moving independent of one another (left, blue), variations in fluorescence intensity measured in the pixel volume over time will be small. If particles are moving together in and out of the pixel volume (right, red), intensity variation will be larger. This can result from bound molecules (i.e. complex) or unbound molecules moving in the same direction ('coordinated movement').

c. A cultured *Drosophila* S2 cell expressing GFP-tagged fibrillarin to mark the nucleolus (left). Inset shows entire nucleus (dotted line) and region of interest (white box). Visual representation of increased variance measured by Number and Brightness (middle), color scale represented in quantification graph (right). Quantification of variance (right) across the hetero-euchromatic border from nucleoplasm to nucleolus (example line drawn in middle). Dotted line represents approximate hetero-euchromatic boundary. Image, variance map, and quantified variance of **d.** HP4 in S2 cells, **e.** HP5 in S2 cells, **f.** HP1□ in mammalian NIH3T3 cells, and **g.** HP1c in S2 cells. **h.** Diffusion rate (*D*) for fibrillarin across the nucleoplasm-nucleolus boundary (left), and HP4 (middle) and HP5 (right) across the euchromatin-heterochromatin boundary. For **c-h**, N=25 nuclei, error bars are SD. **i.** Representative image, variance map, and quantified variance across boundary for HP4 in control cells (bw RNAi, top), HP1a-depleted cells (HP1a RNAi, middle), and HP1a-depleted and rescued cells (HP1a RNAi + mCherry-HP1a, bottom). N=25 nuclei per condition, error bars are SD. **j.** Predictions of inert probe variance and diffusion near 'H2A edges,' which have a >2 fold increase in H2A density (purple bar) with <1.25 fold change in HP1a density (green bar), and 'HP1a edges,' which have >3 fold increase in HP1a density (green bar) with <1.25 fold change in H2A density (purple bar). The Chromatin Compaction model (left) predicts that inert probe variance and diffusion rate would be influenced by increasing H2A density, but unaffected by HP1a density. The Phase Separation model (right) predicts that inert probe variance and diffusion rate would be influenced by HP1a density, but unaffected by H2A density. **k.** Summary of RICS and N&B data. Heterochromatin proteins can move freely in the heterochromatin domain **(i)** but are hindered near the hetero-euchromatic border **(ii)**. Similarly, euchromatic proteins move freely in euchromatin **(iii)** but are hindered near the border **(iv)**, mostly preventing their entry. Euchromatic proteins that do enter heterochromatin move more slowly due to energetically costly interactions with surrounding phase particles **(v)** or crowded environments **(vi)**. **l.** Model of liquid properties influencing heterochromatic domain formation. We speculate that nucleation of heterochromatic (HP1) foci could occur independently of chromatin and H3K9me2/3, then associate with the chromatin fiber (top, left), or accumulation could require H3K9me2/3 for nucleation (top, right). Heterochromatin could spread along the chromatin fiber by liquid wetting of HP1, followed by methylation (HP1 first), or by previously proposed mechanisms involving *cis*-extension of H3K9 methylation, followed by HP1 binding (H3K9me2/3 first). Noncontiguous segments of chromatin (on the same or different chromosomes) can coalesce into one 3D domain, due to liquid-like fusion events between H3K9me2/3:HP1 enriched regions.

Based on the combination of *in vivo* and *in vitro* data presented here, we propose a model where heterochromatin domain formation and behaviors are driven by liquid phase separation, which holistically links emergent properties of the domain to local molecular interactions (Fig. 3h). Some findings, such as the presence of both immobile and mobile HP1 in the domain, are also consistent with canonical HP1:H3K9me2/3 binding models for heterochromatin formation (Elgin & Reuter, 2013). However, binding is not inconsistent with phase separation, and the liquid behaviors, dependence on weak hydrophobic interactions, and protein dynamics, strongly favor the conclusion that heterochromatin domains form via phase separation. We propose that multivalent, weak hydrophobic interactions between HP1 and other heterochromatin components drives initial nucleation and growth of heterochromatic foci. Loss of circularity of HP1a foci coincides with an increase in immobile, chromatin-bound, HP1, resulting in mature domains consisting of both liquid and stable compartments. We propose that the loss of circularity in mature heterochromatin domains is due to inclusion of the DNA/nucleosome polymer (Iborra, 2007), whereas previous examples of phase separated systems have been comprised of smaller independent particles that are able to freely intermix (Brangwynne, Mitchison, & Hyman, 2011; Hyman et al., 2014; P. Li et al., 2012; Zhu & Brangwynne, 2015); however, preferential interactions with nuclear structures could also generate non-spherical domains.

The phase separation model is also attractive because it can account for unusual heterochromatin behaviors described in the literature, and generates alternative,

testable hypotheses about regulation of heterochromatin functions. For example, associations between distal heterochromatic islands and the main domain(Dernburg et al., 1996) is easily accommodated by liquid fusion events that loop the intervening DNA (Extended Data Fig. 3l). Additionally, the phase separation model explains sensitivity of Position Effect Variegation to temperature and heterochromatin protein dosage. The inherent demixing ability of HP1 leads us to speculate that nucleation of HP1-rich domains *in vivo* could occur independent of chromatin and H3K9me2/3, instead of dependent on the methylation mark (Extended Data Fig. 3l). HP1-mediated recruitment of H3K9 methyltransferases that modify adjacent nucleosomes is routinely invoked to explain stochastic *cis*-spreading of heterochromatin and gene silencing(Elgin & Reuter, 2013); however, it is also possible that adjacent sequences (in *cis* or *trans*) are first engulfed by liquid HP1, followed by HMTase recruitment and H3K9 methylation (Extended Data Fig. 3l). Finally, selective permeability imparted by a phase boundary (Extended Data Fig. 3k) provides an alternative mechanism to chromatin compaction for regulating fundamental heterochromatic functions like transcriptional silencing, replication(Taddei, Roche, Sibarita, Turner, & Almouzni, 1999) and prevention of aberrant DNA damage repair (Chiolo et al., 2011; Peng & Karpen, 2008). We speculate that access to the domain could be regulated by binding a transport protein, similar to nuclear pores and importins (Ribbeck & Görlich, 2002), or through post-translational modifications. Alternatively, specific DNA sequences could be moved in and out of the phase, as seen for double-strand breaks in heterochromatin (Chiolo et al., 2011).

More investigations are needed to elucidate how emergent properties of phase separated systems impact genome functions, and in particular to identify the sequence and protein features that regulate inclusion or exclusion from the heterochromatic domain. It has been suggested that phase separation is a general organizing principle in cells, so it will be important to determine if other chromatin domains also form and function via phase separation principles. In sum, these results have led us to a fundamentally different perspective on heterochromatin formation, providing new opportunities for understanding how architectural and biophysical properties influence chromatin domain formation and overall genome function.

Methods

Drosophila embryo imaging. Female *Drosophila* homozygous for GFP-HP1a and RFP-H2Av were crossed to *yw* males and embryos were collected for 2 hours, dechorionated, and imaged every 2 minutes at 60X magnification on a DeltaVision microscope. Images were deconvolved using softWoRx conservative deconvolution, 5 iterations. Quantification of foci number and circularity were performed with FIJI (Schindelin, J., Arganda-Carreras, I., Frise, E., Kaynig, V., Longair, M., Pietzsch, T., et al. (2012). Fiji: an open-source platform for biological-image analysis. *Nature Methods*, *9*(7), 676–682. http://doi.org/10.1038/nmeth.2019). Nuclei were identified after smoothing and 12 pixel rolling ball background subtraction by >85% fluorescence intensity thresholding and size > 2 μm^2. HP1a foci were identified after smoothing and 5 pixel rolling ball background subtraction with HP1a threshold > 95% fluorescence intensity and size > 0.1 μm^2. Foci size, number and circularity measured using the

Analyze Particles function in FIJI. Quantifications result from movies of >75 nuclei each in N = 12 embryos.

Lattice Light Sheet Microscopy (LLSM) was performed on a home-built implementation of the instrument as previously described(B.-C. Chen et al., 2014a). A 30 beam square lattice light sheet, with inner and outer numerical apertures of 0.505 and 0.60 respectively, was generated with a 488 nm input laser and dithered in x over a 5 μm range during each exposure to create a uniform excitation sheet. Z-stacks were collected by synchronously scanning the excitation sheet and detection objective over a 25 μm range in 250 nm steps. The exposure time for each slice in the stack was 10 ms, and the time interval between stacks was 2.025 seconds. The laser power was measured to be ~700 μW at the back aperture. Data was rendered and analyzed using Amira (FEI).

Fluorescence Recovery After Photobleaching (FRAP). Embryos (prepared as above) were imaged every 2 seconds for 30 frames at 100X on a DeltaVision microscope. Three images were pre-bleach, and on the fourth approximately 3 μm^2 was bleached with the 488 nm laser of the Quantifiable Laser Module (QLM). FRAP in S2 cells was performed on selected regions of interest ($2\mu m^2$) using a spinning disk confocal (3i) with 100% power and recovery observed at 2% power, 0.5 second intervals for 30 seconds. Recovery was measured as fluorescence intensity of photobleached area normalized to the intensity of the unbleached heterochromatic area.

Hexanediol treatments. Cultured *Drosophila* S2 cells in Schneiders Medium (Sigma-Aldrich S0146) stably expressing GFP-tagged $HP1a^{WT}$, $HP1a^{I191E}$, or $HP1a^{W200A}$ (in addition to endogenous untagged HP1a) were visualized on a DeltaVision microscope every 5 seconds for 10 minutes. At approximately 2 minutes, normal media was removed and Schneiders Medium containing 10% 1,6-hexanediol (Sigma-Aldrich 240117-50G) by weight was added. After 2 minutes more, media containing hexanediol was removed and replaced with normal Schneiders Medium and recovery was observed for 6 minutes. Image analysis was performed with FIJI. Nuclei were identified after smoothing and 12-pixel rolling ball background subtraction with a >85% H3 fluorescence intensity threshold. This nuclear area was used to calculate nuclear size. The heterochromatin region was identified after smoothing and 3-pixel rolling ball background subtraction with a threshold of >97.5% HP1a fluorescence intensity. Heterochromatic enrichment was calculated by dividing average intensity of the heterochromatic domain in one nucleus by the average intensity of an equally sized region elsewhere in the same nucleus.

Number and Brightness (N&B) and Raster Image Correlation Spectroscopy (RICS). Twenty-five consecutive 256 x 256 pixel images were collected at 16 bit depth with pixel dwell time 6.3 μs and 1 AU using a 63X objective with 10X zoom on a Zeiss LSM710 Confocal. Images were analyzed using SimFCS (Digman et al., 2008; Digman, Wiseman, Horwitz, & Gratton, 2009; Rossow et al., 2010). Variance was quantified by measuring individual pixel variance values across a line crossing the domain edge, from

outside to inside the domain. At least 10 lines per nucleus were measured, and values from 25 nuclei averaged. Center is mean and error bars are standard deviation.

Inert probe properties. Cultured *Drosophila* S2 cells were transiently transfected with CFP-HP1a, mCherry-H2A and YFP-YFP-YFP-NLS, each expressed from a Copia promoter. Nuclei were imaged after three days; twenty-five consecutive 256 x 256 pixel images were collected at 16 bit depth with pixel dwell time 3.1 μs and 1 AU, using a 63X objective with 10X zoom on a Zeiss LSM710 Confocal. To calculate average diffusion rate, scan analysis was performed with a 32 x 32 pixel ROI in simFCS at edges of HP1a domains with minimal H2A change (> 3 fold intensity increase in HP1a, <1.25 fold intensity increase in H2A), and at edges of H2A-dense domains with minimal HP1a change (> 2 fold intensity increase in H2A, <1.25 fold intensity increase in HP1a).

In vitro droplet assays. Recombinant *Drosophila* FLAG-6xHis-HP1a was expressed in *E. coli* and purified in three steps by Ni-NTA and anion exchange chromatography (Source 15Q). The purified protein was also subjected to ultracentrifugation (2 h at 260,000 *g*) to remove insoluble aggregates. Protein was stored in 25 mM HEPES, pH 7.6, 200 mM NaCl, 0.1 mM EDTA, 10% glycerol, 0.01% NP-40, 1 mM DTT, 0.2 mM PMSF, 0.5 mM benzamidine. Protein was added to 5 μL salt buffer (50 mM HEPES, 5 mM DTT, 25-150 mM NaCl) at 0.05, 0.1, 0.25 and 0.5 mg/mL in 20 μL PCR tubes, then 1 mL was trapped between two coverslips and imaged with DIC at 63X on a Zeiss LSM710 confocal. Images were quantified using FIJI. After smoothing and 5-pixel rolling ball background subtraction, droplets were identified with threshold >99.5% intensity and size > 0.1 μm^2. Aspect ratio calculated for N = 3 experiments, each with > 300 droplets. Area probability was calculated from movies taken during droplet formation, where coverslips containing 0.5 mg/mL HP1a in 50 mM NaCl buffer were incubated at 37°C for 5 minutes, then returned to 22°C. Images were taken every 10 seconds for 8 minutes to visualize droplet formation. Number and area of droplets calculated using FIJI with same specifications as above.

Glycerol gradient sedimentation. Samples of purified recombinant HP1a (2.5 mg/ml) were incubated for 1 h at 4°C in buffers containing 50 or 500 mM NaCl and subjected to ultracentrifugation (Beckman SW-41Ti, 41,000 rpm, 287,000 *g*, 18 h at 4°C) on linear 10-45% gradients of glycerol in 10 mM HEPES, 1 mM EDTA, 0.01% NP-40, 1 mM DTT, 0.2 mM PMSF, 0.5 mM benzamidine and 50 or 500 mM NaCl. The gradients were cut into 12 fractions and analyzed by SDS-PAGE and Coomassie staining.

RNAi experiments. dsRNA targeting the *brown* gene sequence or the UTR-exon1 junction of HP1a were made from S2 genomic DNA using a MegaScript T7 Transcription Kit. dsRNA was applied to culture medium on day 1, then on day 2 cells were transfected using Mirus Trans-IT 20-20 with GFP-HP4 alone or with an RNAi-resistant mCherry-HP1a. Cells were imaged on day 5 and collected for knockdown validation by western blot.

Data Availability Statement

The data that support the findings of this study are available from the corresponding author upon request.

Author Contributions

A.R.S. and G.H.K. conceived of experiments. A.R.S. performed *Drosophila*, cell culture, imaging, FRAP, hexanediol, and droplet-formation experiments and analysis. M.M. and X.D. performed and analyzed the lattice light sheet microscopy. A.V.E. and D.V.F. contributed purified HP1a, and performed glycerol gradient experiments. A.R.S. and G.H.K. wrote the manuscript, and all authors contributed ideas and reviewed the manuscript.

Acknowledgements

Funding was provided by National Institute of Health grants R01 GM117420 (GK), and U54-DK107980 and U01-EB021236 (XD), and the California Institute for Regenerative Medicine (CIRM, LA1-08013, XD). We thank Abby Dernburg for use of the spinning disk confocal, Michelle Scott for maintenance of the rastering confocal, Serafin Colmenares for cell lines, Claire Robertson for introduction to RICS and N&B, Astou Tangara for help in assembling and maintaining the LLSM, and Abby Dernburg, Sam Safran and the Karpen lab for helpful comments on the manuscript.

Chapter 3

Shelob Regulates Biophysical Properties and Functions of Heterochromatin

Authors: Amy R. Strom*[1,2], Joel M. Swenson*[1], Serafin U. Colmenares[1], Wilbur K. Mills[1,2], Ryan S. Chung[2], Sylvain V. Costes[1] and Gary H. Karpen[1,2,^]
[1]Division of Biological Systems and Engineering, Lawrence Berkeley National Laboratory, Berkeley, CA 94720, USA
[2]Department of Molecular and Cell Biology, University of California, Berkeley, Berkeley, CA 94720, USA
*Equal contribution
^Correspondence: ghkarpen@lbl.gov (G.H.K.)

Abstract
Constitutive heterochromatin is enriched for repetitive DNAs and specific epigenetic factors and is essential for viability, genome stability, and nuclear architecture. From both genome-wide RNAi and biochemical screens, we previously identified *Drosophila* CG8108, here named Shelob (Seo), as both a component and regulator of heterochromatin. Here we show that *Drosophila* Shelob interacts with Heterochromatin Protein 1a (HP1a), and cytological and genomic analyses demonstrate its localization to the heterochromatin domain. We also show that Shelob is required for organismal viability and heterochromatin functions, including gene silencing, relocalization of heterochromatic repair foci, and organization of repetitive DNAs. Interestingly, increased or decreased Shelob levels alter the biophysical properties of heterochromatic HP1a, including mobility, sensitivity to 1,6-hexanediol, and diffusion rates. Mutant studies revealed that an intrinsically disordered region in Shelob is necessary to alter HP1a's biophysical properties. We conclude that Shelob is an essential protein that regulates the biophysical properties and functions of heterochromatin.

Introduction

The heterochromatin regions of the genome are enriched for simple repetitive DNA sequences (Peacock et al., 1978) and transposons (Carlson & Brutlag, 1978), in contrast to euchromatin, which is predominantly composed of single copy sequences and most of the protein coding genes. Despite being relatively gene-poor, heterochromatin is required for many functions (Bernard et al., 2001; Karpen, Le, & Le, 1996; McKee & Karpen, 1990) including genome integrity (Peng & Karpen, 2009). The defining heterochromatic epigenetic marks are di- and tri-methylation of histone H3 Lys9 (H3K9me2 and me3), hypo-acetylation of histones, and the presence of heterochromatin protein 1a (HP1a). *Drosophila* HP1a-enriched heterochromatin is concentrated in pericentromeric and telomeric regions on all chromosomes, yet these distinct linear chromatin regions usually coalesce into a single heterochromatin domain that is DNA-dense and stains brightly with DAPI (Grewal & Jia, 2007; Kellum, Raff, & Alberts, 1995). Recently, this domain was shown to be formed via phase separation(Strom et al., 2017) (A. G. Larson et al., 2017), similar to other membraneless domains like the nucleolus.

Known examples of phase separation in biological systems are mediated by intrinsically disordered domains and high miultivalency (Hyman et al., 2014). These mediate multiple, weak interactions between molecules that result in liquid-like domains that have both high concentration and high mobility of components. Domains formed by these types of interactions are generally sensitive to addition of the small aliphatic alchohol 1,6-hexanediol, which specifically disrupts the weak hydrophobic interactions and results in dispersion of components (Ribbeck & Görlich, 2002) .

HP1 has orthologs in many eukaryotes including *D. melanogaster* (HP1a), *S. pombe* (Swi6), *A. thaliana* (LHP1), *C. elegans* (HPL) and *H. sapiens* (*CBX1*, *CBX3*, *CBX5*. HP1 proteins possess a chromodomain for binding H3K9me2/3 (Bannister et al., 2001; Lachner, O'Carroll, Rea, Mechtler, & Jenuwein, 2001), a flexible hinge domain that binds RNA/DNA (Maison et al., 2011; Zhao, Heyduk, Allis, & Eissenberg, 2000), and a chromoshadow domain that facilitates protein-protein interactions (Smothers & Henikoff, 2000) and homodimerization (Cowieson et al., 2000). HP1a tethering to a site is sufficient to cause heterochromatinization and silencing (Y. Li, Danzer, Alvarez, Belmont, & Wallrath, 2003), and mutations that abolish HP1a homodimerization, H3K9me/3 binding or interaction with PxVxL motifs lead to a loss of silencing (Hines et al., 2009). Additionally, these proteins exhibit diverse biochemical/biophysical properties *in vivo*. Fluorescence correlation spectroscopy (FCS) and fluorescence recovery after photobleaching (FRAP) identified at least three different dynamic populations of HP1—highly mobile, intermediately mobile and highly stable (Müller et al., 2009). Salt fractionation experiments (Kellum et al., 1995) and size exclusion chromatography (Rosnoblet, Vandamme, Völkel, & Angrand, 2011) also suggest the existence of distinct populations of HP1. Therefore, binding and movement of HP1a may be important for its transcriptional silencing and other functions.

Immuno-precipitation mass spectrometry (IP-MS) studies of HP1a or its orthologs have identified >200 putative HP1 interacting proteins (HPips) (Alekseyenko et al., 2014; Lechner, Schultz, Negorev, Maul, & Rauscher, 2005; Motamedi et al., 2008; Rosnoblet et al., 2011; Ryu et al., 2014; Swenson, Colmenares, Strom, Costes, & Karpen, 2016). Identified HPips play roles in diverse pathways including DNA

replication, transcription elongation, transcription silencing and chromatin remodeling. However, more in-depth molecular studies of identified proteins are required to generate a true understanding of how heterochromatin formation and function are regulated *in vivo*, and if they impact function by regulating LLPS.

We, and others, have previously identified a protein encoded by *CG8108* as a HPip (Alekseyenko et al., 2014; Guruharsha et al., 2011; Swenson et al., 2016). Surprisingly, CG8108 depletion led to increased HP1a fluorescence intensity in a genome-wide RNAi screen (Swenson et al., 2016). Additionally, GFP-tagged CG8108 was found to significantly colocalize with HP1a in a low-resolution imaging screen (Swenson et al., 2016). Here we analyze the localization and functions of CG8108, and demonstrate that it is a heterochromatic protein required for organismal viability and several heterochromatin functions, specifically the DNA damage response, transcriptional silencing, and repeat organization. We further show that CG8108 is a negative regulator of HP1a solubility and diffusion. Overall, we conclude that CG8108 is an essential protein that regulates the biophysical properties and functions of heterochromatin. Based on the results presented here we propose renaming *CG8108* to *Shelob* (*Seo*).

Results

CG8108 interacts with HP1a and localizes to heterochromatin

Shelob is expressed from a gene region on *Drosophila* chromosome 3 in two splice isoforms that differ only in their 3' UTR (Extended Data Figure 1a). The *Shelob* protein contains two C2H2 zinc finger domains and a C2H2-type zinc finger matrin domain (Figure 1a, top). C2H2 zinc fingers have been shown to bind DNA (Wolfe, Nekludova, & Pabo, 2000), RNA (Hall, 2005), and protein (Brayer and Segal, 2008). Much of the rest of the 949aa Shelob protein is predicted to be highly disordered, with PONDR (Xue, Dunbrack, Williams, Dunker, & Uversky, 2010) scores above 0.5, as well as many low-complexity sequences predicted by SEG (Wootton, 1994)(Figure 1a, bottom). Low amino acid sequence complexity and intrinsically disordered regions are associated weak hydrophobic interactions that can contribute to liquid-liquid phase separation. To facilitate investigations into Shelob functions we raised an antibody against amino acids 730-880 present in all Shelob splice isoforms (Figure 1a, top).

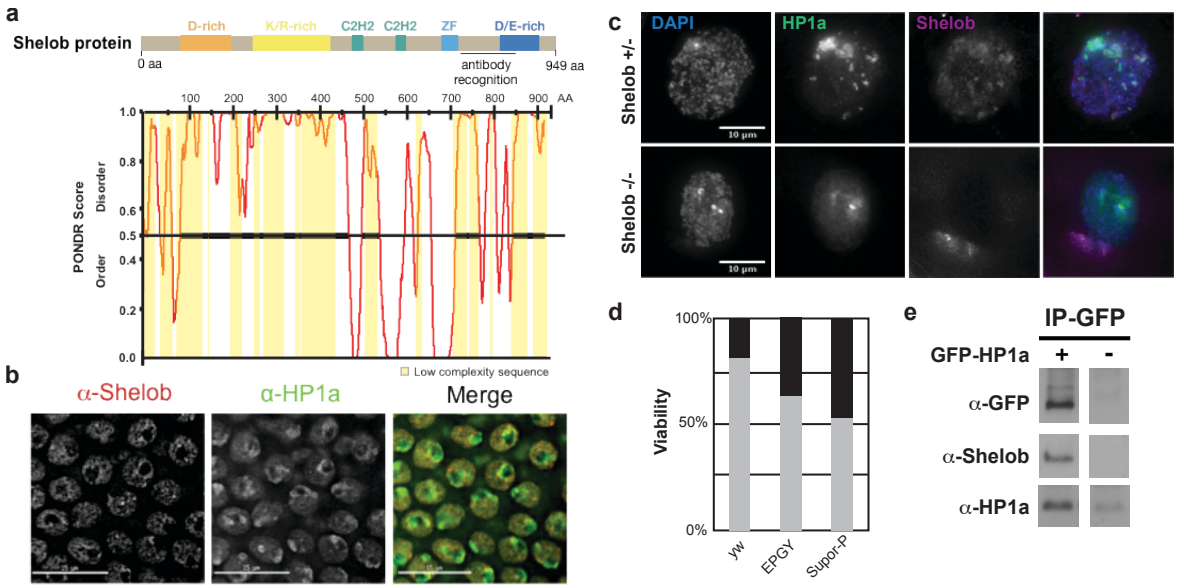

Figure 1: Shelob is an essential gene that localizes to heterochromatin and interacts with HP1a
a. Shelob protein domain diagram and PONDR disorder prediction, where 0.5 and above is considered disordered. Three zinc finger domains are ordered and much of the rest of the protein is highly disordered. Antibody was raised against amino acids 720 – 850. **b.** Third instar eye discs stained with antibodies recognizing Shelob and HP1a reveal extensive co-localization. **c.** Immunofluorescence images of polytene salivary gland nuclei from heterozygous and homozygous mutants of Shelob are stained for Shelob and HP1a. **d.** Viability assays for control embryos and embryos heteroozygous for two different P element insertions that disrupt expression of Shelob. **e.** Immunoprecipitation of GFP in S2 cells transiently transfected for GFP-HP1a (+) or untransfected control (-). Eluate from immunoprecipitations was blotted with antibodies recognizing GFP, Shelob, and HP1a.

To validate that the antibody recognizes Shelob, we analyzed Shelob null mutations caused by P element insertions (*P{SUPor-P}CG8108*^{KG0545} , in the 5' untranslated region, and *P{EPgy2}CG8108*^{EY14316} in the first exon, Extended Data Figure 1a), and observed that a band at 150 kDa is reduced in homozygous mutant embryos (Extended Data Figure 1b). Additionally, we depleted Shelob from S2 cultured cells by RNAi and observed 35-45% protein reduction via western blot (Extended Data Figure 1c). We conclude that the antibody recognizes a 150 kDa product of the Shelob gene.

To visualize cytological localization of Shelob, we used our antibody to stain disc tissue from *Drosophila* larvae, and observed that the protein is nuclear, is excluded from the nucleolus, and largely overlaps with HP1a (Figure 1b). The meshwork pattern, along with its role in silencing (see below), led us to name CG8108 after the fictional spider Shelob (Tolkien, 1954). Nuclear staining was completely abolished in *P{SUPor-P}CG8108*^{KG05452} homozygous 3rd instar wing discs and salivary glands, and nuclear localization of HP1a is disrupted in tissues lacking Shelob (Figure 1c, Extended Data Figure 1d).

Interestingly, neither *P{Epgy2}CG8108*^{EY14316} nor *P{SUPor-P}CG8108*^{KG054522} homozygous mutants developed into adults, demonstrating that Shelob is required for

viability. The hatch rates of *P{EPgy2}CG8108^{EY14316}/TM6* progeny (53%) and *P{SUPor-P}CG8108^{KG05452}/TM6* progeny (64%) were lower than controls (81%) (Figure 1d), indicating that Shelob mutants die during embryogenesis. Some *P{SUPor-P}CG8108^{KG05452}* homozygotes hatch but die during larval and pupal stages.

It could be that Shelob is essential because it regulates its binding partner HP1a, which is also required for viability. To validate our previous finding that Shelob interacts with HP1a (Swenson et al., 2016) we immuno-purified either GFP-tagged HP1a or endogenous Shelob from S2 cells and probed for co-purifying Shelob or HP1a, respectively. The reciprocal IPs confirmed a physical interaction between Shelob and HP1a (Figure 1e, Extended Data Figure 1e).

We also expressed a GFP-tagged *Shelob* under a *Copia* promoter in live S2 cells to visualize colocalization with HP1a. GFP-Shelob signal somewhat overlaps HP1a, but also exists in enriched areas throughout the rest of the nucleus. HP1a-Shelob colocalization is highest during a 1-hour period during interphase, suggesting Shelob localization is regulated by the cell cycle.

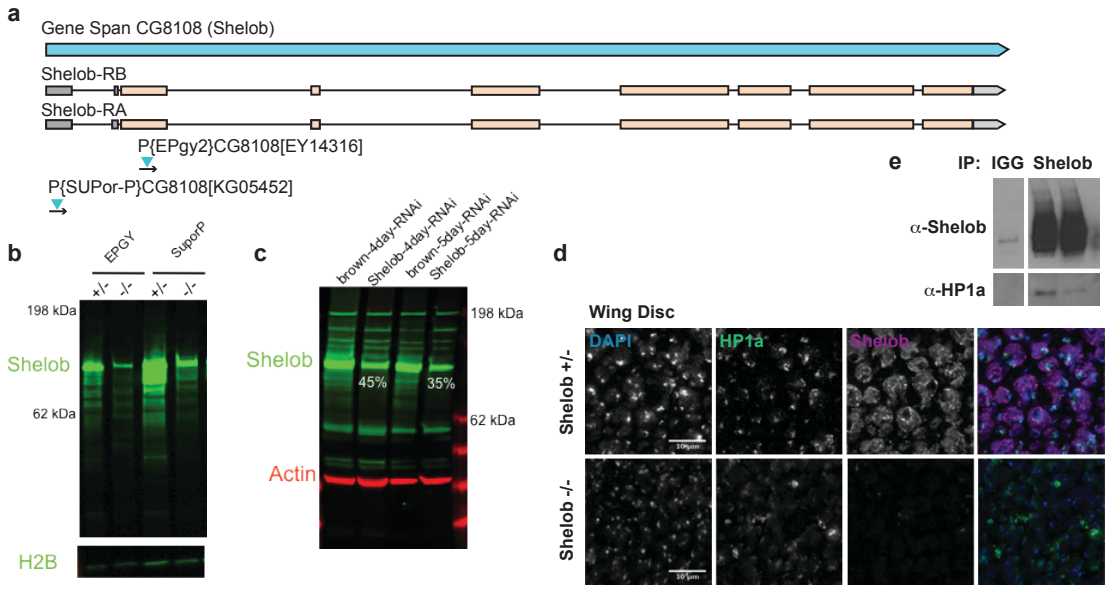

Extended Data Figure 1: Shelob is an essential gene that localizes to heterochromatin and interacts with HP1a

a. Diagram of CG8108 (Shelob) gene span, transcripts, and P-element insertions. **b.** Western blot of extracts from larvae heterozygous or homozygous for mutations in Shelob, H2B as loading control. **c.** Western blot of cell extracts from S2 cultured cells depleted for a control gene (brown) or Shelob for four or five days. **d.** Immunostaining of wing discs from stage-matched 3rd instar larvae heterozygous or homozygous for EPGY Shelob mutation. Scale bars 10 microns. **e.** Immunoprecipitation of control IGG or Shelob from S2 cell extracts. Eluates probed for Shelob and HP1a. Two biological replicates shown.

Shelob mainly binds heterochromatic sequences

To investigate the genomic localization of Shelob and to compare it to HP1a, we performed ChIP-seq in biological duplicate. Consistent with the IF studies, Shelob is distributed throughout the genome, but is densest within heterochromatin (Extended Data Figure 2a). Additionally, Shelob ChIP-seq peaks were enriched for modENCODE

(Kharchenko et al., 2011) chromatin states associated with transcriptional silencing, including those enriched for the repressive Polycomb complex (state 6), canonical heterochromatin marks and proteins (e.g. H3K9me2/3, HP1a, Su(var)3-9, state 7) and another largely devoid of chromatin marks and genes (state 9). Finally, as expected for a heterochromatin protein, Shelob binds repetitive elements; ~50% of all reads map to more than one location in the genome, and ~15% align to repetitive elements identified in Repbase (Jurka, 2000). Shelob binding is particularly enriched for tandem repeats, including the simple repeat AATAT (average fold enrichment [FE] of 109 over input, Extended Data Figure 2b). Based on the biochemical interaction and cytological co-localization between Shelob and HP1a, as well as the Shelob ChIP-seq data, we conclude that Shelob is present in many nuclear locations, but is significantly enriched in heterochromatin.

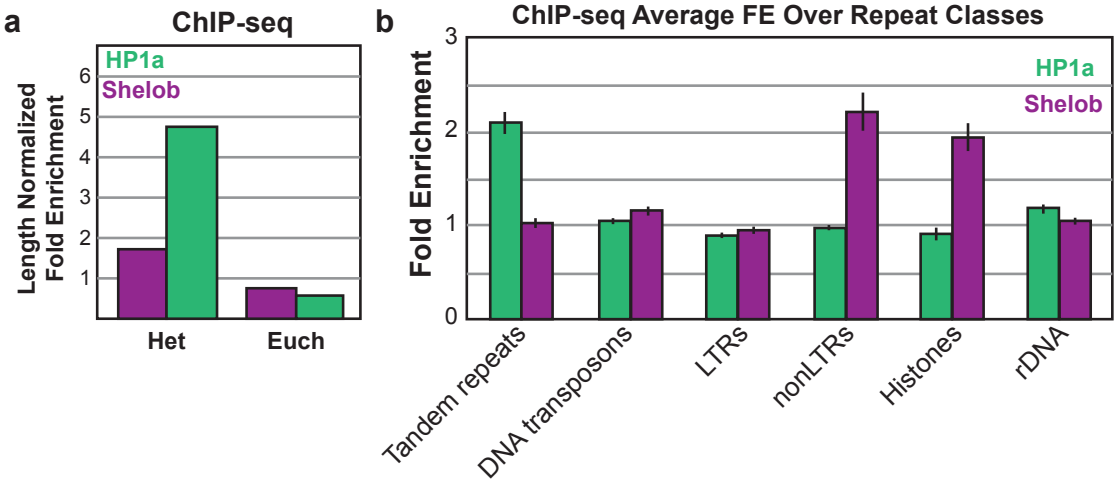

Extended Data Figure 2: Shelob genomically binds heterochromatic sequences
a. ChIP-seq of Shelob and HP1a from S2 cells shows Shelob binds to heterochromatic sequences (Het) more than euchromatic sequences (Euch). These sequences tend to have high enrichment of HP1a. **b.** Breakdown of heterochromatic sequences shows that Shelob preferentially binds nonLTR repeats and histones, while HP1a preferentially binds tandem repeat sequences.

Shelob affects heterochromatic silencing without altering HP1a genomic localization or protein level

Because Shelob localizes to heterochromatin and interacts with HP1a, we tested whether loss of Shelob influences heterochromatin-mediated transcriptional silencing, known as Position Effect Variegation (PEV). *In(3L)BL1* is a chromosome with a large inversion, placing a heterochromatic region near an exogenous *lacZ* gene, which is stochastically silenced and displays a variegated pattern of LacZ expression in tissues (Lu, Bishop, & Eissenberg, 1996). To determine if the *P{EPgy2}CG8108*^{EY14316} allele modified *lacZ* PEV, we stained third-instar salivary glands of flies carrying *P{EPgy2}CG8108*^{EY14316} and compared LacZ (X-gal) staining patterns to flies with a mutation in a known Suppressor of variegation (*Su(var)3-7*^{14}) or wild type flies (Figure 2a, bottom). To quantify transcriptional silencing, we measured total β-galactosidase

activity in cohorts of 5 adult males (Figure 2a, top). *P{EPgy2}CG8108*^{EY14316} significantly suppressed LacZ PEV in both assays, demonstrating that Shelob is required for heterochromatin-induced silencing.

Considering that Shelob might play a role in heterochromatin structure, we investigated if Shelob is required for heterochromatic satellite DNA organization. We used our ChIP-seq data to identify four repetitive DNA elements (AATAT, undeca, AACAC, and 1.686) bound by Shelob (ChIP-seq FEs of 1.5, 2.5, 5, and 100 respectively). Fluorescence in situ hybridization (FISH) revealed an increased number of 1.686 foci in Shelob-depleted S2 cells compared GFP-depleted negative control, but no change in the number of AACAC, AATAT or undeca foci (Figure 2d, Extended Data Figure 3a-c), indicating that Shelob is necessary for the proper organization of the 1.686 repetitive element. Interestingly, Shelob and HP1a are both enriched at AACAC, AATAT and undeca loci in ChIP-seq results, whereas only Shelob is enriched at 1.686.

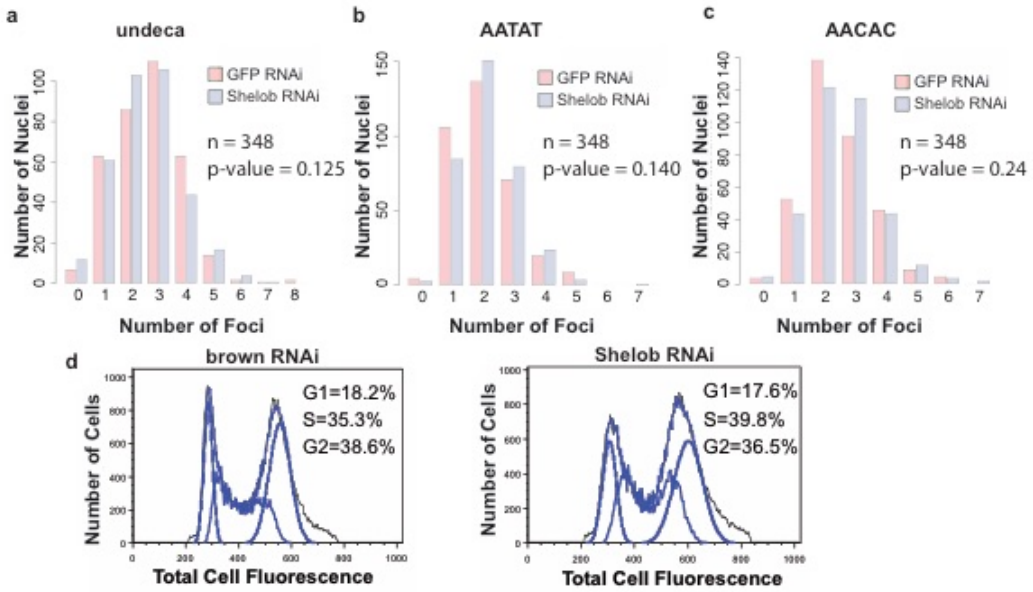

Extended Data Figure 3: Shelob depletion does not affect cell cycle progression or general repeat organization, but prevents DSB response in heterochromatin

a-c. Quantification of number of repetitive element FISH foci from S2 cells treated with RNAi to deplete GFP (control) or Shelob. **d.** Cell cycle analysis by FACS sorting DNA content of control cells and Shelob-depleted cells.

Shelob's role in PEV and direct binding to HP1a suggests that it might mediate other heterochromatin functions. Double-strand breaks (DSBs) in heterochromatic repeated sequences relocalize outside of the heterochromatin domain (Chiolo et al., 2011; Janssen et al., 2016) in order to complete repair. Depletion of HP1a or other heterochromatin proteins results in retention of DSBs in heterochromatin (Chiolo et al., 2011), as indicated by an elevated Pearson correlation coefficient (PCC) between DAPI and the repair foci marker phosphor-H2Av (γH2Av) at 60 minutes post-DSB induction (Figure 2d). S2 cells were treated for 5 days with dsRNA amplicons targeting either *Shelob* or *GFP* (control). *Shelob* depletion showed a significant increase in the PCC between γH2Av and DAPI, 60 minutes post-break induction (Figure 2d,e). We conclude that *Shelob* is required for efficient re-localization of DSBs from heterochromatin.

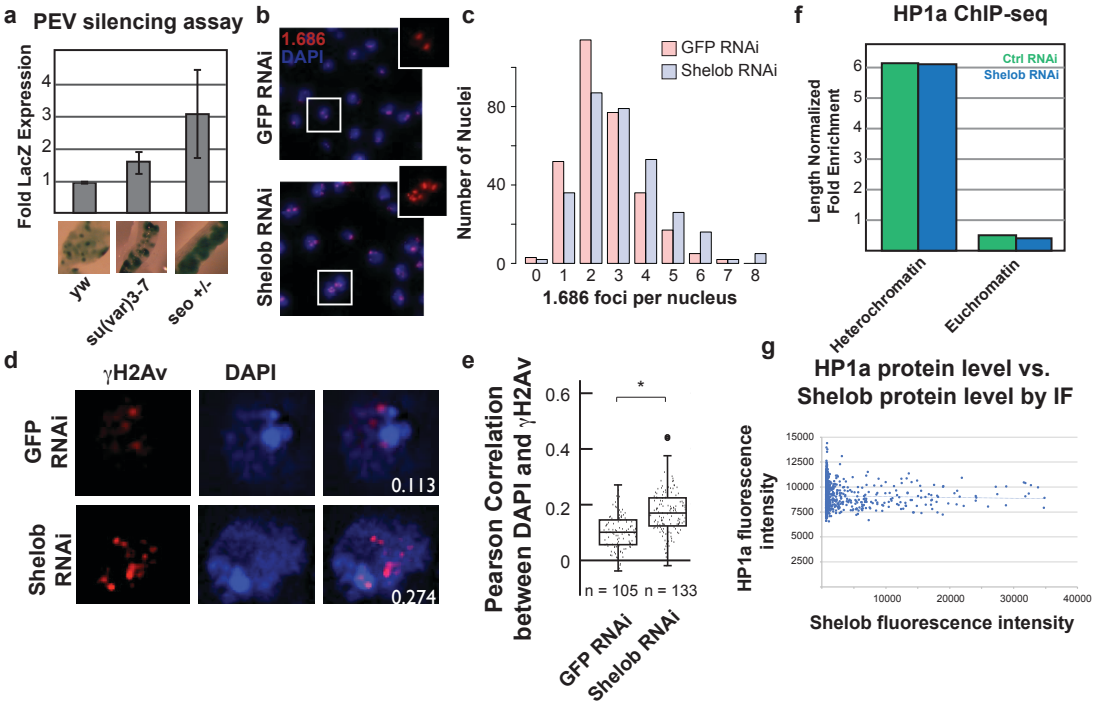

Figure 2: Shelob affects heterochromatic functions without altering HP1a genomic localization or protein level

a. Position effect variegation images (bottom) of 3rd instar larvae salivary glands from control (yw), known heterochromatic protein heterozygous mutant (su(var)3-7) and Shelob heterozygous mutant (seo+/-). Quantification (top) of variegation by Optical Density of enzymatic output from 3 larva of each genotype, error bars are standard deviation, N = 3. **b.** Images and **c.** quantification of FISH for the repetitive element 1.686 in S2 cells depleted for GFP or Shelob. N = 327 cells, p value = 0.027. **d.** Images and **e.** quantification of Pearson Correlation between DAPI and gH2Av in S2 cells treated with 5 Gray irradiation. Bright DAPI staining is AT-rich repetitive heterochromatic sequences and gH2Av is marker of double strand breaks. Higher correlation indicates failure to relocalize breaks outside of heterochromatin. **f.** ChIP-seq of HP1a from S2 cells depleted for control gene (GFP) or Shelob. Shown is fold enrichment of HP1a reads in unique heterochromatic or euchromatic areas of the *Drosophila* genome. **g.** Assay for protein level of HP1a and Shelob by immunofluorescence in S2 cells transiently transfected for a Shelob overexpression construct. Trendline shown, N = 1136 nuclei, $R^2 = 0.05$.

Because loss of Shelob changes the cytological distribution of HP1a in nuclei from larval tissues, we investigated HP1a's genomic distribution by ChIP-seq after Shelob depletion by RNAi, compared to control (GFP depletion). Using a sliding window analysis of HP1a ChIP-seq reads, we observe that in *Shelob*-depleted cells, HP1a's genomic distribution remains largely unchanged (Figure 2f). We observe that Shelob depletion results in some differences in HP1a localization to repetitive elements compared to control depletions, but the effects are overall minor. We conclude that Shelob does not largely affect which DNA sequences are bound by HP1a but could alter HP1a protein level or nuclear organization and positioning of the sequences within the nucleus.

Shelob's influence on heterochromatin silencing could additionally be due to altered protein levels of HP1a. To test whether overexpression of Shelob changes HP1a protein level, we overexpressed Shelob in S2 cells and measured Shelob and HP1a protein levels on a cell-by-cell basis with immunofluorescence. We find that there is no correlation between Shelob level and HP1a level, with R^2=0.05 (Figure 2g).

Shelob alters HP1a's mobile population

Phase separation is responsible for large-scale organization of the heterochromatin domain, including the ability of heterochromatic sequences from multiple chromosomes to organize into a single domain(Strom et al., 2017). Shelob knockdown does not change HP1a genomic localization, but does impair domain formation, indicating it could specifically impact HP1a's phase separation properties without changing its genomic interactions. To determine if Shelob protein level alters heterochromatic phase separation, we treated S2 cells overexpressing Shelob protein with 1,6-hexanediol. In a previous study, we showed that approximately 50% of the HP1a population is sensitive to 1,6-hexanediol in S2 cells, indicating that half of the HP1a is retained in the domain through weak hydrophobic interactions. Here we imaged S2 cells expressing GFP-HP1a and mCherry-Shelob before, during, and after exposure to 1,6-hexanediol to visualize heterochromatic enrichment of HP1a. We observe that increased Shelob expression leads to less HP1a hexanediol sensitivity (Figure 3a,b).

Additionally, we have previously showed that the population of HP1a that is insensitive to hexanediol is correlated with the population determined to be immobile by FRAP (doesn't recover after 30 seconds) (Strom et al., 2017). We asked whether overexpressing Shelob and altering the population of HP1a that is sensitive to hexanediol also changes the % of HP1a that is immobile. In wild-type cells, HP1a has two populations; one 'mobile' population that recovers with $t_{1/2}$ ~ 15 seconds, and one 'immobile' population that does not recover by 30 seconds (Fig 3c,d). Shelob protein levels are highly correlated with HP1a immobile population (Fig 3e). Interestingly, Shelob overexpression does not alter mobility of other heterochromatin proteins HP4 and HP5 (Extended Data Figure 4). We conclude that the immobile population by FRAP is likely the same population that is insensitive to 1,6-hexanediol, and that Shelob protein level directly correlates with the proportion of immobile HP1a.

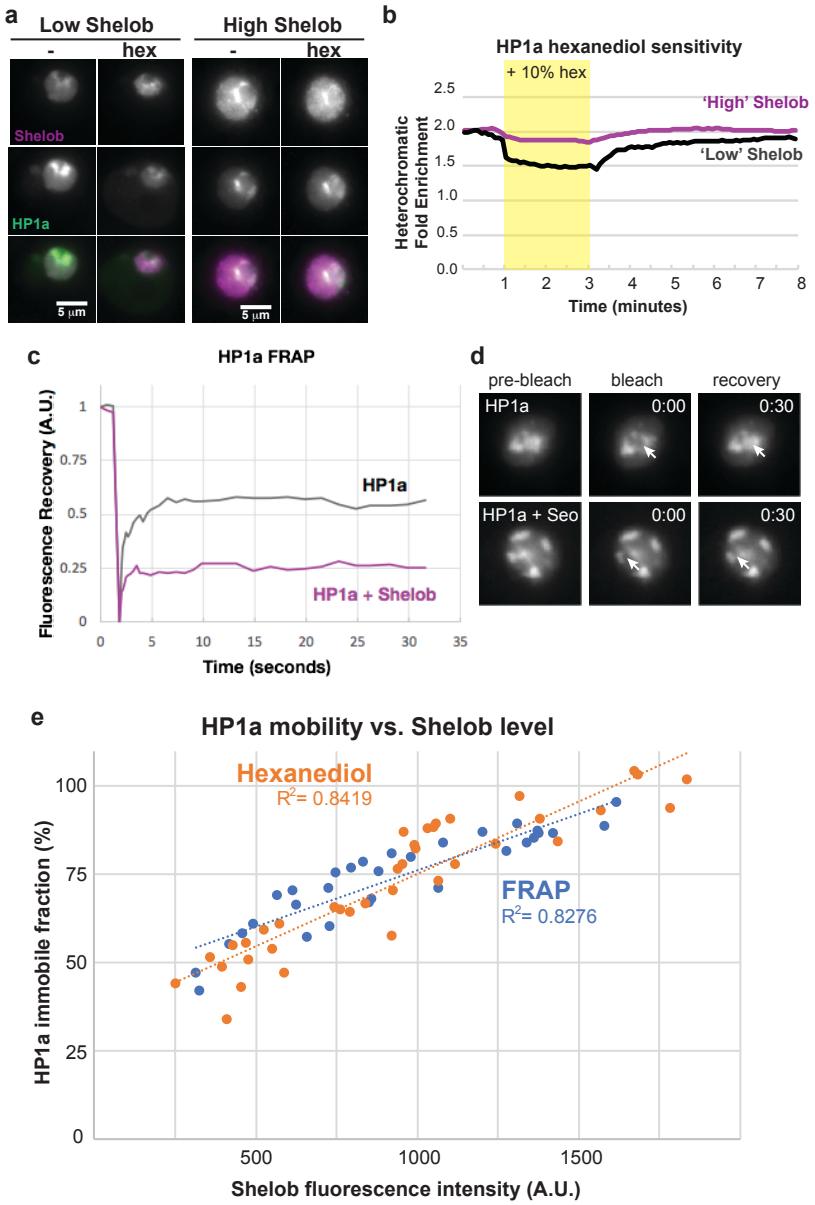

Figure 3: Shelob protein level indirectly correlates with HP1a mobility
a. Images of S2 cells transiently transfected with GFP-HP1a and mCherry-Shelob before and after exposure to media containing 10% 1,6-hexanediol (- and hex, respectively). Low Shelob expression is considered less than 600 A.U. fluorescence intensity, and High Shelob expression is greater than 1200 A.U. fluorescence intensity. **b.** Quantification in high and low Shelob-expressing cells of HP1a enrichment inside heterochromatin before (0-1 minute), during (1-3 minutes) and after (3-8 minutes) exposure to media containing 10% hexanediol. One representative nucleus of each is shown. **c.** Fluorescence Recovery after Photobleaching of HP1a in cells transiently transfected with either GFP-HP1a alone, or GFP-HP1a and mCherry-Shelob. **d.** Fluorescence images of nuclei quantified in c. **e.** Correlation between Shelob fluorescence intensity and HP1a immobile fraction as measured by FRAP (% of HP1a not recovered after 30 seconds) or 1,6-Hexanediol exposure (% of HP1a population not dispersed by 1,6-hexanediol treatment).

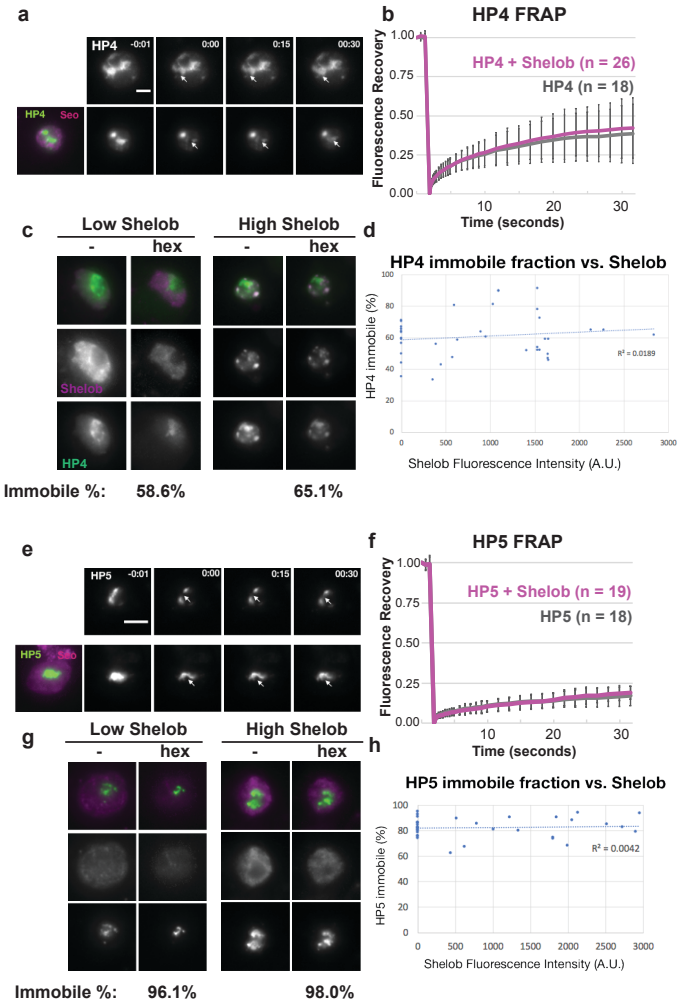

Extended Data Figure 4: Shelob overexpression does not alter HP4 and HP5 mobility
a. FRAP images and **b.** quantification of S2 cells expressing either GFP-HP4 alone or with mCherry-Shelob. **c.** Images and quantification of HP4 hexanediol treatment in low and high Shelob overexpression. **d.** Correlation between Shelob expression level and HP4 mobility is minimal (R^2 = 0.0189). **e.** FRAP images and **f.** quantification of S2 cells expressing either GFP-HP5 alone or with mCherry-Shelob. **c.** Images and quantification of HP5 hexanediol treatment in low and high Shelob overexpression. **d.** Correlation between Shelob expression level and HP5 mobility is minimal (R^2 = 0.0042).

Disordered regions of Shelob are important for its influence on HP1a

To determine which areas of the Shelob protein are important for HP1a regulation, we made three point mutants that prevent function of each of the three zinc finger domains; C550A, C692A, and C721A, and four mutants that express only a portion of the protein; amino acids 1-250, 251-497, 498-730, or 731-949 (Figure 4a, left). Cysteine to alanine point mutations within a zinc finger domain abolish binding to nucleic acid substrates (Bombarda, Cherradi, Morellet, Roques, & Mély, 2002). The 498-730 fragment contains all three zinc finger domains, while 1-250, 251-497 and 731-949 contain no folded domains, but encode highly disordered regions rich in Aspartic acid, arginine and lysine, or aspartate and glutamate, respectively. Each of these constructs was tagged with mCherry and transiently transfected alongside GFP-HP1a into S2 cells.

First, localization of each protein was observed. In wild type cells, HP1a forms a single enriched heterochromatin domain that is usually centrally located in the nucleus, adjacent to the nucleolus. In cells also expressing high levels of full length wild type Shelob, HP1a becomes mislocalized to a larger area of the nucleus and enriched at the nuclear periphery. The three zinc finger point mutants are each still able to relocalize

HP1a to peripheral domains, though the C550A mutant seems to be less stable and does not express as highly as wild type. Shelob 1-250 and 498-730 localize similarly to wild type protein but are unable to relocalize HP1a. 251-497 and 731-949 both have less nuclear enrichment than wild type Shelob and are unable to relocalize HP1a to the nuclear periphery (Figure 4a, right). We conclude that each of the zinc fingers is individually dispensable for HP1a binding and localization, and that the Shelob C-terminal aspartate-rich disordered domain and its zinc fingers are important for its localization, but are insufficient to also relocalize HP1a.

We also tested each mutant for its ability to alter HP1a's sensitivity to 1,6-hexanediol exposure. Cells expressing GFP-HP1a only have about 50% of their HP1a population disperse upon hexanediol exposure. With high levels of wild type Shelob expression, 100% of the HP1a becomes insensitive to hexanediol (Figure 3?). The C550A mutant does not express as highly as wild type does not alter HP1a's hexanediol sensitivity, while C692A seems to act identically to wild type and C721A is only slightly impaired for HP1a immobilization. Though 1-250 and 498-730 have localization similar to the wild type protein, they do not alter HP1a hexanediol sensitivity, consistent with inability to relocalize HP1a. Expression of 251-497 or 731-949 similarly do not alter HP1a sensitivity to hexanediol (Figure 4b).

We conclude that the zinc finger domains of Shelob are important for the protein's stability, but insufficient for its actions on HP1a. Amino acids 1-250 seem to be important for Shelob localization, but also insufficient for its interaction with HP1a. We conclude that Shelob's actions on HP1a require both a localization domain and an interaction domain.

To determine whether altering levels of Shelob might affect HP1a's silencing function through its mobility, we performed FRAP on HP1a in salivary gland nuclei, the same tissue where PEV silencing was measured. Indeed, we find that in Shelob heterozygous mutants, HP1a has increased mobility (Figure 4c). Taken together, these data suggest that Shelob protein level inversely affects HP1a mobility both in cells and in tissues, and that this mobility may be important for heterochromatic functions like transcriptional silencing.

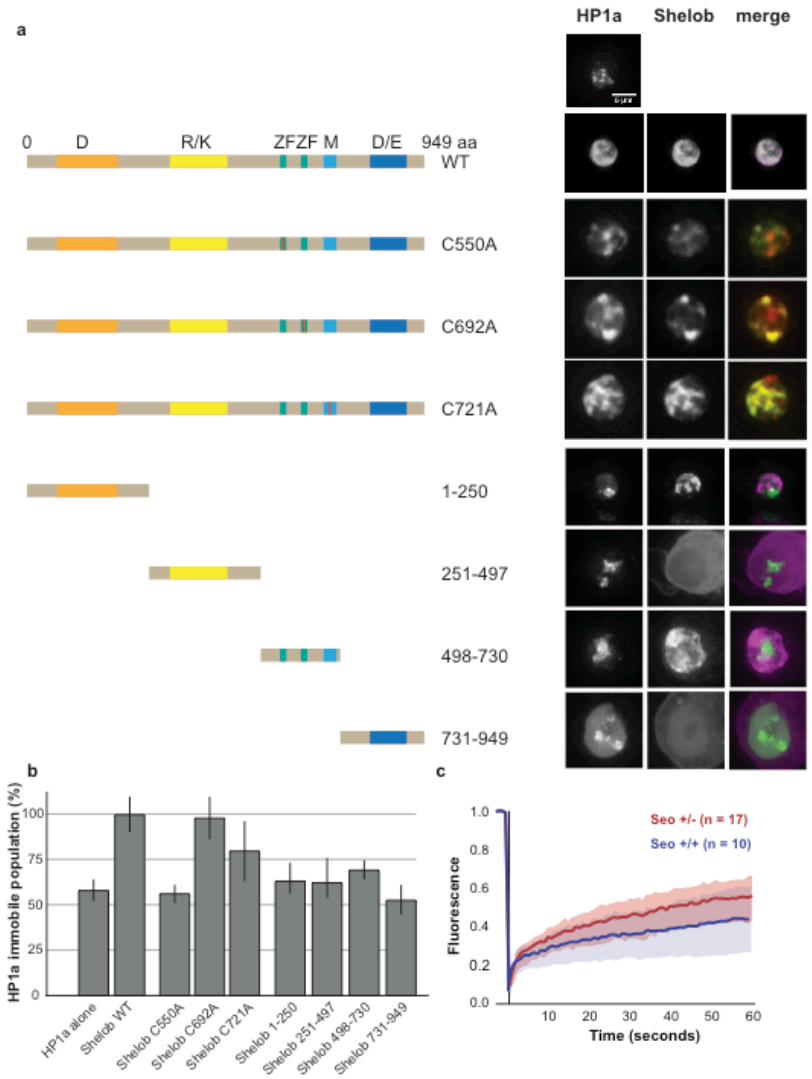

Figure 4: Mutants of Shelob
a. Diagram of Shelob mutations and their localization compared to HP1a at high expression levels. C550A, C692A, and C721A are point mutants that disrupt one of the C2H2 or Matrin zinc finger domains. 1-250, 251-497, 498-730, and 731-949 express only a portion of the wild type protein.
b. Quantification by hexanediol treatment of HP1a immobile population when coexpressed with indicated mutants. Immobile population calculated as % of total heterochromatic enrichment that is insensitive to hexanediol treatment for two minutes. Error bars are standard deviation, N = 8 biological replicates.
c. FRAP of HP1a in salivary gland nuclei dissected from 3rd instar wild type or Shelob heterozygous mutant larvae.

Discussion

Heterochromatin is essential for organismal viability and important cellular functions, and is defined molecularly by the presence of HP1a (reviewed in Eissenberg and Elgin, 2000). Despite the importance of HP1a in regulating heterochromatin and other functions, its mode of action remains unclear. Here we identified Shelob as a novel, functionally relevant component of heterochromatin, and demonstrate both physical interaction and co-localization of Shelob with HP1a, based on biochemical and cytological results. Additionally, we show that Shelob is required for organismal survival and for three aspects of heterochromatin structure or function: transcriptional silencing, DSB re-localization from heterochromatin, and proper organization of the 1.686 satellite. Interestingly, we also show that Shelob regulates the solubility, diffusion and coordinated movement of HP1a. This raises the intriguing possibility that the modulation of the biophysical properties of HP1a is important for regulating its functions, and raises new and important questions as to what other major nuclear processes are governed by a similar phenomenon.

Most heterochromatin proteins studied to date either broadly colocalize with HP1a or occupy a subdomain within the heterochromatin domain (Swenson et al., 2016). Intriguingly, and in contrast, Shelob displays a broad meshwork-like distribution throughout the nucleus with the highest concentrations of Shelob co-localizing with HP1a. Shelob ChIP-seq analysis validated these cytological results by showing that Shelob binds throughout the genome, but is densest in heterochromatin, where HP1a is also highly enriched. It is possible that Shelob interacts with HP1a through one of its zinc fingers. However, direct binding studies using recombinantly expressed Shelob and HP1a proved unsuccessful due to insolubility and toxicity of Shelob expression in E. coli (data not shown), which we speculate is due to the largely unstructured nature of the Shelob protein.

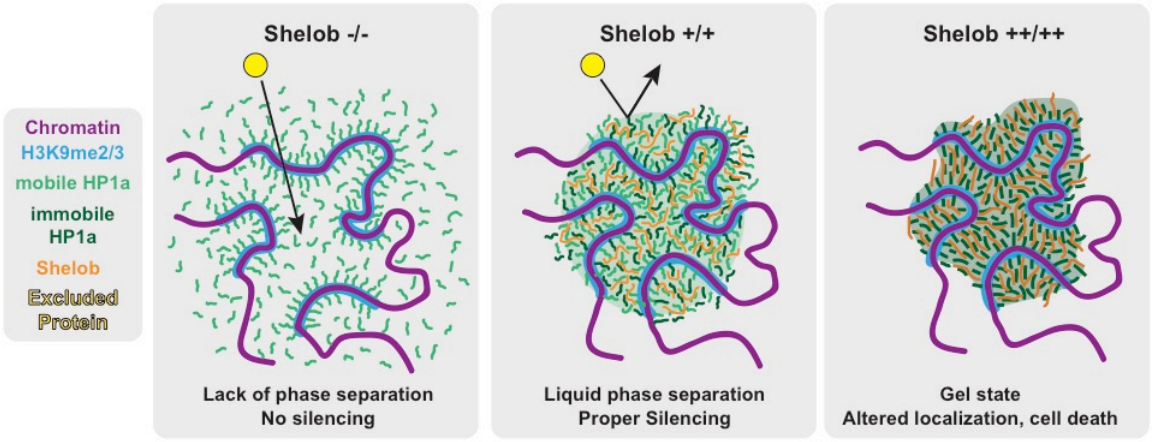

Figure 5: Model of Shelob function
In the wild type case (Shelob +/+), Shelob acts to form HP1a into its proper phase separated organization with 50% mobile and 50% immobile populations, which has normal protein exclusion functions. In Shelob mutants (-/-), HP1a binds to the same genomic sequences and exists at the same total level, but cannot form a phase separated domain, therefore it lacks an immobile population and cannot exclude proteins like polymerases. In Shelob overexpression (++/++), the balance of HP1a mobility shifts to 100% immobile, forming a gel-like state, which is also mislocalized to the nuclear periphery, and leads to cell death.

Functionally, Shelob was first identified in a genome-wide RNAi screen as a regulator of HP1a. In the absence of Shelob, HP1a cytological localization was altered (Swenson et al., 2016), yet we could not detect any obvious changes in HP1a's ChIP-seq enrichment profile. It was therefore perplexing that Shelob depletion led to a decrease in HP1a-associated functions, such as heterochromatic DSB re-localization and silencing of a reporter gene. Thus, we tested if Shelob regulates the biophysical properties of heterochromatin, and found that indeed HP1a's mobility by FRAP and sensitivity to 1,6-hexanediol are decreased as Shelob protein levels increase. Previously, we determined that phase separation properties of HP1a are important for selective permeability of the domain—specifically the exclusion of non-heterochromatic proteins (Strom et al., 2017). Shelob's influence on HP1a's mobility suggests that it might be altering HP1a's phase separation properties and thus its selective permeability. HP1a self-association that results in phase separation is mediated by the

flexible hinge and N-terminal extension on HP1a (A. G. Larson et al., 2017) and is separate from HP1a's dimerization and H3K9me2/3 binding. We propose that CG8108 specifically affects HP1a self-association without altering dimerization or H3K9me2/3 binding, which would explain the phenotype where HP1a protein exists at the same levels in the nucleus and binds to the same genomic sequences, but is deficient in silencing and DNA repair. Together, these results suggest that Shelob promotes HP1a phase separation, and that loss of Shelob results in increased HP1a solubility, loss of selective permeability and thus loss of heterochromatic functions like DSB movement and transcriptional silencing.

Similar to HP1a (Aucott et al., 2008; Chiolo et al., 2011), Shelob is required for organismal viability, is a dominant suppressor of position effect variegation and is required for an efficient DSB response in heterochromatin. We show here that Shelob regulates the biophysical properties of heterochromatin, and speculate that the tight regulation of the biophysical properties of HP1a is essential for normal HP1a function (Figure 5). Further studies are needed to determine if Shelob binding to HP1a and regulating HP1a solubility are separable functions. It is possible that Shelob mediates its affects on HP1a function through post-translational modifications rather than direct binding.

To our knowledge, this is the first report of a primarily unstructured protein modulating heterochromatin function, and raises the possibility that the unstructured regions in this protein play a critical functional role. Intrinsically disordered proteins are implicated in forming organized membraneless subcompartments like stress granules (Molliex et al., 2015), nucleoli (Brangwynne et al., 2011) and P granules (Brangwynne et al., 2009). It is intriguing that these functions of unstructured proteins likely depend on creating membraneless 'domains' separate from the surrounding environment, through phase separation mechanisms. In fact, many HPips were identified in a screen for proteins that contain low-complexity sequences (Kato et al., 2012), and heterochromatin has now been shown to form a coherent domain through phase separation mechanisms (Strom et al., 2017). It has been difficult to determine if phase separation is important for playing a functional role in biological contexts beyond compartmentalization and protein localization, because most perturbations that would affect phase separation result in dissolution of the entire domain, as observed for the heterochromatin domain upon loss of HP1a (Strom et al). Here we examined a protein that altered heterochromatic function without significantly changing domain formation, perhaps revealing a role for phase separation in genome functions that is separable from domain formation.

Here we have identified a novel component of heterochromatin that is essential for organismal viability. Furthermore, we demonstrate that Shelob regulates heterochromatin functions, specifically re-localization of DSBs from heterochromatin, organization of repetitive elements and heterochromatin-mediated gene silencing. Importantly, we propose that Shelob regulates heterochromatin through the modulation of the biophysical properties of HP1a. We speculate that other cellular components are regulated via targeted changes in their biophysical properties. Further validation and elucidation of this model should prove to be an exciting area of research.

Methods

HP1a level analysis. S2 cells were transiently transfected with pCopia::mCherry-CG8108. After 3 days, cells were fixed in 4% Paraformaldehyde for 5 minutes, washed three times for 5 minutes in 0.25% PBST, permeabilized for one hour in 1% PBST, blocked for 30 minutes in 5% FBS in 0.25% PBST, incubated overnight in primary antibody solution (α-HP1a, α-mCherry) at 4 degrees, washed three times for 5 minutes, incubated two hours in secondary antibody solution, washed three times for 10 minutes in 0.25% PBST, and mounted in VectaShield mounting medium with DAPI. Images were obtained on a Nikon Ti2 scanning confocal microscope. Quantification of fluorescent intensity of each nucleus was performed with a custom macro in FIJI.

1,6-hexanediol treatment**.** S2 cells expressing constructs of interest were imaged on a Deltavision Spectris microscope (GE Healthcare). Images were collected every five seconds for eight minutes, and cells were exposed to media containing 10% hexanediol for two minutes, starting at minute two.

Fluorescence Recovery After Photobleaching (FRAP). S2 cells expressing constructs of interest were plated at $1x10^6$ cells/mL in an 8-well chamber slide from Ibidi (Cat. No. 80826) and imaged on an Deltavision Spectris microscope (GE Healthcare). Nuclei were imaged 3 times pre-bleach, bleached with 100% laser power with 405 nm laser, then observed on an adaptive time scale for 30 seconds. Quantification of bleached area fluorescence was performed in FIJI, normalized for expression level and extent of bleaching.

Transient transfection of *Drosophila* S2 cells. Logarithmically growing S2 cells ($1.2x10^6$ cells/mL) were plated and allowed to grow overnight (O/N). Plasmid was mixed with serum free Schneiders media (SFM) (Invitrogen, Carlsbad, CA) (0.4 μg plasmid:100 μL SFM), then 0.5 μL:0.4 μg of TransIT-2020 (TransIT-2020 MIR 5400; MirusBio) was added and allowed to incubate at room temperature (RT) for 30 minutes. Transfection was accomplished by adding this mixture to cells dropwise, which were harvested or fixed after 72 hours.

RNAi. MEGAscript® T7 Kit (Ambion AM1334) was used per manufacturer's recommendations to produce dsRNA. T7 primer pairs for the targets are listed if different from DRSC, lower case denotes T7-polymerase binding site: mCherry 5' taatacgactcactatagggGAGGATAACATGGCCATC 3' and 5' taatacgactcactatagggTTCAGCTTCAGCCTCT 3', brown (DRSC04005), GFP 5' taatacgactcactatagggGACGTAAACGGCCACAAGTT 3' and 5' taatacgactcactatagggGAACTCCAGCAGGACCATGT 3', HP1a 5' taatacgactcactatagggCCCTCTGGCAATAAATCAAAA 3' and 5' taatacgactcactatagggTTAATCTTCATTATCAGAGTACCA 3', Shelob (DRSC25065, DRSC09675, DRSC30844). DOTAP (Roche, Basel, Switzerland: 11 202 375 001) mediated transfection was used per manufacturer's recommendations with 10 μg dsRNA used per $1x10^6$ cell/mL in a 6-well plate.

Co-immunoprecipitations of GFP-tagged HP1a and endogenous Shelob. $2x10^7$ S2 cells (for HP1a IP: cells were transfected with pCopia-LAP-HP1a (plasmid construction as described (Chiolo et al., 2011) or mock transfected for 72 hours) were harvested at 600 r.c.f for 5 minutes and flash frozen in liquid nitrogen. Next, pellets were resuspended in 200 μL of Buffer A (0.05% NP-40, 50 mM Hepes pH 7.6, 10 mM KCl, 3 mM MgCl2, 10% Glycerol, 5 mM NaF, 5 mM β-Glycerophosphate, 1 mM Benzamidine, 1X protease inhibitor cocktail (Roche: 11 836 170 001), 1 mM PMSF, 25 mM NEM, 1:1000 Phosphatase Inhibitor Cocktail 2 (Sigma-Aldrich, St. Louis, MO: P5726), 1:1000 Phosphatase Inhibitor Cocktail 3 (Sigma-Aldrich: P0044). 10 U benzonase (EMD Millipore, Hayward, CA: 80601-766) per 37 μg chromatin (estimated by A_{260} reading) was incubated at 4°C with mixing for 30 minutes. 0.5 mM EDTA was added to stop the reaction and HP1a was extracted on ice with 300 mM NaOAc for 1 hour with mixing. Cell extracts were cleared by centrifuging at 16,100 r.c.f. for 10 minutes at 4°C and the supernatant was removed to a new tube. For IPs of GFP-tagged HP1a, 3 μg of goat anti-GFP antibody (Rockland/VWR, Limerick, PA: RL600-101-215) and 10 μL protein G beads (GE Life Sciences, Marlborough, MA: 17-0618-01) were mixed with sample O/N at 4°C. For IPs of Shelob, 3 μg of rabbit anti-Shelob antibody and 10 μL protein G beads were mixed with sample O/N at 4°C. Bound material was washed four times with Buffer A at 4°C while mixing. Liquid was removed and beads resuspended in 25 μL of Laemmli loading buffer.

Antibodies for IFs and western blots. Primary antibodies were rabbit anti-GFP (Western blot (WB): 1:1,000) (Invitrogen: A11122), rabbit anti-Shelob (WB: 1:5,000; IF:1:500) (generated via genetic immunization by SDIX, Newark, Delaware), rabbit anti-H2B (WB: 1:5,000) (Millipore: 07-371), rabbit anti-wa184 (HP1a) (WB: 1:500) (kind gift from Sarah Elgin), mouse anti-C1A9 (HP1a) (IF: 1:1,000) (Developmental Studies Hybridoma Bank, University of Iowa, Iowa City, Iowa: C1A9c), rabbit anti-HA (IF: 1:1,000) (Cell Signaling: 3724S), 1:1,000 rabbit anti-γH2Av (Rockland/VWR: VWR #600-401-914) and 1:1,000 mouse beta-Actin (Abcam, Cambridge, United Kingdom: 8224). Alexa secondary antibodies (Invitrogen) were used for IF (1:500). HRP-conjugated antibodies were used for ECL-based Westerns (1:5,000). IRDye® secondaries (Licor) were used for Odyssey-based Westerns (1:10,000).

Western blots. Protein samples were heated to 65°C for 5 minutes, centrifuged and separated on a 4-12% SDS-PAGE gel, transferred to nitrocellulose membrane, incubated in blocking buffer (0.5% non-fat milk in 15 mM Tris-HCl pH 7.5, 150 mM NaCl, 0.05% Tween-20 for blots visualized with ECL, 0.167% non-fat milk in a 1:2 ratio Odyssey® Blocking Buffer (Li-cor 927-40000) for blots visualized with Odyssey imager for 30 minutes and primary antibodies were incubated in blocking buffer at 4C O/N, secondary antibodies were incubated in blocking buffer at RT for 1 hour. Membranes were washed 3 times (5 minutes each) with TBST (ECL) or PBST (Odyssey) between primary and secondary incubation and after secondary incubation. Super Signal West Dura Extended Duration Substrate (Pierce #34075) was used for ECL, Clean-Blot IP Detection Reagent (Thermo Scientific/Pierce PI21230) was used to detect only native GFP after GFP-IP.

Immunofluorescence and FISH. "Regular IF" was performed by fixing cells onto a slide with 4% paraformaldehyde (PFA) in PBST (PBS + 0.4% Triton-X 100). 100 μL of cells were dropped onto a slide, in this way multiple experimental conditions can be processed in parallel to limit differences between samples. Slides were incubated in PBST + 5% Fetal Calf Serum (FCS) (blocking buffer) at RT for 30 minutes to block. Primary antibodies were incubated in blocking buffer at 4°C O/N, secondary antibodies were incubated in blocking buffer at RT for 1 hour. Slides were washed 3 times (5 minutes each) with PBST between primary and secondary incubation and after secondary incubation. Slides were washed again in PBS and DNA was stained with 0.2ug/ml of DAPI in PBS for 5 min at room temperature, washed with PBS and mounted in Vectashield (VWR H-1000).

Triton extraction and cytospin IF were performed similarly to "regular IF". For triton extraction cells were incubated in PBST (0.2% Triton-X 100) for 5 minutes prior to fixation. For cytospin cells were loaded into a dual-chamber Cytospin funnel and spun for 10 minutes at 900 r.p.m. (90 r.c.f.) in a Shandon Cytospin 3.

FISH samples were fixed in 4% PFA in PBST. Next, the slides were washed for 20 minutes in PBST at RT, 30 minutes in 2X sodium citrate buffer with 0.1% Tween-20 (SSCT) at 37°C, then 5 minutes at 50°C and 40 minutes at 70°C. Slides were incubated with heat-denatured 2.5 ng/μL of bicyclic nucleic acids (BNA) probes (Integrated DNA Technologies) in 50% formamide, 2X sodium citrate buffer and 10% Dextran Sulfate for 3 hours at 37°C for AACAC and 1.686; 18°C for AATAT; 50°C for undeca. BNA probe sequences are listed: (undeca: FAM/CAGT/iBNA-A/iBNA-meC/GGG/iBNAA/C/iBNA-meC/AGT/iBNA-A/iBNA-meC/GGG, 1.686: Cy5/CAAT/iBNA-A/GA/iBNA-meC/A/iBNA-A/T/iBNA-A/GA/iBNA-meC/iBNA-A/ATAG, AATAT: HEX/AATAT/iBNA-A/iBNA-A/T/iBNA-A/T/iBNA-A/iBNA-A/T/iBNA-A/T/iBNA-A/iBNA-A/TAT, AACAC: Cy-5/AACAC/iBNA-A/A/iBNA-meC/A/iBNA-meC/A/iBNA-A/C/iBNA-A/C/iBNA-A/ACAC).

Cell cycle analysis movie. Images were taken as z-stacks with 0.2 um increments using a 60X oil immersion objective (NA 1.40) Deltavision Spectris microscope (GE Healthcare) and images were deconvolved using SoftWoRx (Applied Precision, LLC). Time-lapse images were acquired once every 20 minutes. Image analysis was performed as described previously (Swenson et al., 2016).

Flow Cytometry. 5x10^6 cells were harvested at 600 r.c.f for 5 minutes and washed with 5 mL of cold PBS+ (calcium and magnesium free PBS with 1% glucose, 10mM EDTA and 0.5% BSA), spun for 5 minutes at 300 r.c.f. and resuspended (R/S) in 1 mL of cold PBS+. Cells were fixed by adding 10 mL of cold EtOH dropwise while mixing and incubated for >1 hour at -80°C. Cells were pelleted for 3 minutes at 200 r.c.f. and R/S in cold PBS+ at 2x10^6 cells/mL. 1 mL of cells was mixed with 20 μL of RNase A (Sigma R5250; 29mg/mL) and 50 μL Propidium Iodide (Molecular Probes P3566; 1mg/mL in ddH20) and incubated for 30 minutes at 37°C in the dark. Cells were filtered (35 um) in a polystyrene tube and analyzed using BD Biosciences FACSCalibur flow cytometer. Doublets were eliminated using PI-fluorescence-area vs PI-fluorescence-width plots and cell cycle stage was determined by a Watson Pragmatic model. Training and experimental design support provided by Michelle Scott at the LBNL FACS Facility.

ChIP-Seq and Data Analysis. ChIP-Seq was performed as described previously (Hawkins et al., 2010; O'Geen et al., 2011). Briefly, $2.2x10^7$ cells were fixed and used per ChIP, chromatin was sonicated using a Biorupter (Diagenode) to fragment DNA to 200 - 1,000 bp. Chromatin was immunoprecipitated using 5 μL of a polyclonal anti-HP1a antibody (552) and Protein G magnetic beads. Libraries were prepared per manufacturer's recommendations using TruSeq™ DNA Sample Prep Kit (Illumina FC-121-1001). Libraries were sequenced (50 base-pair single-end reads) at the Vincent J. Coates Genomics Sequencing Laboratory using a HiSeq2000 Sequencer (Illumina). The FASTX-Toolkit (http://hannonlab.cshl.edu/fastx_toolkit/) was used to filter Shelob sequencing reads to have a phred score greater than or equal to 20. Bowtie software was used to map reads to either the *Drosophila* reference genome (fb5.22) or unmapped repeats.

A pileup was generated for each ChIP-seq and input experiment using SAMtools mpileup (Li et al., 2009). Fold-enrichment (FE) was calculated using a sliding window with a window size of 1,000 bps and a step-size of 100 bps. A length normalized FE of windows for each region (e.g. 2L) was determined as follows: [# of windows with FE > 2 in region X / # of windows in region X] / [# of windows with FE > 2 in the entire genome / # of windows in entire genome] so that a value > 1 indicates that the FE is more enriched in that region than the genome average enrichment. Windows were regularized by excluding windows with 150 or more bases with no (i.e. 0) coverage. We defined heterochromatin as 2LHet, 2Lh, 2RHet, 2R, 3LHet, 3Lh, 3RHet, XHet, YHet and Xh and euchromatin as 2R, 2L, 3R and 3L. For browsing tracks on IGV, Macs2 (Feng et al., 2012) and SPP (Kharchenko et al., 2008) were used to normalize ChIP and input sequences and Macs2 broadPeak was used to identify peaks.

β-Galactosidase Activity (Measuring whole fly PEV). *P{EPgy2}CG8108^{EY14316}* was obtained from the Bloomington *Drosophila* Stock Center and In(3L)BL1 was a generous gift from Joel Eissenberg. Protocol was performed as described previously (Lu et al., 1996) with minor modifications. Five adult males aged 2-6 days after eclosion were heat shocked for 45 minutes and recovered for 1.75 hours at RT. OD_{574} readings were derived from a 35 μL extract of flies and readings were collected at 30, 60, 90, 120 and 180 minutes. Endogenous β-Galactosidase activity was subtracted from *yw/yw* flies and *CG8108^{EY14316}/In(3L)BL1*, *Su(var)3-7^{14}/In(3L)BL1* readings were normalized to yw;+/*/In(3L)BL1* flies. X-gal staining for analysis of PEV in individual tissues was performed as in (Lu et al., 1996).

Hatch Rate. *P{EPgy2}CG8108^{EY14316}/[TM6. SbTbe]*, *P{SUPor-P}CG8108^{KG05452}/[TM6. SbTbe]* and *ry/[TM6. SbTbe]* heterozygous virgin females were mated to their siblings and allowed to lay eggs on apple juice plates for ~4 hours. Unhatched and hatched eggs were counted ~40 hours later. *P{SUPor-P}CG8108^{KG05452}* was obtained from the Bloomington *Drosophila* Stock Center.

Chapter 4

Heterochromatin in Aging and Longevity

Authors: Amy R. Strom, Debbie Staijen, Braeden K. Ego, Gary H. Karpen

Abstract:

Decline of cellular and tissue function is an inevitable outcome of age common to all forms of life. Many mechanisms have been identified that contribute to aging phenotypes, and when experimentally manipulated, can lead to increased or decreased longevity in various organisms. While many lifespan-extending manipulations can be attributed to maintenance of tissue homeostasis, some aging mechanisms are highly conserved across distant species and can be connected to fundamental cellular processes. Maintenance of chromatin landscapes and cellular differentiation are critical for maintaining cellular function during aging, and overexpression of a key chromatin protein, Heterochromatin Protein 1a (HP1a) has been shown to increase lifespan in *Drosophila* when expressed under a heat shock promoter. However, the cellular and physiological mechanisms of this lifepan extension, and whether these mechanisms are conserved, are unknown. Here, we show that gut tissues mediate HP1a-dependent lifespan extension in *Drosophila*, connecting the fundamental process of chromatin organization to physiological aging resulting from gut barrier dysfunction.

Introduction

There is conflicting data about the role of heterochromatin in aging and longevity, even about changes in protein level and epigenetic marks over time. Some groups have published that heterochromatin protein levels decrease with age, but others find that they stay the same. Some studies of heterochromatic epigenetic marks find that they decrease over time, while others find that the total genomic levels stay the same but the distribution changes.

In general, it is agreed that in young tissue there is a distinct heterochromatin domain, cytologically and genomically. Heterochromatin proteins and epigenetic marks are strongly enriched at repetitive pericentromeric sequences and are depleted from the bulk of chromosome arms and active gene regions. In older tissues, this contrast is lowered and though changes in total levels of proteins and epigenetic marks may not be consistent, their localization is decidedly altered (Sen, Shah, Nativio, & Berger, 2016). H3K9me2/3 can be found at low levels throughout the genome, such that its levels at heterochromatic sequences is reduced compared to young tissues, but its levels at euchromatic sequences is raised in comparison to younger tissues(Wood et al., 2016).

Drosophila is often used as a model organism for aging studies—the relatively short lifespan and high level of conservation with aging mechanisms in mammals (He & Jasper, 2014) has led to multiple fundamental discoveries in the field. Of note are studies of gut barrier dysfunction, which is the method by which fruit flies are thought to die in a laboratory environment. In all animals, the gut contains thousands of microbes that aid in food digestion and hormonal signaling, but can become pathological if allowed to enter the blood stream. Usually, young animals have a healthy gut barrier and no microbes can move from the gut lumen to the blood stream or hemolymph, while older animals or those that have been exposed to certain toxins tend to accumulate gut fissures that allow movement of microbes into other tissues, which results in systemic infection (L. Wang, Karpac, & Jasper, 2014). In flies, the mechanism of gut barrier dysfunction arising from gut stem cell dysplasia is well-studied. In humans, gut barrier dysfunction can arise from acute assaults like strong antibiotics or chemotherapy, or from long-term processes like general aging. The fruit fly model system has also been used to investigate influence of other tissues on aging phenotypes, including muscle- and neuro-degeneration, hormonal signaling and others.

Overexpression of Heterochromatin Protein 1a (HP1a) in some contexts has been linked to extended lifespan. Expression of HP1a in flies under a heat shock promoter that drives low level overexpression (1.25 fold over endogenous), in all tissues throughout the entire lifespan of the fly, leads to an approximately 25% increase in lifespan (K. Larson et al., 2012). In this study, authors found that HP1a overexpression prevented accumulation of rDNA extrachromosomal circles, which provides a possible mechanism by which nuclear organization could affect overall organismal aging through gross metabolic changes. However, a fly with a genomic duplication of the endogenous HP1a locus (such that the animal has two copies of the HP1a gene both driven by the endogenous promoter) does not increase lifespan (Frankel & Rogina, 2005). This difference suggests that promoter, genomic context, tissue differences or other factors could be critical.

Here we investigate specifics of heterochromatin-mediated lifespan extension using the GeneSwitch system. Because aging studies are very dependent on chromosomal context, most experiments begin by crossing an allele of interest into a common genomic background up to 10 times in order to isolate the allele and ensure that no unknown gene changes are altering experimental results. This process is unnecessary with an experimental advancement like GeneSwitch; a Gal4-based expression system in which genetically identical siblings can be tested side by side with and without addition of a small molecule hormone, RU486. The GeneSwitch protein is a fusion of the DNA-binding domain of Gal4 with the transcriptional activator domain of the mammalian Estrogen Receptor (Figure 1). This results in a protein that is expressed and maintained in the cytosol, but will only enter the nucleus and drive expression by binding to the Upstream Activating Sequence (UAS) in the presence of RU486. Using this tool and tissue-specific GeneSwitch drivers, we investigated the timing, location and level of HP1a overexpression needed to drive heterochromatin-mediated lifespan extension. Our results suggest that HP1a overexpression only in neuronal glia, fat body, or gut are sufficient to significantly extend lifespan, greatly refining our understanding of the role of chromatin organization in tissue homeostasis and longevity.

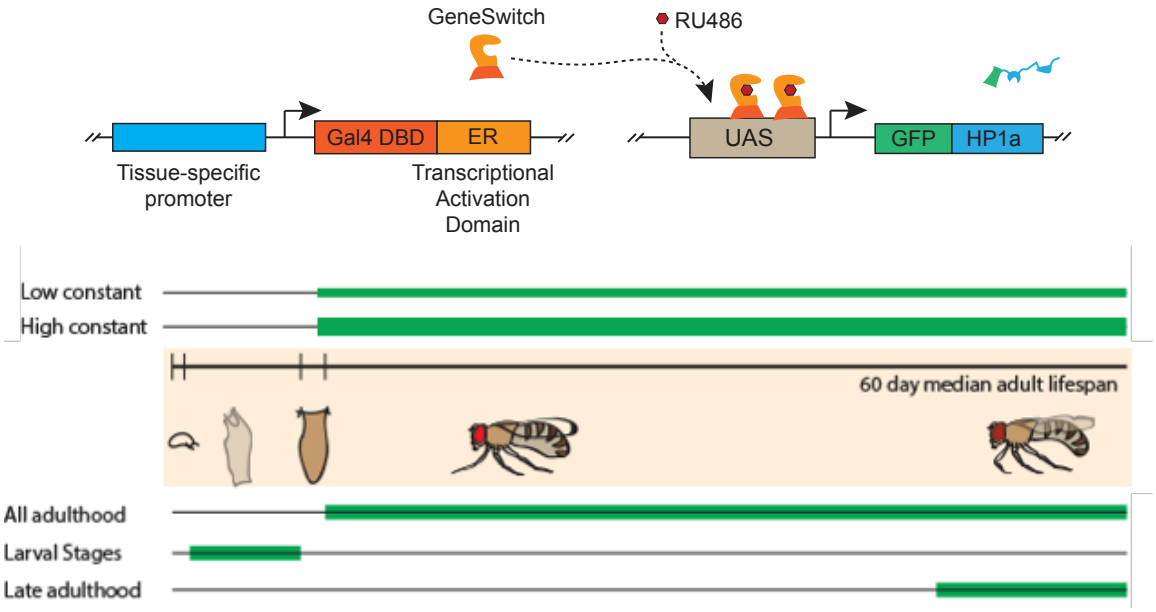

Figure 1: Experimental setup for investigating HP1a-mediated lifespan extension
GeneSwitch constructs can be driven in a tissue-, level- and temporal- specific manner by addition of varying levels of RU486 to fly media. In these experiments, we drove four levels of expression of GFP-HP1a in larval, all adult or late adult stages, and measured lifespan changes.

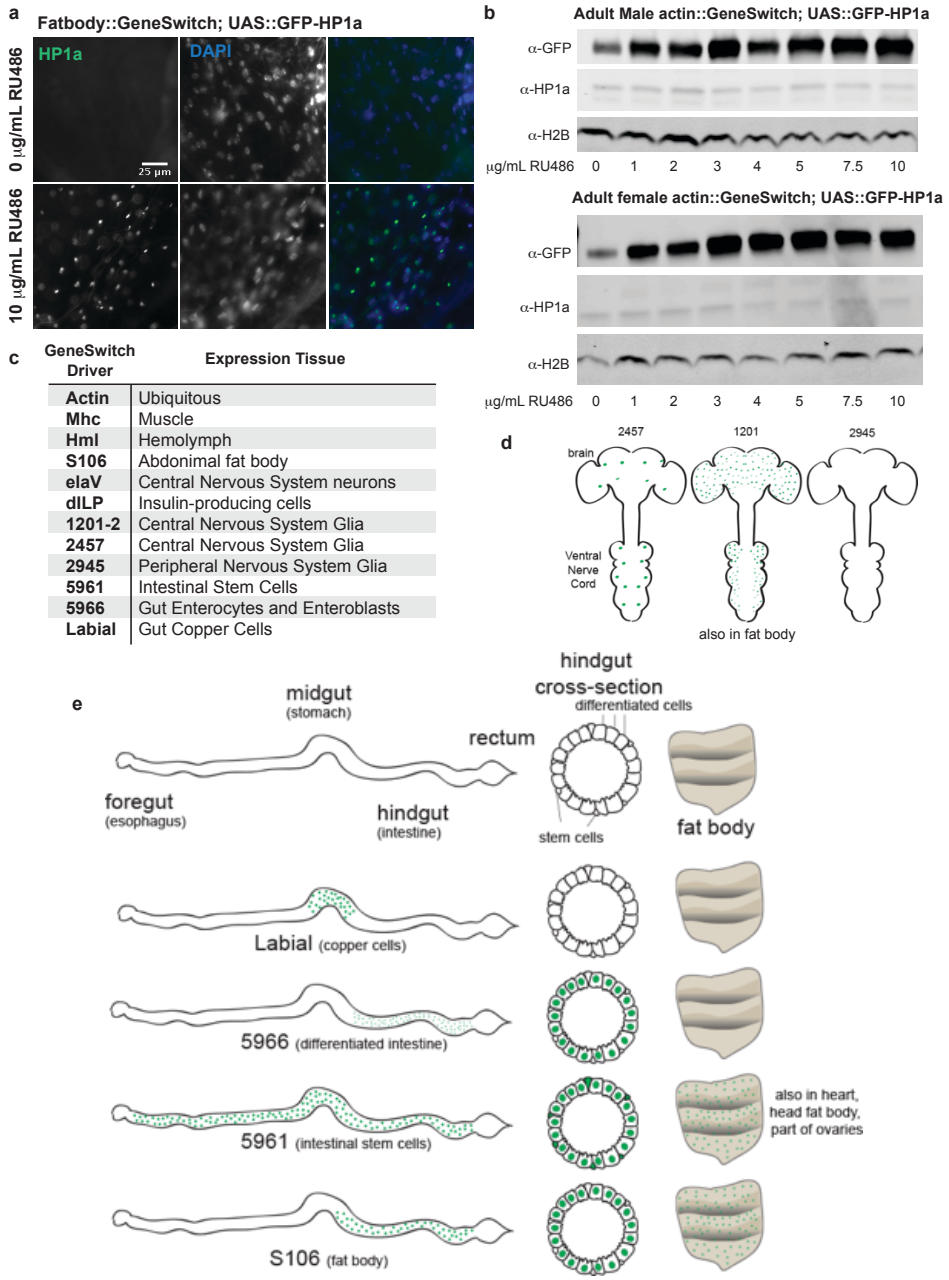

GeneSwitch Driver	Expression Tissue
Actin	Ubiquitous
Mhc	Muscle
Hml	Hemolymph
S106	Abdonimal fat body
elaV	Central Nervous System neurons
dILP	Insulin-producing cells
1201-2	Central Nervous System Glia
2457	Central Nervous System Glia
2945	Peripheral Nervous System Glia
5961	Intestinal Stem Cells
5966	Gut Enterocytes and Enteroblasts
Labial	Gut Copper Cells

Extended Data Figure 1: Characterization of the GeneSwitch System drivers
a. Images of dissected fat body tissue from adult females of genotype S106::GeneSwitch; UAS::GFP-HP1a, fed 0 or 10 µg/mL RU486 for 48 hours before dissection. Expression of GFP-HP1a is inducible and nuclear, as expected for HP1a protein. **b.** Western blots of extracts from three adult male (top) and female (bottom) flies fed 1, 2, 3, 4, 5, 7.5, or 10 µg/mL RU486 for 48 hours before assay. Blots stained for GFP-HP1a, endogenous HP1a, and H2B as loading control. Expression of GFP-HP1a is inducible to differing levels depending on concentration of RU486 fed to the animal. **c.** Table of GeneSwitch drivers used in this study and their expression tissue. **d.** Characterization of expression tissues for glial (**d.**) and gut (**e.**) drivers. Adult males and females were fed 10 µg/mL RU486 for 48 hours, then dissected and *ex vivo* tissues immediately visualized for expression data.

Results

Characterization of the GeneSwitch System and drivers used in this experiment

To ensure that the GeneSwitch system indeed drives tissue-, temporal- and dose-specific expression of the UAS::HP1a-GFP transgene, we dissected relevant tissues from adult flies fed 0 or 10 μg/mL RU486, and mounted them in media containing DAPI to visualize nuclei. *Ex vivo* tissues were immediately imaged, and we found that each driver was capable of RU486-dependent GFP-HP1a expression (Extended Data Figure 1a). GFP-HP1a localizes to the nucleus, where it is enriched in a DAPI-rich subnuclear heterochromatic compartment, as expected. To determine the level of overexpression of GFP-HP1a in the GeneSwitch system, we performed western blots on cell extracts from adult male or female actin::GeneSwitch; UAS::GFP-HP1a flies fed for 48 hours with 0, 1, 2, 3, 4, 5, 7.5 or 10 μg/mL RU486. Anti-GFP antibody binding demonstrates that GFP-HP1a is expressed in increasing levels dependent on RU486 concentration. Blotting for endogenous HP1a shows there is no change in the endogenous level of HP1a. We chose a list of twelve GeneSwitch drivers that represent a diverse range of tissues previously shown to be involved in aging and longevity (Extended Data Figure 1c). Additionally, we verified expression patterns of each driver by dissecting a panel of tissues from adults (Extended Data Figure 1d).

HP1a overexpression in larvae? causes lethality

One possible explanation of how epigenetic marks change with age is that compartmentalization between different types of chromatin is lost over time. If chromatin compartmentalization is established during development and slowly lost during aging, we might expect that boosting levels of chromatin proteins during development would establish a stronger compartmentalization and result in longer lifespan. To test this, we took 24 hour 1st instar larvae of genotype actin::GeneSwitch; UAS::GFP-HP1a and provided them with food containing 0, 0.1, 1 or 10 μg/mL RU486. We found that 97% of larvae fed 0 μg/mL RU486 survived to pupariation, but almost 100% of larvae fed 0.1, 1 or 10 μg/mL RU486 died before pupariation (Figure 1a). To ensure that lethality was due to HP1a overexpression and not some other result of RU486 consumption, we repeated the experiment with larvae that had either actin::GeneSwitch or UAS::GFP-HP1a, but not both. Indeed, larvae with only one or the other piece of the Geneswitch system had similar survival rates to 0 μg/mL RU486 control. This suggested that the chosen concentrations of RU486 drove levels of HP1a overexpression that are too high and result in lethality, so we repeated the experiment with a lower range of RU486 concentrations.

With very low levels of overexpression (0.001 μg/mL RU486 in food), larvae can survive through pupal stages and eclose as adults. With increasing concentrations (0.005, 0.01, 0.05, 0.1 μg/mL), an increasing proportion of the larvae have defects or die, while siblings with 0 μg/mL food survive with no issue (Figure 1a). Surviving larvae and pupae from intermediate concentrations of RU486 (X-Y)have phenotypes indicative

of lack of ecdysone signaling. In developing Drosophila, Ecdysone is a steroid hormone that is released in large pulses just before each molting stage between 1st and 2nd instar larvae, 2nd and 3rd instar, and just before pupation. Deceased larvae from this experiment failed to molt, as evidenced by two pairs of mouthhooks (Figure 1b, bottom). Animals that make it to pupation are smaller than their non-drug treated siblings, and have mis-shapen, lighter-color pupal casings (Figure 1b, top). These tend to die as pupa or fail to properly eclose as adults. Lighter-color pupal casings are also indicative of lack of ecdysone signaling, as ecdysone is responsible for tanning of the pupal casing and hardening of adult cuticle.

The animals that do make it to adulthood have misshapen forelimbs consistent with lack of cuticle hardening (not shown). Ecdysone is also involved in post-eclosion cuticle hardening through a downstream hormone pathway including the ecdysteroid bursicon and its receptor rickets. These results lead us to conclude that overexpression of HP1a during larval development is not responsible for lifespan extension and is in fact detrimental to the development of the organism, likely through preventing a response to ecdysone hormone.

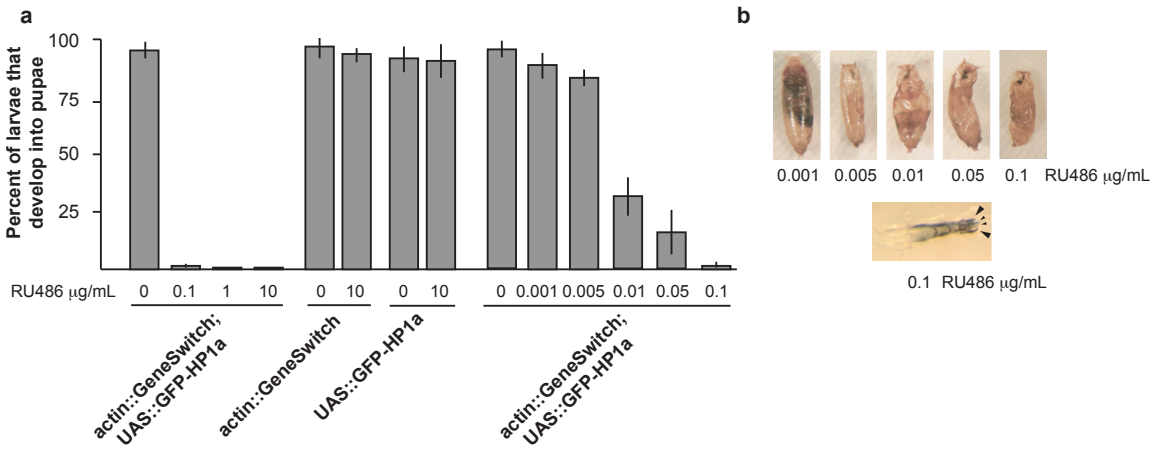

Figure 2: Larval overexpression of GFP-HP1a results in lethality
a. Percent of larvae of indicated genotype that develop into pupae after treatment with RU486, which causes GeneSwitch to express UAS::GFP-HP1a if both are present. N = 3 biological replicates of 60 larvae each. **b.** Representative images of pupae from indicated concentration of RU486 (top). Dissected larval mouthhook showing two pairs of hooks, large arrows and small arrows, which indicates lack of molting.

HP1a overexpression in gut and fat body tissues extends adult lifespan

To determine which tissues are responsible for heterochromatin-dependent lifespan extension, we performed longevity assays on separated virgin females and males expressing each tissue-specific driver, fed either 0 or 10 μg/mL RU486 throughout their adult life, which evades larval or pupal lethality. We find that ubiquitous expression of GFP-HP1a through the Actin5C::GeneSwitch driver does not extend adult lifespan. Interestingly, overexpression of HP1a in adult stages seems to have no impact on lifespan in males or females, even though overexpression in larvae was so detrimental to development. Three glia drivers (2945, 2457 and 1201-2) had no impact on female lifespan. Glial driver 1201-2 did extend lifespan by a significant amount (20%)

in males, but this result is complicated by the fact that this driver is also expressed in abdominal fat body (see Discussion). Neuronal driver elaV, muscle driver Mhc, hemolymph cell driver Hml and insulin-producing cells driver dILP8 also did not have any significant effects on male or female lifespan. Intriguingly, four tissue-specific drivers did significantly lengthen lifespan—5961 (intestinal stem cells), 5966 (gut enterocytes and enteroblasts), Labial (gut copper cells), and S106 (fat body) extended female lifespan by 10%, 5%, 7% and 12%, respectively. These data are summarized in Figure 3.

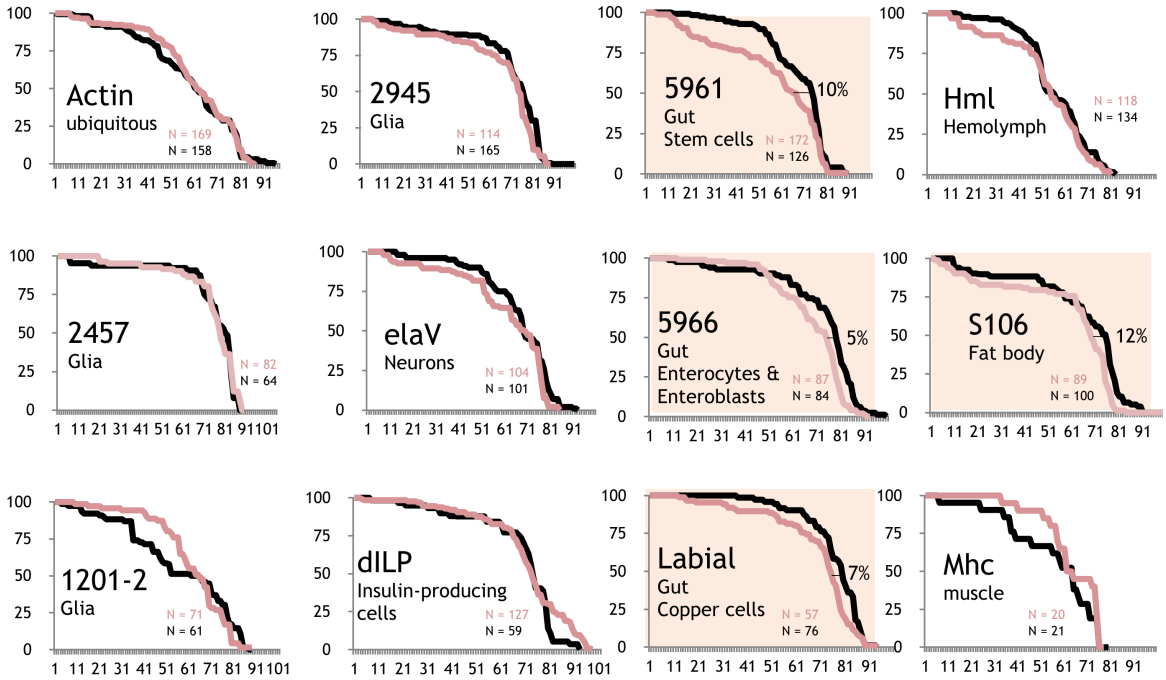

Figure 3: Tissue-specific expression of GFP-HP1a in gut tissues leads to lifespan extension
Longevity assays from adult females with indicated tissue-specific GeneSwitch drivers fed 0 (pink) or 10 (black) μg/mL RU486 throughout their lifespan. Drivers that resulted in significant difference between expressing and non-expressing are highlighted, and percent of average lifespan increase is indicated.

HP1a overexpression late in life does not extend lifespan

In order to develop therapies that might mitigate aging phenotypes, it is pertinent to determine which aspects of aging are reversible, and when they have impact. To determine whether HP1a overexpression is able to mediate lifespan extension when applied only late in life, we first aged flies to 40 days without RU486 and then began expression of GFP-HP1a by feeding 10 μg/mL RU486. For this assay, we tested only those tissue specific drivers that resulted in lifespan extension when active throughout the entire fly lifespan—5966 (intestinal stem cells), S106 (fat body), 5961 (enterocytes and enteroblasts), Labial (copper cells), and 1201-2 (glia). We found that there was no lifespan extension when GFP-HP1a was overexpressed under control of any of these drivers when induced from 40 days onward (Figure 4).

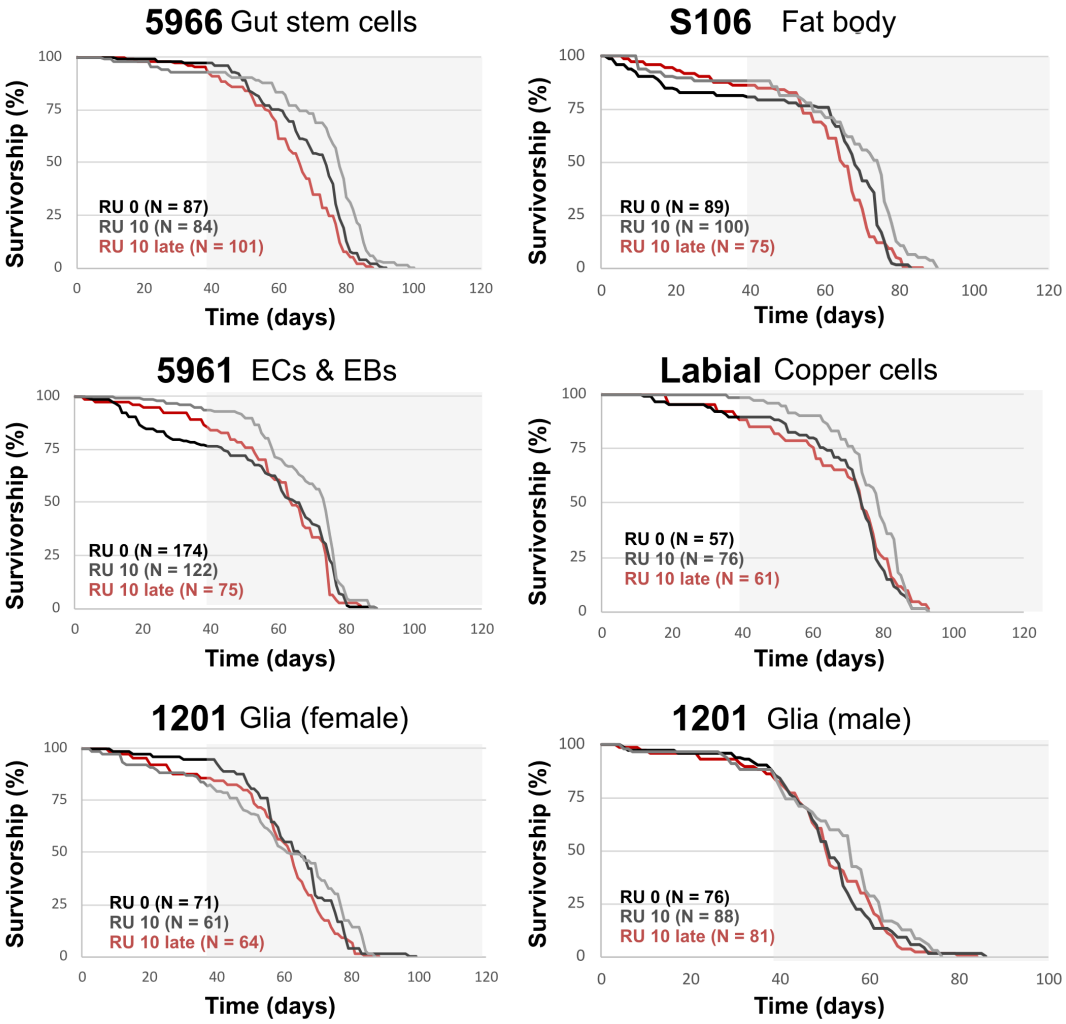

Figure 4: Late life overexpression of HP1a does not lead to lifespan extension
Longevity assays from adult females or males with indicated tissue-specific GeneSwitch drivers fed 0 μg/mL RU486 for days 0-39 and 10 μg/mL RU486 from day 40 onward (indicated by shaded regions). Survivorship curves from late life overexpression (RU 10 late, red lines) are shown in comparison to control (RU 0, black) and whole-life overexpression (RU 10, gray) for each genotype. None of the tissue specific drivers tested resulted in significant lifespan extension in this assay.

Discussion

Here we investigated the tissue specificity, timing, and level of HP1a overexpression sufficient for lifespan extension. We tested whether overexpression of GFP-HP1a at specific times or in specific tissues via the GeneSwitch system is sufficient for heterochromatin-mediated lifespan extension. Larval expression of GFP-HP1a led to potent lethality, even with very low levels of RU486 exposure. Escapees have defects indicative of impaired ecdysone signaling, suggesting that increased HP1a during development could prevent proper transcriptional responses to ecdysteroid hormones. However, tissue-specific overexpression of HP1a in adult gut and fat body resulted in lifespan extension, while overexpression in other tissues including neurons,

muscle and hemolymph did not. This indicates that the primary tissue mediating heterochromatin-related lifespan extension is the gut, and potentially glia and/or fat body. Interestingly, both stem cell and differentiated cell drivers in the gut lead to lifespan extension. Finally, overexpression of HP1a beginning at 40 days of age, after aging effects have begun to take hold, is not sufficient to reverse aging phenotypes and extend lifespan. This likely means that heterochromatin-mediated lifespan extension occurs through a preventative process rather than a reversible one.

Ecdysteroid hormones are indispensable for insect development. Ecdysone pulses trigger large transcriptional program shifts at key developmental moments, including molting and eclosion (Richards, 1997). One of the main functions of HP1a is transcriptional silencing of heterochromatic sequences, and maintenance of genome integrity. Extreme sensitivity of larvae to HP1a protein expression level and presence of mutations that phenocopy ecdysone receptor mutants (Loveall & Deitcher, 2010; Peng & Karpen, 2008) suggest that HP1a overexpression in larvae could be preventing activation of ecdysone-induced transcriptional programs. It would be interesting to test if HP1a is specifically silencing primary ecdysone response genes at these stages, or if it is promoting general transcriptional silencing and therefore preventing downstream ecdysone responses. Ecdysone is also used to signal hormonal changes during adult fly lifespan; it regulates key aspects of reproduction and metabolism, and flies that are heterozygous for ecdysone receptor mutations have increased lifespan (Simon, Shih, Mack, & Benzer, 2003). If HP1a overexpression is specifically preventing activation of ecdysone response genes, heterochromatin-mediated lifespan extension could be explained through the same mechanism as heterozygous ecdysone receptor mutants.

Utilization of the powerful Geneswitch system demonstrated that HP1a overexpression in specific adult tissues and cell types is sufficient for significant lifespan extension. Specifically, expression in muscles, neurons, hemolymph, and most glial subtypes did not extend lifespan**.** Thus, heterochromatin integrity does not need to be maintained in all adult tissues to ensure a normal or extended lifespan. At this time, we do not have direct evidence to identify specific mechanisms, but both molecular and cellular impacts can be proposed based on what is known about the potential roles of these tissue and cell types in lifespan and aging.

Intestinal homeostasis is closely linked to lifespan in *Drosophila.* The gut is a tissue with high cell turnover – differentiated cells exposed to the lumen of the gut are constantly exposed to oxidative damage and toxic insults, therefore they live only a short time before they are sloughed off and replaced with new cells(L. Wang et al., 2014). This process places high demand on intestinal stem cells, which must continue to divide and replace damaged cells throughout the lifespan of the fly. In young flies, with each division, intestinal stem cells self renew and produce an enteroblast, which subsequently differentiates into a micropiliated enterocyte responsible for nutrient absorbtion, or an enteroendocrine cell, responsible for hormonal signaling relating to hunger and satiety (Jiang & Edgar, 2009; Posovszky & Wabitsch, 2015a; 2015b). These cells are spatially organized in the gut in a way that maintains gut barrier function and prevents microbes inside the gut lumen from entering the hemolymph (Figure 5). With increasing age, the enteroblasts produced by the intestinal stem cells tend to mis-differentiate, and instead of fully committing to either a completely differentiated lineage, or continue to express stem cell markers(Jeon et al., 2018; Purnell, 2015). This leads to

disorganization of gut tissue and formation of fissures that allow microbes from the gut lumen to leak out into other tissues. Leaky gut can lead to systemic infection and death (Rera, Clark, & Walker, 2012). We found that overexpression of HP1a in either intestinal stem cells, or in enteroblasts and enterocytes, is sufficient to extend lifespan significantly. If HP1a expression in these cell types helps maintain intestinal homeostasis, heterochromatin-mediated lifespan extension could be due to longer maintenance of gut barrier function.

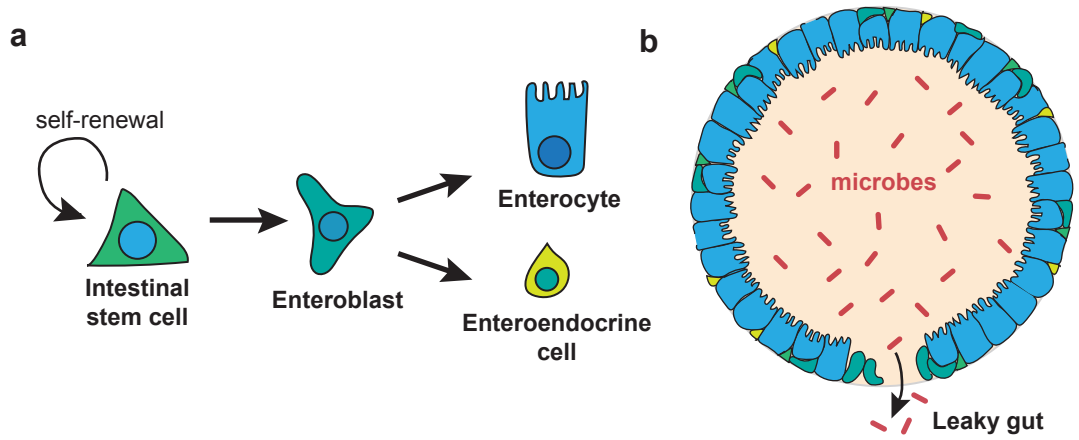

Figure 5: Intestinal stem cell differentiation and gut barrier dysfunction
a. Diagram of self-renewal and differentiation pathways for hindgut cells. Intestinal stem cells self-renew and produce enteroblasts. Enteroblasts can differentiate into enterocytes or enteroendocrine cells. **b.** Visualization of a cross-section of the hindgut. In young tissues, differentiated enteroblasts provide a barrier that prevents microbes from the gut lumen from entering other tissues. In aged tissues, misdifferentiation of enteroblasts can lead to fissures that allow microbes to leak into other tissues, causing systemic infection and death.

The fat body in *Drosophila* is a metabolic and immune organ important for regulating immunosenescence and inflammation. Senescence and inflammation are related processes that increase with organismal age. Senescence is the process by which cells, often in response to damage, to permanently exit the cell cycle. It is associated with an excretory phenotype that promotes inflammation and recruits migrating immune cells to kill and recycle the senescent cell (H. Chen, Zheng, & Zheng, 2014b; Coppé, Desprez, Krtolica, & Campisi, 2010; Ito & Igaki, 2016). Senescence is important for proper organ function and wound healing, but long-term accumulation and failure to clear senescent cells leads to prolonged inflammation, which exacerbates aging phenotypes . These processes are well conserved from insect to mouse to human. In *Drosophila*, the fat body loses heterochromatin over time through a process that involves downregulation of lamin B. Normally, lamin B-associated chromatin domains, which are enriched for immune responsive genes in the fat body, are heterochromatinized and silenced. However, during aging, lamin B is specifically downregulated in fat body tissues and these immune responsive genes become activated. In particular, Peptidoglycan Recognition Proteins (PGRPs) are expressed from the fat body and directly contribute to intestinal stem cell dysplasia and leaky gut (H. Chen et al., 2014b). Here we showed that overexpression of HP1a in fat body cells

leads to lifespan extension. This could be due to maintenance of heterochromatin in fat body cells, which prevents senescent secretory pathway activation and PGRP expression (Guo, Karpac, Tran, & Jasper, 2014).

Copper cells are the equivalent of the stomach in *Drosophila* guts. They are acid-producing cells similar to mammalian parietal cells that are required for proper breakdown of consumed nutrients. Compartmentalization of this function within the gut tissue is important for nutrient absorption and metabolism, in addition to determining microbiota count and content in the gut lumen. This influence over gut microbiota links copper cell function to intestinal dysplasia. Specifically, chronic activation of JAK/STAT signaling in copper cells induces commensal dysbiosis and gut barrier dysfunction (H. Li, Qi, & Jasper, 2016). Inhibition of JAK/STAT in copper cells prevents age-related dysplasia and commensal dysbiosis, and extends lifespan. Interestingly, accumulation of unphosphorylated STAT promotes constitutive heterochromatin formation (Yan, Lim, Shi, Dutta, & Li, 2011). Here we showed that overexpression of HP1a in copper cells is sufficient to induce lifespan extension. It is possible that increased levels of HP1a in copper cells has a similar function to inhibiting JAK/STAT in these cells, which would result in preventing age-related dysplasia and systemic infections.

Glia are involved in many physiological processes important for aging, including maintenance of neurons, immune signaling, and metabolism. Connections between neuronal glia and longevity are numerous, but also tenuous (Hwangbo et al., 2004; Mühlig-Versen et al., 2005; Sanchez et al., 2006; Technau, 2007). Interestingly, our data showed that HP1a expression from one glia driver extended lifespan only in male flies. There is an example of male-specific lifespan extension mechanism –expression of Apolipoprotein D is sex-specifically altered in aging male flies, which alters neuronal and glial metabolism and leads to changes in response to oxidative stress (Ruiz, Sanchez, Canal, Acebes, & Ganfornina, 2011). HP1a in glia could be involved in oxidative stress response and connected via this pathway to longevity, but testing this hypothesis requires direct analyses.

In fact, oxidative stress and subsequent accumulation of unresolved DNA damage is an often-cited mechanism for irreversible age-dependent decline(M. C. Wang, Bohmann, & Jasper, 2003). Tissues tied to aging phenotypes tend to be metabolically active, and are disproportionately subject to oxidative stress. HP1a plays a specific role in repairing DNA damage, especially of repetitive heterochromatic sequences that tend to aberrantly recombine during repair and can lead to chromosomal rearrangements or extrachromosomal circles. In fact, this function of HP1a was invoked in an earlier study of HP1a's contribution to lifespan extension through maintenance of rDNA repeats and prevention of multinucleolar phenotype in older tissues(K. Larson et al., 2012). HP1a's role in preventing aberrant recombination could have cumulative effects on aging, especially in metabolically active tissues that have high DNA damage load. This mechanism is irreversible—once DNA damage is aberrantly repaired or unrepaired, it will not revert back to the original sequence. In this study, we found that overexpression of HP1a later in life does not lead to lifespan extension, which suggests that the mechanism of heterochromatin-mediated lifespan extension is preventative but not reversible. It is possible that this mechanism involves HP1a's role in DNA damage repair, as the consequences of improper repair are irreversible.

Taken together, these data suggest multiple roles for heterochromatin that could contribute to lifespan extension by maintenance of tissue homeostasis, differentiation and genomic integrity. While the true molecular mechanism of HP1a-dependent lifespan extension is as yet unknown, we have shown that basic chromatin organization contributes in a tissue-specific manner to physiological processes of aging.

Acknowledgements

We thank Heinrich Jasper for discussion and generous gift of GeneSwitch fly lines.

Methods

GeneSwitch fly lines (table of Bloomington order numbers)

Stock Name	Obtained from:	Description of expression
UAS::GFP-HP1a	Nystul lab, UCSF. Originally created by Fang Lin Sun in China	Expresses GFP-tagged HP1a in tissues activated by Gal4 or GeneSwitch
Actin5C::GeneSwitch	Bloomington Stock 9431	Drives ubiquitous expression of UAS
elaV::GeneSwtich	Bloomington Stock 43642	All neurons throughout development
GSG2457::GeneSwitch	Bloomington Stock 40992	CNS and PNS glia
GSG1201-2::GeneSwitch	Bloomington Stock 40320	Subset of glia
GSG2945::GeneSwitch	Bloomington Stock 40275	Subset of glia
S106::GeneSwitch	Bloomington stock 8151	Adult abdominal fat body
Labial::GeneSwitch	Heinrich Jasper lab, Buck Institute, CA	Copper cells of midgut
5966::GeneSwitch	Heinrich Jasper lab, Buck Institute, CA	Enteroblasts and post-mitotic enterocytes
5961::GeneSwitch	Heinrich Jasper lab, Buck Institute, CA	Intestinal stem cells
Hml::GeneSwitch	Heinrich Jasper lab, Buck Institute, CA	Hemolymph
dILP::GeneSwitch	Heinrich Jasper lab, Buck Institute, CA	Neurosecretory cells producing dILP6
Mhc::GeneSwitch	Heinrich Jasper lab, Buck Institute, CA	Muscles

Larval feeding of RU486. 3 mL of water plus indicated concentration of RU486 or ethanol for control was mixed with one gram of Formula 4-24 Drosophila instant Medium, Blue per vial. Adult *actin::GeneSwitch* male flies were mated to *UAS::GFP-HP1a* female flies and vice versa, then placed in small egg collection chambers. Eggs were collected for approximately four hours and aged twenty-four hours. Sixty hatchlings were transferred to each vial with indicated concentration of RU486, and raised at 25 degrees for eight days. Number of pupae were counted on days 8, 9 and 10.

Adult feeding RU486. Plastic vials containing standard drosophila media R recipe (yeast, agar, molasses, corn meal, water) were obtained from the facility on UC Berkeley's campus. Indicated concentration of RU486, or ethanol for control, was mixed and distributed 60 μL onto the top of the food in each vial via repeat pipette. Liquid was spread onto top of entire food by gentle rotation, and let dry for at least 45 minutes before adding flies.

Expression Validation. Adult flies from *driver::GeneSwitch* crossed to *UAS::GFP-HP1a* were collected less than 8 hours after eclosion and males and females were separated.

Flies were fed on RU486-containing food for 48 hours, then dissected, mounted in VectaShield mounting medium with DAPI and visualized immediately for live GFP fluorescence. Tissues visualized from each individual: brain, head fat body, flight muscle, heart, ventral nerve cord, leg, gut, crop, gonads, abdominal fat body. To measure expression level, three adults were homogenized per sample in 30 μL Lysis buffer (150 mM NaCl, 1% Triton X-100, 50 mM TrisCl pH 7.4), treated with 1 μL Benzonase for one hour spinning at 4 degrees, added 6 μL Laemmli loading buffer, boiled at 100 degrees C for 5 minutes, spun one minute at 20,000 x g and run on a denaturing SDS-PAGE gel. Gel was transferred to nitrocellulose membrane and blotted with antibodies recognizing GFP, HP1a, and H2B.

Longevity assays. Adult flies were collected upon eclosion and separated by sex into vials of no more than 20 individuals. RU486-containing food was prepared fresh each time, and flies were put to sleep with gentle Carbon Dioxide treatment, and transferred to new vials every 3-4 days. Upon transfer, number of remaining living flies was recorded. For late-in-life expression, flies were aged on food containing no RU486 for 40 days, then transferred to food containing indicated concentrations of RU486 for their remaining lifespan.

General Summary and Future Directions

***In vitro* reconstitution of constitutive heterochromatin liquid-like properties**

We have shown that Drosophila HP1a protein, when purified in vitro, can spontaneously demix from aqueous solution. In a companion paper, Larson et al. found that the human homolog, HP1α, is also capable of droplet formation. To understand how this property is connected to chromatin regulation, we are interested to follow up by testing the influence of chromatin on these in vitro droplets. There are numerous examples of lowering critical concentration of phase separating proteins in solution by adding DNA or RNA (Han et al., 2012) (Brangwynne et al., 2009) (Mitrea et al., 2018) (Patel et al., 2015) (Maharana et al., 2018). Larson et al. also showed that adding DNA to HP1a *in vitro* can lower its critical concentration. In future experiments, we aim to determine if DNA is partitioned naturally into the droplets, whether addition of DNA alters properties of droplet formation and growth, whether methylated nucleosomes are preferentially partitioned into the phase. HP1a directly interacts with H3K9me2/3 and therefore we might expect that nucleosomes methylated at H3K9 would partition preferentially inside the droplets, while unmethylated nucleosomes would have no preference, or partition outside. It will be pertinent to test nucleosome partitioning with *in vitro* purified HP1a.

Additionally, we are curious to investigate the role of Shelob on molecular structure of HP1a-nucleosome interactions. Given our results that Shelob alters the mobility of HP1a toward immobility, we might expect that adding Shelob to the in vitro system would lead to gel-like instead of liquid-like droplets; loss of fusion ability, or irreversibility. However, because of preliminary evidence that Shelob alters HP1a mobility through post-translational modifications, adding Shelob to *in vitro* droplets may have no effect unless the active enzyme is present. In this case, we might turn to the list of HP1a interactors to identify which enzymes might modify HP1a with the modifications that we found in mass spec.

The goal of these *in vitro* experiments is to create a simplified system that closely mimics in vivo domain formation and permeability properties. Of particular interest is the role of the chromatin polymer itself in these droplets. Other examples of membraneless organelles consist of proteins and RNAs but lack the added complexity of a large polymer. Specific *in vitro* experiments will determine methods of specifying which regions of chromatin should partition into or out of the droplet, and how this might be regulated *in vivo*. We expect that selective permeability of the phase separated domain determines which proteins can access the sequences partitioned inside; it will be a great experimental advantage to be able to recreate this system *in vitro* and investigate particular aspects of partitioning and selectivity.

In vivo functions of phase separation

We have demonstrated that heterochromatin droplets arise via liquid-like processes including nucleation, growth, fusion, and look toward further investigating each of these properties. Nucleation of the liquid-phase separated nucleolus is initiated at the rDNA locus, which leads to well-controlled timing and number of nucleoli forming in each nucleus (S. C. Weber & Brangwynne, 2015). To determine if heterochromatin body nucleation is similarly nucleated on the chromatin fiber, we visualized formation of heterochromatin domains in early embryos of Drosophila mutant for su(var)3-9, the histone methyltransferase responsible for depositing H3K9me2/3 (Figure 1). Without this mark, HP1a should not be able to interact directly with chromatin. We expected that, because HP1a is capable of forming droplets when purified *in vitro*, that without H3K9me2/3, it would be able to form droplets *in vivo*, but not be able to load chromatin into the droplets. We find that unlike wild type embryos which exhibit synchronous nucleation and growth of domains in cycles 11-14, in the mutants lacking H3K9me2/3, no nucleation of droplet formation occurs until very late cycle 13. Even in cycle 14, domains do not form in a manner indicative of nucleation and growth—instead they seem to accumulate HP1a in a pattern that already resembles the shape of the coalesced final domain in cycle 14 of wild type embryos. This could indicate that H3K9me2/3 is a necessary staging platform for synchronous domain initiation, similar to the rDNA locus in nucleolar formation. We had hypothesized that fusion of HP1a droplets would be a necessary process for gathering distal heterochromatin domains into a single locus, but this experiment suggests there may be an additional organizing factor.

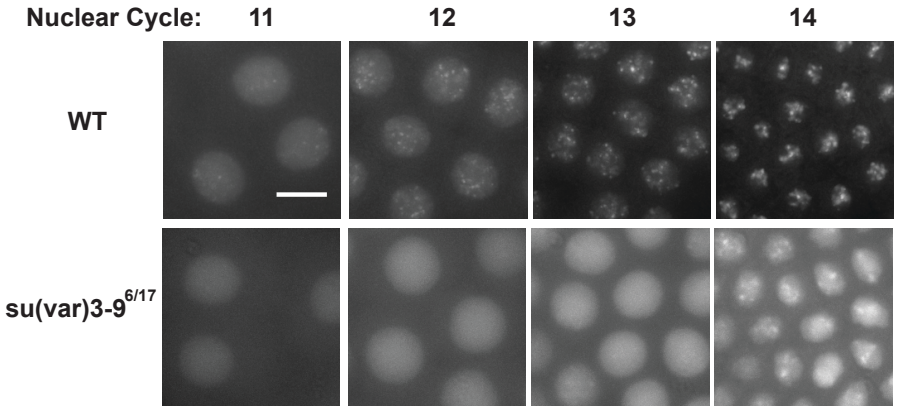

Figure 1: The role of H3K9methylation in HP1a domain formation
Wild type embryos (top) form visible HP1a-rich foci starting at cycle 11 that nucleate, grow, and dissolve again upon mitosis in a liquid-like manner. In su(var)3-9 transheterozygous null embryos, HP1a does not accumulate into foci until cycle 14, and even then is diminished.

To further investigate growth properties of the domains during initial heterochromatin establishment, we can attempt to alter HP1a protein dosage in the early embryo. In a phase separation model we expect that higher concentrations of HP1a will lead to larger heterochromatin domains. Initial attempts at this experiment have failed due to technical issues, and could suggest that HP1a levels in the embryo are tightly regulated. We hope to compare domain growth rates and final domain size to

our *in vitro* experiments with added DNA and chromatin, to determine whether the *in vitro* system is properly representing the *in vivo* system.

Another interesting dial to turn is temperature—phase separated systems are very sensitive to temperature, such that raising temperature should result in smaller and less enriched domains up until a critical temperature at which no domain is able to form (Figure 2). Raising the temperature in a liquid-liquid phase separated system leads to mixing of the two phases, and the ratio of concentrations of dense and light phase can inform about the shape of the two-phase region of the phase diagram (Figure 2). Initial experiments with tissues from adult Drosophila tissues and cultured S2 cells suggest that in vivo heterochromatin domains are indeed sensitive to temperature manipulations and have a critical temperature around 40 degrees centigrade. We are curious to determine whether this critical temperature of in vivo domains matches that of in vitro ones, and whether addition of DNA and chromatin to in vitro domains alters critical temperature. Additionally, we might expect that manipulating levels of Shelob protein, if truly altering the material state of the heterochromatin domain may alter the temperature sensitivity of the domain. Finally, we hypothesize that the human version of the protein might have a higher critical temperature than the Drosophila version, because endothermic resting temperature of 37 degrees is very close to the measured critical temperature 40 degrees, and domain dissolution by temperature increase could be very dangerous. Indeed, *C elegans* are ectothermic organisms that specify germline via localization of p granules in the embryo. P granules are phase separated and dissolve at specific temperature, as stated above. C elegans become sterile at the exact temperature that p granules dissolve. Interestingly, in an evolutionary study of closely related C elegans populations collected from a volcanic island such that worms from the higher elevations on the island were more adapted to colder climate and worms collected from lower elevations were more adapted to warmer climate, those adapted to warmer climate were more able to withstand temperature increase and

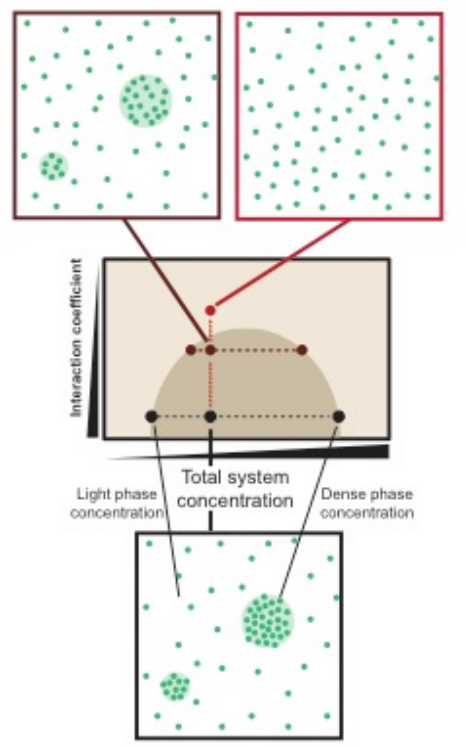

Figure 2: Temperature and phase separation If a system's total concentration of phase-separating protein (green) is within the two-phase regime (black outline), it will phase separate into a dense phase that has concentration equal to the critical concentration at right edge of two-phase regime, and light phase that has concentration equal to the critical concentration at the left edge of the two-phase regime. Increasing temperature will move this system upwards on the diagram (dark red outline) such that a new ratio between dense and light phases is established that represents the two critical concentrations. Increasing temperature even more (bright red outline) moves the system outside of the two-phase into the one-phase regime.

maintain fertility. When investigated, it was found that their p granules stayed present until higher temperature (Delgadillo & Hyman, dissertation 2015). In this way, temperature can control formation of phase-separated nuclear and cytoplasmic membraneless organelles, and result in physiological outcomes.

New Holistic model of the Nucleus: A multi-phase conglomerate

Through the data presented here, we have created a model of the nucleus as a conglomerate of multiple phase-separated systems (Figure 3). The nucleolus, heterochromatin, and other nuclear bodies are each a unique liquid, whose properties are defined by the component proteins, RNAs, and chromatin within. Each compartment has a nuclear position defined by its interaction with other compartments, and a size and number defined by its growth- or nucleation-limited properties. Selective permeability of every type of domain concentrates a unique set of factors within it, allowing for functionalization. Some of these functionalized compartments contain chromatin, targeted to the domain based on their compartment identity, which could be imparted by epigenetic modifications. This model allows for unique regulation of each compartment, but coordinated regulation of all sequences within the compartment.

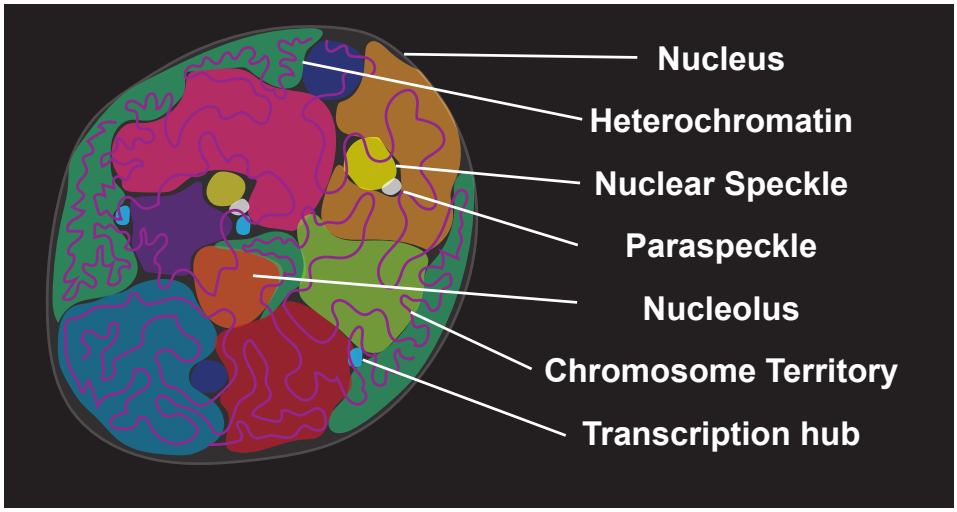

Figure 3: Model of the nucleus
Functionalized compartments within the nucleus are phase-separated, including heterochromatin and nucleoli. Compartmentalization by phase separation allows for coordinated regulation of the chromatin within the domain.

Compartments within compartments

Imagining the nucleus as multiple phase separated compartments invokes stimulating questions of compartment miscibility and interaction. Compartmentalization of sequences allows for a larger unit of regulation so that instead of regulating thousands of unique interactions, the nucleus can rearrange a specific set of loci in a coordinated manner. How this regulation takes place is an open area of examination. One interesting example of a specific region of DNA quickly changing compartments upon an environmental cue is relocalization of DNA double strand breaks from inside heterochromatin. Poly ADP-ribosylation of proteins at the site of double strand breaks

creates a new phase separated compartment (Altmeyer et al., 2015) that exists within heterochromatin, and is able to accumulate early repair proteins. However, proteins that act late in the DSB repair pathway, like rad51, cannot enter into the heterochromatin domain, and therefore cannot load into the repair focus until it is physically moved outside of the heterochromatin area (Figure 4) (Chiolo et al., 2011). This regulation of compartments is potentially a generalizable mechanism that would represent phase-controlled regulation of chromatin locus localization and function. We can use this example to investigate what controls protein accessibility to certain compartments, whether epigenetic modifications determine domain localization, and if liquid-liquid phase separation is required for the function of proper DNA damage repair of repetitive sequences.

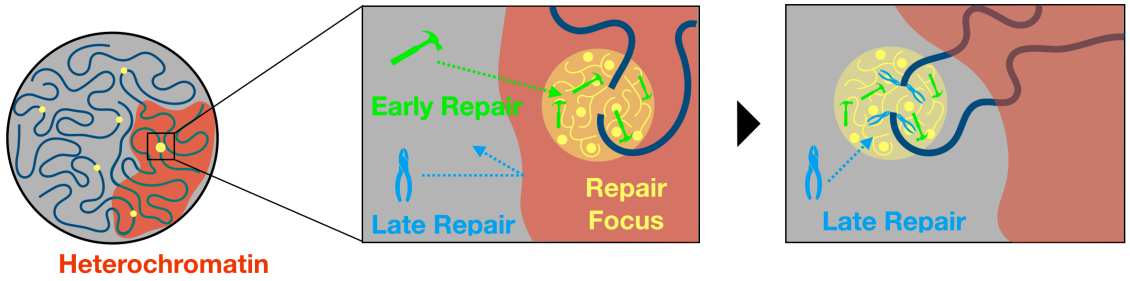

Figure 4: Repair focus movement mediates proper repair of DSBs in repetitive sequences
Double strand breaks, induced by irradiation, that occur inside the heterochromatin domain are able to load early repair proteins (green) but late repair proteins (blue) are prevented from accessing the break until it is physically moved outside of the heterochromatin domain (right).

The field of biological phase separation is relatively new and many fundamental questions remain, including which compartments are formed via phase separation, and how they interact with each other, how many proteins or RNAs are capable of demixing and can we predict which they are. Especially relevant to nuclear function and organization are how phase-separated compartments are regulated, how proteins and chromatin sequences are specified as belonging to a specific compartment, and how each compartment's environment influences its function. Experiments presented here begin to understand phase separation of nuclear compartments but much more work is necessary to understand phase-separation-dependent nuclear organization and eventually utilize that understanding.

Bibliography

Alekseyenko, A. A., Gorchakov, A. A., Zee, B. M., Fuchs, S. M., Kharchenko, P. V., & Kuroda, M. I. (2014). Heterochromatin-associated interactions of Drosophila HP1a with dADD1, HIPP1, and repetitive RNAs. *Genes & Development*, *28*(13), 1445–1460. http://doi.org/10.1101/gad.241950.114

Altmeyer, M., Neelsen, K. J., Teloni, F., Pozdnyakova, I., Pellegrino, S., Grøfte, M., et al. (2015). Liquid demixing of intrinsically disordered proteins is seeded by poly(ADP-ribose). *Nature Communications*, *6*(1), 8088. http://doi.org/10.1038/ncomms9088

Aten, J. A., Stap, J., Krawczyk, P. M., van Oven, C. H., Hoebe, R. A., Essers, J., & Kanaar, R. (2004). Dynamics of DNA double-strand breaks revealed by clustering of damaged chromosome domains. *Science*, *303*(5654), 92–95. http://doi.org/10.1126/science.1088845

Aucott, R., Bullwinkel, J., Yu, Y., Shi, W., Billur, M., Brown, J. P., et al. (2008). HP1-beta is required for development of the cerebral neocortex and neuromuscular junctions. *The Journal of Cell Biology*, *183*(4), 597–606. http://doi.org/10.1083/jcb.200804041

Bancaud, A., Huet, S., Daigle, N., Mozziconacci, J., Beaudouin, J., & Ellenberg, J. (2009). Molecular crowding affects diffusion and binding of nuclear proteins in heterochromatin and reveals the fractal organization of chromatin. *The EMBO Journal*, *28*(24), 3785–3798. http://doi.org/10.1038/emboj.2009.340

Bannister, A. J., Zegerman, P., Partridge, J. F., Miska, E. A., Thomas, J. O., Allshire, R. C., & Kouzarides, T. (2001). Selective recognition of methylated lysine 9 on histone H3 by the HP1 chromo domain. *Nature*, *410*(6824), 120–124. http://doi.org/10.1038/35065138

Bernard, P., Maure, J. F., Partridge, J. F., Genier, S., Javerzat, J. P., & Allshire, R. C. (2001). Requirement of heterochromatin for cohesion at centromeres. *Science*, *294*(5551), 2539–2542. http://doi.org/10.1126/science.1064027

Bombarda, E., Cherradi, H., Morellet, N., Roques, B. P., & Mély, Y. (2002). Zn(2+) binding properties of single-point mutants of the C-terminal zinc finger of the HIV-1 nucleocapsid protein: evidence of a critical role of cysteine 49 in Zn(2+) dissociation. *Biochemistry*, *41*(13), 4312–4320. http://doi.org/10.1021/bi015956g

Brangwynne, C. P., Eckmann, C. R., Courson, D. S., Rybarska, A., Hoege, C., Gharakhani, J., et al. (2009). Germline P granules are liquid droplets that localize by controlled dissolution/condensation. *Science*, *324*(5935), 1729–1732. http://doi.org/10.1126/science.1172046

Brangwynne, C. P., Mitchison, T. J., & Hyman, A. A. (2011). Active liquid-like behavior of nucleoli determines their size and shape in Xenopus laevis oocytes. *Proceedings of the National Academy of Sciences of the United States of America*, *108*(11), 4334–4339. http://doi.org/10.1073/pnas.1017150108

Brower-Toland, B., Findley, S. D., Jiang, L., Liu, L., Yin, H., Dus, M., et al. (2007). Drosophila PIWI associates with chromatin and interacts directly with HP1a. *Genes & Development*, *21*(18), 2300–2311. http://doi.org/10.1101/gad.1564307

Brundin, P., Melki, R., & Kopito, R. (2010). Prion-like transmission of protein aggregates in neurodegenerative diseases. *Nature Reviews. Molecular Cell Biology*, *11*(4), 301–307. http://doi.org/10.1038/nrm2873

Brutlag, D., Carlson, M., Fry, K., & Hsieh, T. S. (1978). DNA sequence organization in Drosophila heterochromatin. *Cold Spring Harbor Symposia on Quantitative Biology*, *42 Pt 2*, 1137–1146.

Carlson, M., & Brutlag, D. (1978). One of the copia genes is adjacent to satellite DNA in Drosophila melanogaster. *Cell*, *15*(3), 733–742.

Chen, B.-C., Legant, W. R., Wang, K., Shao, L., Milkie, D. E., Davidson, M. W., et al. (2014a). Lattice light-sheet microscopy: imaging molecules to embryos at high spatiotemporal resolution. *Science*, *346*(6208), 1257998. http://doi.org/10.1126/science.1257998

Chen, H., Zheng, X., & Zheng, Y. (2014b). Age-associated loss of lamin-B leads to systemic inflammation and gut hyperplasia. *Cell*, *159*(4), 829–843. http://doi.org/10.1016/j.cell.2014.10.028

Chiolo, I., Minoda, A., Colmenares, S. U., Polyzos, A., Costes, S. V., & Karpen, G. H. (2011). Double-strand breaks in heterochromatin move outside of a dynamic HP1a domain to complete recombinational repair. *Cell*, *144*(5), 732–744. http://doi.org/10.1016/j.cell.2011.02.012

Clemson, C. M., Hall, L. L., Byron, M., McNeil, J., & Lawrence, J. B. (2006). The X chromosome is organized into a gene-rich outer rim and an internal core containing silenced nongenic sequences. *Proceedings of the National Academy of Sciences of the United States of America*, *103*(20), 7688–7693. http://doi.org/10.1073/pnas.0601069103

Coppé, J.-P., Desprez, P.-Y., Krtolica, A., & Campisi, J. (2010). The senescence-associated secretory phenotype: the dark side of tumor suppression. *Annual Review of Pathology*, *5*(1), 99–118. http://doi.org/10.1146/annurev-pathol-121808-102144

Dernburg, A. F., Broman, K. W., Fung, J. C., Marshall, W. F., Philips, J., Agard, D. A., & Sedat, J. W. (1996). Perturbation of nuclear architecture by long-distance chromosome interactions. *Cell*, *85*(5), 745–759.

Digman, M. A., Dalal, R., Horwitz, A. F., & Gratton, E. (2008). Mapping the number of molecules and brightness in the laser scanning microscope. *Biophysical Journal*, *94*(6), 2320–2332. http://doi.org/10.1529/biophysj.107.114645

Digman, M. A., Wiseman, P. W., Horwitz, A. R., & Gratton, E. (2009). Detecting protein complexes in living cells from laser scanning confocal image sequences by the cross correlation raster image spectroscopy method. *Biophysical Journal*, *96*(2), 707–716. http://doi.org/10.1016/j.bpj.2008.09.051

Elgin, S. C. R., & Reuter, G. (2013). Position-effect variegation, heterochromatin formation, and gene silencing in Drosophila. *Cold Spring Harbor Perspectives in Biology*, *5*(8), a017780–a017780. http://doi.org/10.1101/cshperspect.a017780

Falahati, H., Pelham-Webb, B., Blythe, S., & Wieschaus, E. (2016). Nucleation by rRNA Dictates the Precision of Nucleolus Assembly. *Current Biology : CB*, *26*(3), 277–285. http://doi.org/10.1016/j.cub.2015.11.065

Feric, M., Vaidya, N., Harmon, T. S., Mitrea, D. M., Zhu, L., Richardson, T. M., et al. (2016). Coexisting Liquid Phases Underlie Nucleolar Subcompartments. *Cell*, *165*(7), 1686–1697. http://doi.org/10.1016/j.cell.2016.04.047

Fischle, W., Tseng, B. S., Dormann, H. L., Ueberheide, B. M., Garcia, B. A., Shabanowitz, J., et al. (2005). Regulation of HP1-chromatin binding by histone H3

methylation and phosphorylation. *Nature*, *438*(7071), 1116–1122. http://doi.org/10.1038/nature04219
Frankel, S., & Rogina, B. (2005). Drosophila longevity is not affected by heterochromatin-mediated gene silencing. *Aging Cell*, *4*(1), 53–56. http://doi.org/10.1111/j.1474-9726.2005.00143.x
Greil, F., de Wit, E., Bussemaker, H. J., & van Steensel, B. (2007). HP1 controls genomic targeting of four novel heterochromatin proteins in Drosophila. *The EMBO Journal*, *26*(3), 741–751. http://doi.org/10.1038/sj.emboj.7601527
Grewal, S. I. S., & Jia, S. (2007). Heterochromatin revisited. *Nature Reviews. Genetics*, *8*(1), 35–46. http://doi.org/10.1038/nrg2008
Grousl, T., Ivanov, P., Frýdlová, I., Vasicová, P., Janda, F., Vojtová, J., et al. (2009). Robust heat shock induces eIF2alpha-phosphorylation-independent assembly of stress granules containing eIF3 and 40S ribosomal subunits in budding yeast, Saccharomyces cerevisiae. *Journal of Cell Science*, *122*(Pt 12), 2078–2088. http://doi.org/10.1242/jcs.045104
Guo, L., Karpac, J., Tran, S. L., & Jasper, H. (2014). PGRP-SC2 promotes gut immune homeostasis to limit commensal dysbiosis and extend lifespan. *Cell*, *156*(1-2), 109–122. http://doi.org/10.1016/j.cell.2013.12.018
Guruharsha, K. G., Rual, J.-F., Zhai, B., Mintseris, J., Vaidya, P., Vaidya, N., et al. (2011). A Protein Complex Network of Drosophila melanogaster. *Cell*, *147*(3), 690–703. http://doi.org/10.1016/j.cell.2011.08.047
Han, T. W., Kato, M., Xie, S., Wu, L. C., Mirzaei, H., Pei, J., et al. (2012). Cell-free formation of RNA granules: bound RNAs identify features and components of cellular assemblies. *Cell*, *149*(4), 768–779. http://doi.org/10.1016/j.cell.2012.04.016
He, Y., & Jasper, H. (2014). Studying aging in Drosophila. *Methods (San Diego, Calif.)*, *68*(1), 129–133. http://doi.org/10.1016/j.ymeth.2014.04.008
Heard, E., & Bickmore, W. (2007). The ins and outs of gene regulation and chromosome territory organisation. *Current Opinion in Cell Biology*, *19*(3), 311–316. http://doi.org/10.1016/j.ceb.2007.04.016
Hinde, E., Cardarelli, F., & Gratton, E. (2015). Spatiotemporal regulation of Heterochromatin Protein 1-alpha oligomerization and dynamics in live cells. *Scientific Reports*, *5*(1), 12001. http://doi.org/10.1038/srep12001
Hines, K. A., Cryderman, D. E., Flannery, K. M., Yang, H., Vitalini, M. W., Hazelrigg, T., et al. (2009). Domains of heterochromatin protein 1 required for Drosophila melanogaster heterochromatin spreading. *Genetics*, *182*(4), 967–977. http://doi.org/10.1534/genetics.109.105338
Huber, G. (1991). Scheidegger"s rivers, Takayasu"s aggregates and continued fractions. *Physica a: Statistical Mechanics and Its Applications*, *170*(3), 463–470. http://doi.org/10.1016/0378-4371(91)90001-S
Hwangbo, D. S., Gershman, B., Gersham, B., Tu, M.-P., Palmer, M., & Tatar, M. (2004). Drosophila dFOXO controls lifespan and regulates insulin signalling in brain and fat body. *Nature*, *429*(6991), 562–566. http://doi.org/10.1038/nature02549
Hyman, A. A., Weber, C. A., & Jülicher, F. (2014). Liquid-liquid phase separation in biology. *Annual Review of Cell and Developmental Biology*, *30*(1), 39–58. http://doi.org/10.1146/annurev-cellbio-100913-013325

Iborra, F. J. (2007). Can visco-elastic phase separation, macromolecular crowding and colloidal physics explain nuclear organisation? *Theoretical Biology & Medical Modelling*, *4*(1), 15. http://doi.org/10.1186/1742-4682-4-15
Ito, T., & Igaki, T. (2016). Dissecting cellular senescence and SASP in Drosophila. *Inflammation and Regeneration*, *36*(1), 25. http://doi.org/10.1186/s41232-016-0031-4
Janssen, A., Breuer, G. A., Brinkman, E. K., van der Meulen, A. I., Borden, S. V., van Steensel, B., et al. (2016). A single double-strand break system reveals repair dynamics and mechanisms in heterochromatin and euchromatin. *Genes & Development*, *30*(14), 1645–1657. http://doi.org/10.1101/gad.283028.116
Jenuwein, T., & Allis, C. D. (2001). Translating the histone code. *Science*, *293*(5532), 1074–1080. http://doi.org/10.1126/science.1063127
Jeon, H.-J., Kim, Y.-S., Kim, J.-G., Heo, K., Pyo, J.-H., Yamaguchi, M., et al. (2018). Effect of heterochromatin stability on intestinal stem cell aging in Drosophila. *Mechanisms of Ageing and Development*. http://doi.org/10.1016/j.mad.2018.04.001
Jiang, H., & Edgar, B. A. (2009). EGFR signaling regulates the proliferation of Drosophila adult midgut progenitors. *Development (Cambridge, England)*, *136*(3), 483–493. http://doi.org/10.1242/dev.026955
Jurka, J. (2000). Repbase update: a database and an electronic journal of repetitive elements. *Trends in Genetics : TIG*, *16*(9), 418–420.
Karpen, G. H., Le, M. H., & Le, H. (1996). Centric heterochromatin and the efficiency of achiasmate disjunction in Drosophila female meiosis. *Science*, *273*(5271), 118–122.
Kato, M., Han, T. W., Xie, S., Shi, K., Du, X., Wu, L. C., et al. (2012). Cell-free formation of RNA granules: low complexity sequence domains form dynamic fibers within hydrogels. *Cell*, *149*(4), 753–767. http://doi.org/10.1016/j.cell.2012.04.017
Kellum, R., Raff, J. W., & Alberts, B. M. (1995). Heterochromatin protein 1 distribution during development and during the cell cycle in Drosophila embryos. *Journal of Cell Science*, *108 (Pt 4)*, 1407–1418.
Kramer, S., Queiroz, R., Ellis, L., Webb, H., Hoheisel, J. D., Clayton, C., & Carrington, M. (2008). Heat shock causes a decrease in polysomes and the appearance of stress granules in trypanosomes independently of eIF2(alpha) phosphorylation at Thr169. *Journal of Cell Science*, *121*(Pt 18), 3002–3014. http://doi.org/10.1242/jcs.031823
Lachner, M., O'Carroll, D., Rea, S., Mechtler, K., & Jenuwein, T. (2001). Methylation of histone H3 lysine 9 creates a binding site for HP1 proteins. *Nature*, *410*(6824), 116–120. http://doi.org/10.1038/35065132
Larson, A. G., Elnatan, D., Keenen, M. M., Trnka, M. J., Johnston, J. B., Burlingame, A. L., et al. (2017). Liquid droplet formation by HP1α suggests a role for phase separation in heterochromatin. *Nature*, *547*(7662), 236–240. http://doi.org/10.1038/nature22822
Larson, K., Yan, S.-J., Tsurumi, A., Liu, J., Zhou, J., Gaur, K., et al. (2012). Heterochromatin formation promotes longevity and represses ribosomal RNA synthesis. *PLoS Genetics*, *8*(1), e1002473. http://doi.org/10.1371/journal.pgen.1002473
Lechner, M. S., Schultz, D. C., Negorev, D., Maul, G. G., & Rauscher, F. J. (2005). The mammalian heterochromatin protein 1 binds diverse nuclear proteins through a

common motif that targets the chromoshadow domain. *Biochemical and Biophysical Research Communications*, *331*(4), 929–937. http://doi.org/10.1016/j.bbrc.2005.04.016
Lee, D. Y., Hayes, J. J., Pruss, D., & Wolffe, A. P. (1993). A positive role for histone acetylation in transcription factor access to nucleosomal DNA. *Cell*, *72*(1), 73–84.
Li, H., Qi, Y., & Jasper, H. (2016). Preventing Age-Related Decline of Gut Compartmentalization Limits Microbiota Dysbiosis and Extends Lifespan. *Cell Host & Microbe*, *19*(2), 240–253. http://doi.org/10.1016/j.chom.2016.01.008
Li, P., Banjade, S., Cheng, H.-C., Kim, S., Chen, B., Guo, L., et al. (2012). Phase transitions in the assembly of multivalent signalling proteins. *Nature*, *483*(7389), 336–340. http://doi.org/10.1038/nature10879
Li, Y., Danzer, J. R., Alvarez, P., Belmont, A. S., & Wallrath, L. L. (2003). Effects of tethering HP1 to euchromatic regions of the Drosophila genome. *Development (Cambridge, England)*, *130*(9), 1817–1824.
Lian, X. J., & Gallouzi, I.-E. (2009). Oxidative Stress Increases the Number of Stress Granules in Senescent Cells and Triggers a Rapid Decrease in p21waf1/cip1 Translation. *The Journal of Biological Chemistry*, *284*(13), 8877–8887. http://doi.org/10.1074/jbc.M806372200
Lin, Y., Protter, D. S. W., Rosen, M. K., & Parker, R. (2015). Formation and Maturation of Phase-Separated Liquid Droplets by RNA-Binding Proteins. *Molecular Cell*, *60*(2), 208–219. http://doi.org/10.1016/j.molcel.2015.08.018
Loveall, B. J., & Deitcher, D. L. (2010). The essential role of bursicon during Drosophila development. *BMC Developmental Biology*, *10*(1), 92. http://doi.org/10.1186/1471-213X-10-92
Lu, B. Y., Bishop, C. P., & Eissenberg, J. C. (1996). Developmental timing and tissue specificity of heterochromatin-mediated silencing. *The EMBO Journal*, *15*(6), 1323–1332.
Maharana, S., Wang, J., Papadopoulos, D. K., Richter, D., Pozniakovsky, A., Poser, I., et al. (2018). RNA buffers the phase separation behavior of prion-like RNA binding proteins. *Science*, eaar7366. http://doi.org/10.1126/science.aar7366
Maison, C., Bailly, D., Roche, D., Montes de Oca, R., Probst, A. V., Vassias, I., et al. (2011). SUMOylation promotes de novo targeting of HP1α to pericentric heterochromatin. *Nature Genetics*, *43*(3), 220–227. http://doi.org/10.1038/ng.765
Mao, Y. S., Zhang, B., & Spector, D. L. (2011). Biogenesis and function of nuclear bodies. *Trends in Genetics : TIG*, *27*(8), 295–306. http://doi.org/10.1016/j.tig.2011.05.006
McKee, B. D., & Karpen, G. H. (1990). Drosophila ribosomal RNA genes function as an X-Y pairing site during male meiosis. *Cell*, *61*(1), 61–72.
Mitrea, D. M., Cika, J. A., Guy, C. S., Ban, D., Banerjee, P. R., Stanley, C. B., et al. (2016). Nucleophosmin integrates within the nucleolus via multi-modal interactions with proteins displaying R-rich linear motifs and rRNA. *eLife*, *5*, D181. http://doi.org/10.7554/eLife.13571
Mitrea, D. M., Cika, J. A., Stanley, C. B., Nourse, A., Onuchic, P. L., Banerjee, P. R., et al. (2018). Self-interaction of NPM1 modulates multiple mechanisms of liquid-liquid phase separation. *Nature Communications*, *9*(1), 842. http://doi.org/10.1038/s41467-018-03255-3

Molliex, A., Temirov, J., Lee, J., Coughlin, M., Kanagaraj, A. P., Kim, H. J., et al. (2015). Phase separation by low complexity domains promotes stress granule assembly and drives pathological fibrillization. *Cell*, *163*(1), 123–133. http://doi.org/10.1016/j.cell.2015.09.015

Motamedi, M. R., Hong, E.-J. E., Li, X., Gerber, S., Denison, C., Gygi, S., & Moazed, D. (2008). HP1 proteins form distinct complexes and mediate heterochromatic gene silencing by nonoverlapping mechanisms. *Molecular Cell*, *32*(6), 778–790. http://doi.org/10.1016/j.molcel.2008.10.026

Mühlig-Versen, M., da Cruz, A. B., Tschäpe, J.-A., Moser, M., Büttner, R., Athenstaedt, K., et al. (2005). Loss of Swiss cheese/neuropathy target esterase activity causes disruption of phosphatidylcholine homeostasis and neuronal and glial death in adult Drosophila. *The Journal of Neuroscience : the Official Journal of the Society for Neuroscience*, *25*(11), 2865–2873. http://doi.org/10.1523/JNEUROSCI.5097-04.2005

Müller, K. P., Erdel, F., Caudron-Herger, M., Marth, C., Fodor, B. D., Richter, M., et al. (2009). Multiscale analysis of dynamics and interactions of heterochromatin protein 1 by fluorescence fluctuation microscopy. *Biophysical Journal*, *97*(11), 2876–2885. http://doi.org/10.1016/j.bpj.2009.08.057

Noll, M., & Kornberg, R. D. (1977). Action of micrococcal nuclease on chromatin and the location of histone H1. *Journal of Molecular Biology*, *109*(3), 393–404.

Patel, A., Lee, H. O., Jawerth, L., Maharana, S., Jahnel, M., Hein, M. Y., et al. (2015). A Liquid-to-Solid Phase Transition of the ALS Protein FUS Accelerated by Disease Mutation. *Cell*, *162*(5), 1066–1077. http://doi.org/10.1016/j.cell.2015.07.047

Peacock, W. J., Lohe, A. R., Gerlach, W. L., Dunsmuir, P., Dennis, E. S., & Appels, R. (1978). Fine structure and evolution of DNA in heterochromatin. *Cold Spring Harbor Symposia on Quantitative Biology*, *42 Pt 2*, 1121–1135.

Peng, J. C., & Karpen, G. H. (2008). Epigenetic regulation of heterochromatic DNA stability. *Current Opinion in Genetics & Development*, *18*(2), 204–211. http://doi.org/10.1016/j.gde.2008.01.021

Peng, J. C., & Karpen, G. H. (2009). Heterochromatic genome stability requires regulators of histone H3 K9 methylation. *PLoS Genetics*, *5*(3), e1000435. http://doi.org/10.1371/journal.pgen.1000435

Posovszky, C., & Wabitsch, M. (2015a). Regulation of appetite, satiation, and body weight by enteroendocrine cells. Part 1: characteristics of enteroendocrine cells and their capability of weight regulation. *Hormone Research in Paediatrics*, *83*(1), 1–10. http://doi.org/10.1159/000368898

Posovszky, C., & Wabitsch, M. (2015b). Regulation of appetite, satiation, and body weight by enteroendocrine cells. Part 2: therapeutic potential of enteroendocrine cells in the treatment of obesity. *Hormone Research in Paediatrics*, *83*(1), 11–18. http://doi.org/10.1159/000369555

Purnell, B. A. (2015). Heterochromatin in aging stem cells. *Science*, *348*(6239), 1102–1104. http://doi.org/10.1126/science.348.6239.1102-r

Rera, M., Clark, R. I., & Walker, D. W. (2012). Intestinal barrier dysfunction links metabolic and inflammatory markers of aging to death in Drosophila. *Proceedings of the National Academy of Sciences of the United States of America*, *109*(52), 21528–21533. http://doi.org/10.1073/pnas.1215849110

Ribbeck, K., & Görlich, D. (2002). The permeability barrier of nuclear pore complexes appears to operate via hydrophobic exclusion. *The EMBO Journal*, *21*(11), 2664–2671. http://doi.org/10.1093/emboj/21.11.2664

Richards, G. (1997). The Ecdysone Regulatory Cascades in Drosophila (Vol. 5, pp. 81–135). Elsevier. http://doi.org/10.1016/S1566-3116(08)60036-5

Richmond, T. J., & Davey, C. A. (2003). The structure of DNA in the nucleosome core. *Nature*, *423*(6936), 145–150. http://doi.org/10.1038/nature01595

Rosnoblet, C., Vandamme, J., Völkel, P., & Angrand, P.-O. (2011). Analysis of the human HP1 interactome reveals novel binding partners. *Biochemical and Biophysical Research Communications*, *413*(2), 206–211. http://doi.org/10.1016/j.bbrc.2011.08.059

Rossow, M. J., Sasaki, J. M., Digman, M. A., & Gratton, E. (2010). Raster image correlation spectroscopy in live cells. *Nature Protocols*, *5*(11), 1761–1774. http://doi.org/10.1038/nprot.2010.122

Ruiz, M., Sanchez, D., Canal, I., Acebes, A., & Ganfornina, M. D. (2011). Sex-dependent modulation of longevity by two Drosophila homologues of human Apolipoprotein D, GLaz and NLaz. *Experimental Gerontology*, *46*(7), 579–589. http://doi.org/10.1016/j.exger.2011.02.014

Ryu, H.-W., Lee, D. H., Florens, L., Swanson, S. K., Washburn, M. P., & Kwon, S. H. (2014). Analysis of the heterochromatin protein 1 (HP1) interactome in Drosophila. *Journal of Proteomics*, *102*, 137–147. http://doi.org/10.1016/j.jprot.2014.03.016

Sanchez, D., López-Arias, B., Torroja, L., Canal, I., Wang, X., Bastiani, M. J., & Ganfornina, M. D. (2006). Loss of glial lazarillo, a homolog of apolipoprotein D, reduces lifespan and stress resistance in Drosophila. *Current Biology : CB*, *16*(7), 680–686. http://doi.org/10.1016/j.cub.2006.03.024

Sen, P., Shah, P. P., Nativio, R., & Berger, S. L. (2016). Epigenetic Mechanisms of Longevity and Aging. *Cell*, *166*(4), 822–839. http://doi.org/10.1016/j.cell.2016.07.050

Simon, A. F., Shih, C., Mack, A., & Benzer, S. (2003). Steroid control of longevity in Drosophila melanogaster. *Science*, *299*(5611), 1407–1410. http://doi.org/10.1126/science.1080539

Smothers, J. F., & Henikoff, S. (2000). The HP1 chromo shadow domain binds a consensus peptide pentamer. *Current Biology : CB*, *10*(1), 27–30.

Strom, A. R., Emelyanov, A. V., Mir, M., Fyodorov, D. V., Darzacq, X., & Karpen, G. H. (2017). Phase separation drives heterochromatin domain formation. *Nature*, *547*(7662), 241–245. http://doi.org/10.1038/nature22989

Swenson, J. M., Colmenares, S. U., Strom, A. R., Costes, S. V., & Karpen, G. H. (2016). The composition and organization of Drosophila heterochromatin are heterogeneous and dynamic. *eLife*, *5*, 1445. http://doi.org/10.7554/eLife.16096

Taddei, A., Roche, D., Sibarita, J. B., Turner, B. M., & Almouzni, G. (1999). Duplication and maintenance of heterochromatin domains. *The Journal of Cell Biology*, *147*(6), 1153–1166.

Technau, G. M. (2007). Fiber number in the mushroom bodies of adult Drosophila melanogaster depends on age, sex and experience. *Journal of Neurogenetics*, *21*(4), 183–196. http://doi.org/10.1080/01677060701695359

Urieli-Shoval, S., Gruenbaum, Y., Sedat, J., & Razin, A. (1982). The absence of detectable methylated bases in Drosophila melanogaster DNA. *FEBS Letters*, *146*(1), 148–152.
Vasquez, P. A., Hult, C., Adalsteinsson, D., Lawrimore, J., Forest, M. G., & Bloom, K. (2016). Entropy gives rise to topologically associating domains. *Nucleic Acids Research*, *44*(12), 5540–5549. http://doi.org/10.1093/nar/gkw510
Wang, L., Karpac, J., & Jasper, H. (2014). Promoting longevity by maintaining metabolic and proliferative homeostasis. *The Journal of Experimental Biology*, *217*(Pt 1), 109–118. http://doi.org/10.1242/jeb.089920
Wang, M. C., Bohmann, D., & Jasper, H. (2003). JNK signaling confers tolerance to oxidative stress and extends lifespan in Drosophila. *Developmental Cell*, *5*(5), 811–816.
Weber, S. C., & Brangwynne, C. P. (2015). Inverse size scaling of the nucleolus by a concentration-dependent phase transition. *Current Biology : CB*, *25*(5), 641–646. http://doi.org/10.1016/j.cub.2015.01.012
Wolfe, S. A., Nekludova, L., & Pabo, C. O. (2000). DNA recognition by Cys2His2 zinc finger proteins. *Annual Review of Biophysics and Biomolecular Structure*, *29*(1), 183–212. http://doi.org/10.1146/annurev.biophys.29.1.183
Wood, J. G., Jones, B. C., Jiang, N., Chang, C., Hosier, S., Wickremesinghe, P., et al. (2016). Chromatin-modifying genetic interventions suppress age-associated transposable element activation and extend life span in Drosophila. *Proceedings of the National Academy of Sciences of the United States of America*, *113*(40), 11277–11282. http://doi.org/10.1073/pnas.1604621113
Wootton, J. C. (1994). Non-globular domains in protein sequences: automated segmentation using complexity measures. *Computers & Chemistry*, *18*(3), 269–285.
Xue, B., Dunbrack, R. L., Williams, R. W., Dunker, A. K., & Uversky, V. N. (2010). PONDR-FIT: a meta-predictor of intrinsically disordered amino acids. *Biochimica Et Biophysica Acta*, *1804*(4), 996–1010. http://doi.org/10.1016/j.bbapap.2010.01.011
Yan, S.-J., Lim, S. J., Shi, S., Dutta, P., & Li, W. X. (2011). Unphosphorylated STAT and heterochromatin protect genome stability. *FASEB Journal : Official Publication of the Federation of American Societies for Experimental Biology*, *25*(1), 232–241. http://doi.org/10.1096/fj.10-169367
Yuan, K., & O'Farrell, P. H. (2016). TALE-light imaging reveals maternally guided, H3K9me2/3-independent emergence of functional heterochromatin in Drosophila embryos. *Genes & Development*, *30*(5), 579–593. http://doi.org/10.1101/gad.272237.115
Zhao, T., Heyduk, T., Allis, C. D., & Eissenberg, J. C. (2000). Heterochromatin protein 1 binds to nucleosomes and DNA in vitro. *The Journal of Biological Chemistry*, *275*(36), 28332–28338. http://doi.org/10.1074/jbc.M003493200
Zhu, L., & Brangwynne, C. P. (2015). Nuclear bodies: the emerging biophysics of nucleoplasmic phases. *Current Opinion in Cell Biology*, *34*, 23–30. http://doi.org/10.1016/j.ceb.2015.04.003